

Field Observations During Wind Turbine Foundation Installation at the Block Island Wind Farm, Rhode Island

Appendix D: Underwater Sound Monitoring Reports



US Department of the Interior
Bureau of Ocean Energy Management
Office of Renewable Energy Programs



Field Observations During Wind Turbine Foundation Installation at the Block Island Wind Farm, Rhode Island

Appendix D: Underwater Sound Monitoring Reports

May 2018

Authors (in alphabetical order):

Jennifer L. Amaral, Robin Beard, R.J. Barham, A.G. Collett, James Elliot, Adam S. Frankel,
Dennis Gallien, Carl Hager, Anwar A. Khan, Ying-Tsong Lin, Timothy Mason, James H. Miller,
Arthur E. Newhall, Gopu R. Potty, Kevin Smith, and Kathleen J. Vigness-Raposa

Prepared under BOEM Award

Contract No. M15PC00002,

Task Order No. M16PD00031

By

HDR

9781 S Meridian Boulevard, Suite 400

Englewood, CO 80112

**U.S. Department of the Interior
Bureau of Ocean Energy Management
Office of Renewable Energy Programs**



Report

Underwater Acoustic Measurements of the Construction of the Block Island Wind Farm

February
2018

James H. Miller¹, Gopu R. Potty¹, Ying-Tsong Lin², Arthur E. Newhall², Kathleen J. Vigness-Raposa³, Jennifer L. Amaral^{1,3}, and Adam S. Frankel³

¹University of Rhode Island, Narragansett, Rhode Island, USA

²Woods Hole Oceanographic Institution, Woods Hole, Massachusetts, USA

³Marine Acoustics, Inc., Middletown, Rhode Island, USA

Acknowledgements

The authors wish to gratefully acknowledge the assistance of:

Mary Boatman and Stan Labak of BOEM

Randy Gallien, Anwar Khan, and Jamey Elliot of HDR, Inc.

Steve Crocker of the Naval Undersea Warfare Center

Aileen Kenney of Deepwater Wind

Tim Mason of Subacoustech

Art Popper of the University of Maryland

Tony Hawkins of Loughline

John Kemp, James Dunn, Meghan Donohue, and Peter Koski of WHOI

Hui-Kwan Kim, Fred Pease, Rob Freeland, Melodie Ross, Tyler Blanpied, Peter Ouellette, John King, Chip Heil, and Amin Mivechi of the University of Rhode Island

Jen Daniels of Tetrattech

Brandon Southall of Southall Env. Assoc.,

Charles Greene of Greeneridge Sciences

Bill Ellison and Andrew White of Marine Acoustics, Inc.

Peter Dahl of the University of Washington

Table of Contents

Overview of Report	1
1. Introduction	3
1.1 Purpose of the Report.....	3
1.2 Prior Work	4
1.3 Site Description	4
1.4 Foundation Description.....	6
1.5 Turbine Description.....	8
1.6 Modeling Pile Driving	8
2. Monitoring Construction of the Block Island Wind Farm	11
2.1 Towed Hydrophone Array Results	13
2.2 Preliminary Results for the Geophysical Sled	16
2.2.1 Tetrahedral Array Results.....	17
2.2.2 Geophone Results.....	19
2.2.3 Fish Hearing and Effect of Noise and Particle Motion	21
2.3 Vertical Hydrophone Array Results	22
2.4 Summary of Measurements During Construction.....	24
3. Fin Whale Vocalizations	27
4. Conclusions and Recommended Next Steps	29
References	31

Figures

Figure 1. Location of the wind turbines in the Block Island Wind Farm. The soundings are in feet. (Deepwater Wind, 2017)	3
Figure 2. On the left, the measurement setup as described by Betke (2004) for monitoring underwater noise from an offshore wind turbine in water 10 m deep. On the right, the 1/3-octave band levels measured 110 m from the turbine for different operating conditions. Wind speeds are measured at the hub height.....	4
Figure 3. The Laurentide Ice Sheet and the Wisconsinan Glacier is shown overlying North America. The marine geology of the wind farm site near Block Island, Rhode Island is dominated by debris left from the glaciation.	5
Figure 4. A photo of Mohegan Bluffs on the south side of Block Island illustrates the geology of the area where the sediment consists of heterogeneous over-consolidated gravels, sands, silts, clays, cobbles, and boulders.	5
Figure 5. Bathymetry in the area of Block Island.....	6
Figure 6. An aerial view of the Block Island Wind Farm and Block Island. The numbers refer to the ID numbers from Table 1.	7

Figure 7. One of the foundations of the Block Island Wind Farm is shown to the right of the Lift Barge Robert.....7

Figure 8. Reinhall Dahl (2011) modeled the creation of an acoustic wave in the water from a vertical pile. The speed of the compressional wave in the pile is about 5015 m/s and much greater than the water sound speed of about 1500 m/s. This creates a Mach wave which propagates at an angle of about 17° from the vertical.8

Figure 9. A finite element simulation using ABAQUS of the acoustic effects of impact pile driving into an elastic sea bottom is shown. The water depth is about 12 m and chosen to match the scenario modeled in Reinhall and Dahl (2011). The y-axis is depth below the water. The x-axis is range in meters. The pressure field is plotted in the water between -4 and +2 kPa. Pressures above 2 kPa are shown in gray and pressures below -4 kPa are shown in black. The magnitude of the particle velocity in sediment is shown between 0 and 0.005 m/s. Particle velocity magnitudes greater 0.005 m/s is shown in gray.9

Figure 10. Locations of the Geophysical Sled 500 meters from wind turbines 3 and 4, the Vertical Hydrophone Arrays at 7.5 and 15 km distance and the Towed Hydrophone Array tracks. 11

Figure 11. A graphic illustrating the equipment used to monitor sounds from pile driving during the construction of the Block Island Wind Farm. 12

Figure 12. The left photo shows the towed array trailing aft of the Research Vessel Shanna Rose and the data collection equipment in the lab of the vessel is shown on the right photo..... 13

Figure 13. (Left) Track lines from September 2, 2015. (Right) Track lines from September 17, 2015. 13

Figure 14. Time series (left) and spectrogram (right) taken from a 30-second file when the vessel was 5.25 km from pile driving of leg A2 on WTG 3 on September 2, 2015 14

Figure 15. Peak to peak received level calculated on all of the hammer strikes from the three different pile driving events plotted over distance of the array from the turbine being worked on..... 15

Figure 16. Kurtosis calculated using September 17, 2015 data, presented as a function of distance from WTG #5..... 15

Figure 17. (Left and Center) Images of the geophysical sled before deployment. These two photos show the tetrahedral array of hydrophones with a spacing of 0.5 m. (Right) photo of the surface floats for the sled with WTG#4 in the background. 16

Figure 18. An underwater photo taken by a GoPro camera mounted on the bow of the sled shows the tetrahedral array of hydrophones is maintained despite the sled landing on its side..... 17

Figure 19. (Left) Spectrogram of data from a single tetrahedral array hydrophone and (Right) acoustic pressure signals on the four channels of the tetrahedral array collected on October 25, 2015. 18

Figure 20. Particle velocity calculated for one hammer strike. Left panel shows the values in mm/s and the right panel shows the magnitude of the total velocity (vector sum) in dB re nm/s..... 18

Figure 21. An example of the particle velocity data (in mm/s in three mutually perpendicular directions) from the 3-axis geophone deployed off the geophysical sled (left panel). Right panel shows the acoustic pressure measured by the hydrophone co-located with the geophone. 19

Figure 22. Particle velocity magnitude of the total velocity (vector sum) in dB re nm/s measured by the geophone (left panel). Right panel shows the magnitude of the total velocity (vector sum) calculated from the tetrahedral array data. Note that the start times (x-axis) are arbitrary.....20

Figure 23. Spectra of the particle velocity (red) and acoustic pressure (blue) measured on the seabed using the co-located geophone and hydrophone. Note that the amplitudes are normalized using the peak values. The difference in frequency content between the hydrophone and geophone response is apparent.20

Figure 24. Spectra of the particle acceleration (black) in the water column estimated using the tetrahedral array (left panel) and measured on the seabed using the geophone (right panel). The acceleration levels are compared with published behavioral audiograms of some fishes. The audiogram data is from: Atlantic salmon (Hawkins & Johnstone, 1978), Plaice & Dab (Chapman and Sand, 1974), Atlantic cod (Chapman & Hawkins, 1973).22

Figure 25. Vertical hydrophone array moorings with SHRUs were deployed at 7.5 and 15 km from the Block Island Wind Farm WTG#323

Figure 26. In the top panel, a signal pile driving event is shown from SHRU 913 deployed at 7.5 km from WTG#3. While some clipping is evident in the high gain hydrophones, the low gain hydrophone shows no clipping.....24

Figure 27. A summary of measurements on September 2 and 15, 2015 for the towed hydrophone array, measurements of the tetrahedral hydrophone array and vertical hydrophone arrays on October 25, 2015. There are significant differences between the sensors even at the same range. It is hypothesized that the varying pile rake causes the difference.25

Figure 28. Fin whale acoustic signals spanning about 20 hours are shown on the top panel. The approach, closest point of approach (CPA) around 10 hours and the departure of the whale are seen. In the bottom right panel, the peak SPL in dB re 1 μ Pa is shown as dots. A CPA range of 500 m and an 8 m/s speed for the whale seems to fit the data well. Source level is about 186 dB re 1 μ Pa at 1 m.27

Figure 29. Transmission loss vs. range for a 20 Hz signal in a waveguide of depth 50 meters and a source depth of 25 m.28

Tables

Table 1.	Locations of the Block Island Wind Farm turbines. (Deepwater Wind, 2017).	6
Table 2.	Pile driving activities and associated monitoring efforts are shown. This report documents the results of the Towed Hydrophone Array led by Marine Acoustics, Inc. and the Geophysical Sled and Vertical Array Moorings led by the University of Rhode Island and Woods Hole Oceanographic Institution. Note that 14 of 16 days when pile driving occurred had acoustic monitoring.....	11
Table 3.	Locations and depths of the acoustic moorings.	12

Overview of Report

This is a report that documents the preliminary findings of the acoustic monitoring of the construction of the Block Island Wind Farm. These measurements include estimates of particle motion obtained using a tetrahedral hydrophone array, acoustic pressure measurements from the same tetrahedral hydrophone array, a towed hydrophone array, two vertical multiple-hydrophone arrays, and a 4-channel geophone array. A preliminary numerical model of the three-dimensional underwater sound propagation in the Block Island Wind Farm area is presented. In addition, analysis of fin whale vocalizations south of Rhode Island that were recorded during the monitoring effort is described.

Many environmental studies have been conducted in Europe in conjunction with pile driving for offshore wind turbine construction. See for example Carstensen et al. (2006), Tougaard et al. (2009), Bailey et al. (2010), and Thompson et al. (2013).

Although the United States can leverage lessons learned from these studies, until recently the lack of construction in U.S. waters has hindered the collection of site and activity specific environmental information unique to eastern U.S. offshore areas. The construction of offshore wind facilities in U.S. Federal and state waters provides an opportunity to collect information to address key questions and improve analyses of the environmental effects of offshore wind development. The Bureau of Ocean Energy Management (BOEM), a part of the U.S. Department of the Interior, established the program entitled Real-Time Opportunity for Development Environmental Observations (RODEO) to study the environmental effects of the Block Island Wind Farm during construction and operational periods. The program managers at BOEM are Drs. Mary Boatman and Stan Labak. The project is managed for BOEM by HDR, Inc. of Athens, Georgia.

A number of wind farms have been proposed in the waters south of New England. The Block Island Wind Farm (BIWF) is the first offshore wind farm in the United States. A study on the potential environmental effects of the wind farm has been reported. (Miller, et al., 2010). The wind farm consists of five 6-MW wind turbines sited about 5 km southeast of Block Island, Rhode Island. The developer of the BIWF is Deepwater Wind and also has plans for a future 200-turbine development between Block Island and Martha's Vineyard.

Construction on the foundations of the BIWF started in the summer and fall of 2015. The five lattice jacket foundations were successfully installed in about 28 meters of water. The RODEO team monitored construction of the foundations for visual impacts, air acoustic impacts, and underwater acoustic impacts during the time period from 2 September 2015 through 6 November 2015. In addition, the team detected vocalizations from fin whales and other marine mammals in both time periods.

This page intentionally left blank.

1. Introduction

1.1 Purpose of the Report

This report describes the preliminary observations of the sound during periods of construction of the Block Island Wind Farm. **Figure 1** shows the locations of the five wind turbines about 3 nm to the southeast of Block Island, Rhode Island.

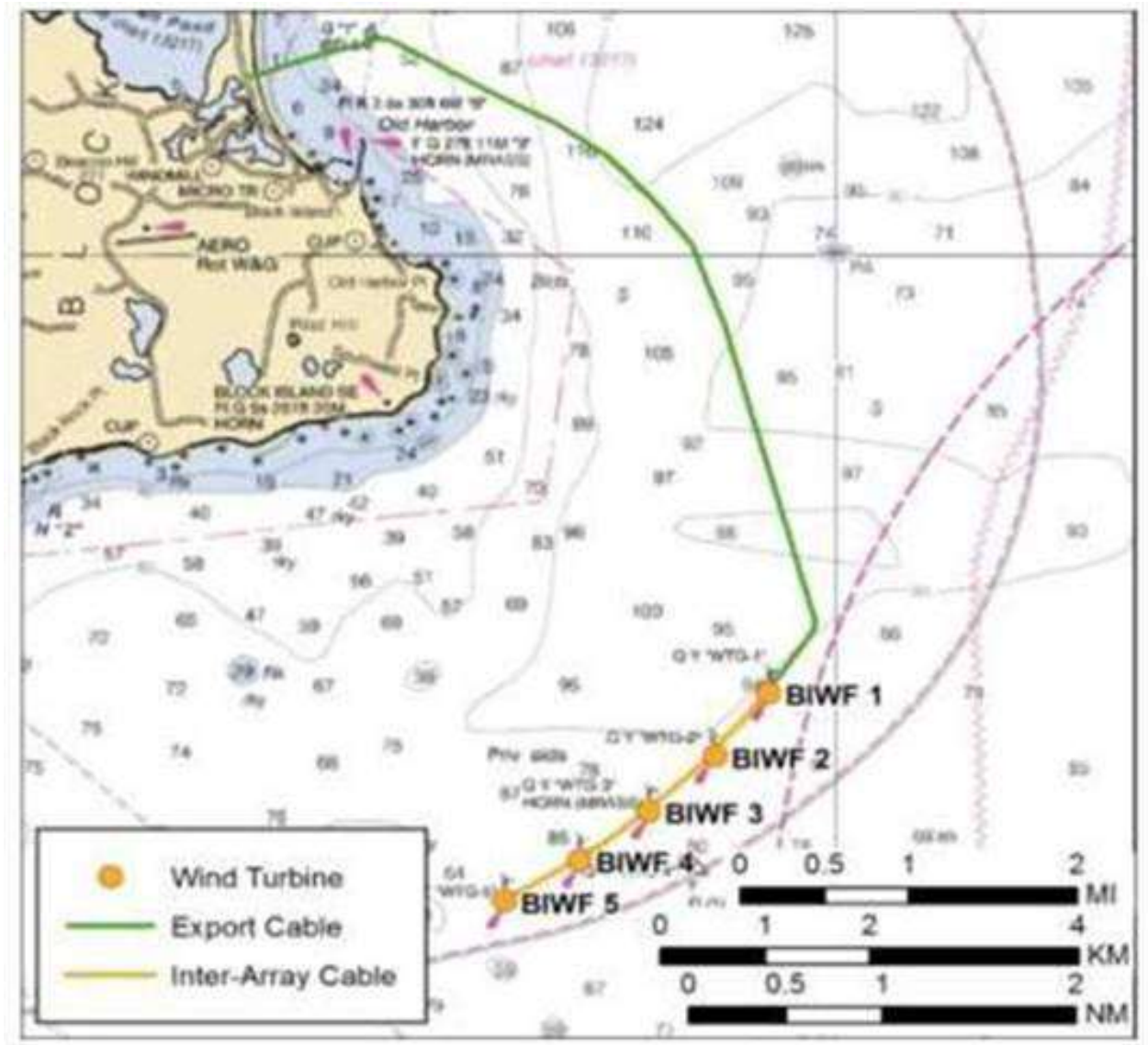


Figure 1. Location of the wind turbines in the Block Island Wind Farm. The soundings are in feet. (Deepwater Wind, 2017)

1.2 Prior Work

There has been a large number of offshore wind farms built in Europe. One of the most useful papers is by Klaus Betke (2004) and his colleagues at ITAP in Oldenburg, Germany. They showed noise from construction and operation of a wind turbine. In particular, they showed the variability of radiated noise from the turbine with various power production levels and wind speeds at shown in **Figure 2**.

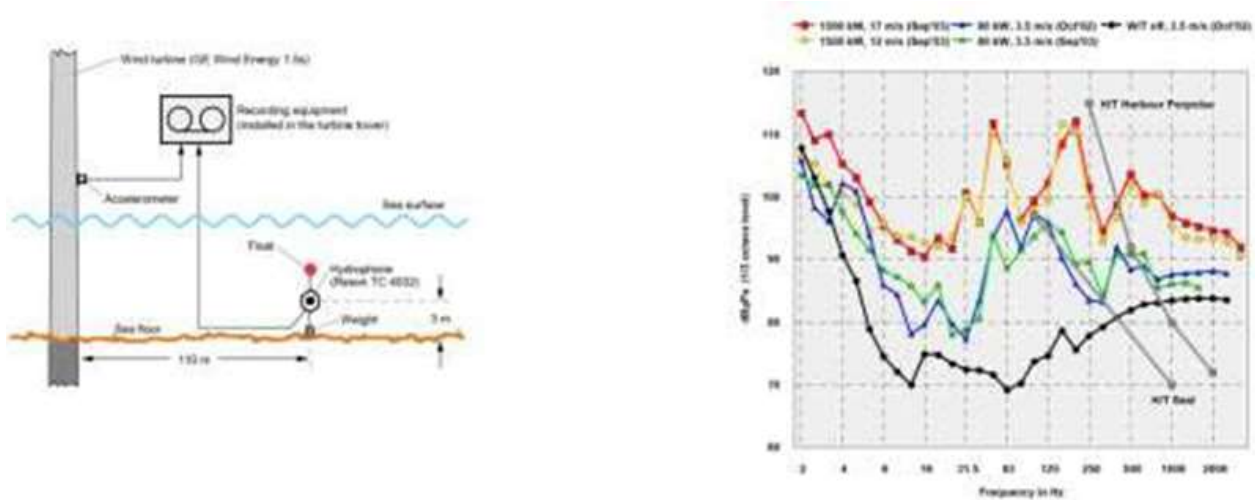


Figure 2. On the left, the measurement setup as described by Betke (2004) for monitoring underwater noise from an offshore wind turbine in water 10 m deep. On the right, the 1/3-octave band levels measured 110 m from the turbine for different operating conditions. Wind speeds are measured at the hub height.

The data from the Betke et al. (2004) report was used to predict the operational noise from the five wind turbines of the Block Island Wind Farm. The results of that study can be found in the Ocean Special Area Management Plan (OSAMP, 2008) and in Miller, et al. (2010).

1.3 Site Description

The site for the Block Island Wind Farm is shown in **Figure 1**. The five turbines are sited in an arc approximately 3 nm south of Block Island, Rhode Island. The geology of the site is complicated due to the debris collected by the Wisconsin Glacier and deposited 20,000 years ago. **Figure 3** shows the extent of the glaciation. The sediment consists of heterogeneous over-consolidated gravels, sands, silts, clays, cobbles, and boulders as illustrated by the photo of Mohegan Bluffs on the south side of Block Island as shown in **Figure 4**.

The bathymetry in the area of the BIWF is shown in **Figure 5**.

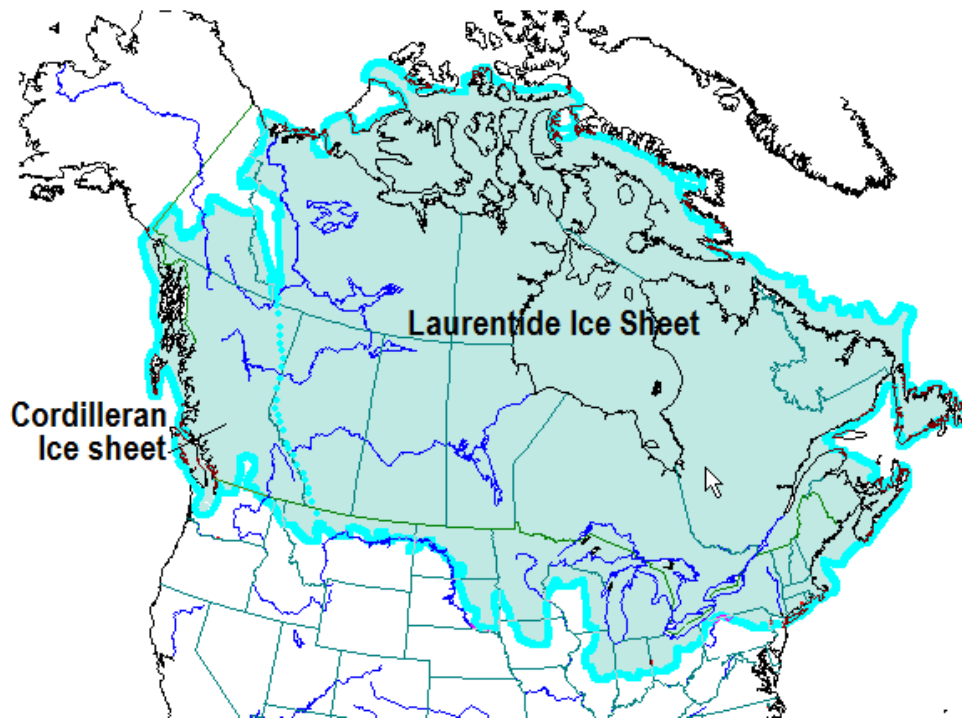


Figure 3. The Laurentide Ice Sheet and the Wisconsinan Glacier is shown overlying North America. The marine geology of the wind farm site near Block Island, Rhode Island is dominated by debris left from the glaciation.



Figure 4. A photo of Mohegan Bluffs on the south side of Block Island illustrates the geology of the area where the sediment consists of heterogeneous over-consolidated gravels, sands, silts, clays, cobbles, and boulders.

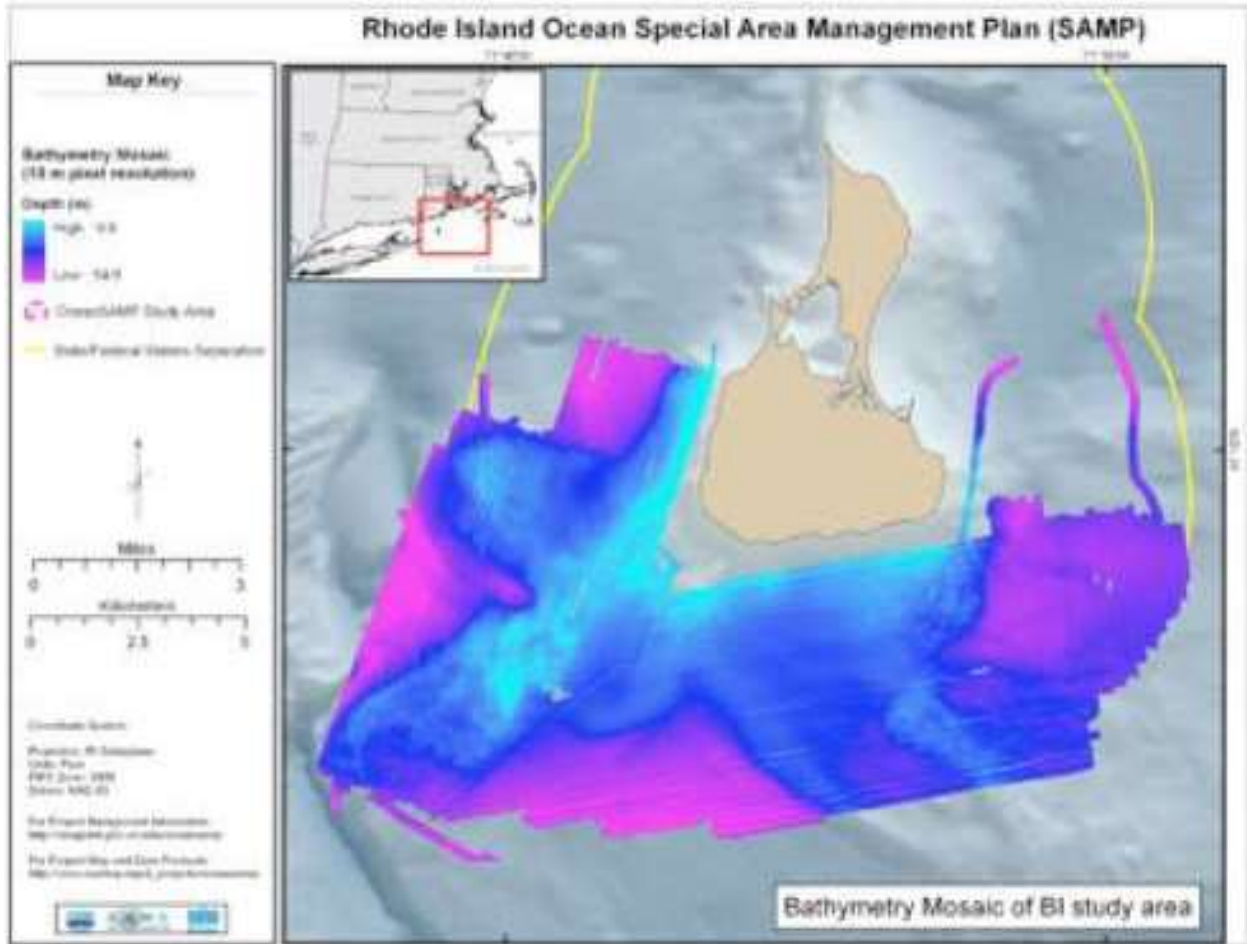


Figure 5. Bathymetry in the area of Block Island.

1.4 Foundation Description

The wind turbine locations are given in **Table 1** and an aerial view is shown in **Figure 6**.

Table 1. Locations of the Block Island Wind Farm turbines. (Deepwater Wind, 2017).

ID	Latitude	Longitude
BIWF 1	41°7.546' N	71°30.451' W
BIWF 2	41°7.193' N	71°30.837' W
BIWF 3	41°6.883' N	71°31.270' W
BIWF 4	41°6.609' N	71°31.744' W
BIWF 5	41°6.380' N	71°31.258' W



Figure 6. An aerial view of the Block Island Wind Farm and Block Island. The numbers refer to the ID numbers from Table 1.

Each Wind Turbine Generator (WTG) is attached to the seafloor using a four-leg jacket foundation secured with four through-the-leg foundation piles. The jackets consist of hollow steel tubular members joined together in a lattice structure, which sit on the seabed supporting the WTG. The diameter of each pile is 50 in. (127 cm), with a maximum wall thickness of 1.5 in (3.8 cm). The foundation piles were inserted into the legs and driven to a depth of up to 250 ft (76.2 m) below the mudline. The piles were driven at an angle of 13.27° with the vertical. This is shown in **Figure 7**.



Figure 7. One of the foundations of the Block Island Wind Farm is shown to the right of the Lift Barge Robert.

Pile driving operations carried out in 2015 to insert the piles into the seabed generated intense impulsive sound that radiated into the surrounding air, water and sediment. Our team deployed

a number of instruments to monitor this noise at several locations from 500 m to 15 km from the pile driving.

1.5 Turbine Description

The turbines used in the Block Island Wind Farm are five GE Haliade 150-6MW wind turbines each with a 150 m diameter blades. The turbines are equipped with a direct drive permanent magnet generator, with no gearbox coupled to the generator. The turbines are of variable speed and each blade has independent pitch control. The cut-in wind speed is 3 m/s. The cut-out wind speed is 25 m/s averaged over 10 minutes.

1.6 Modeling Pile Driving

Reinhall and Dahl (2011) have done modeling and measurement of vertical pile driving. When the hammer strikes the pile, a compression wave produces a local radial deformation due to Poisson's effect. This radial deformation propagates down the pile. The speed of the wave in the steel shell of the pile that is surrounded by water is about 5015 m/s and much greater than water sound speed of 1500 m/s. The pile driving creates a Mach wave in the water and sediment with angle of 17° with vertical. See **Figure 8**.

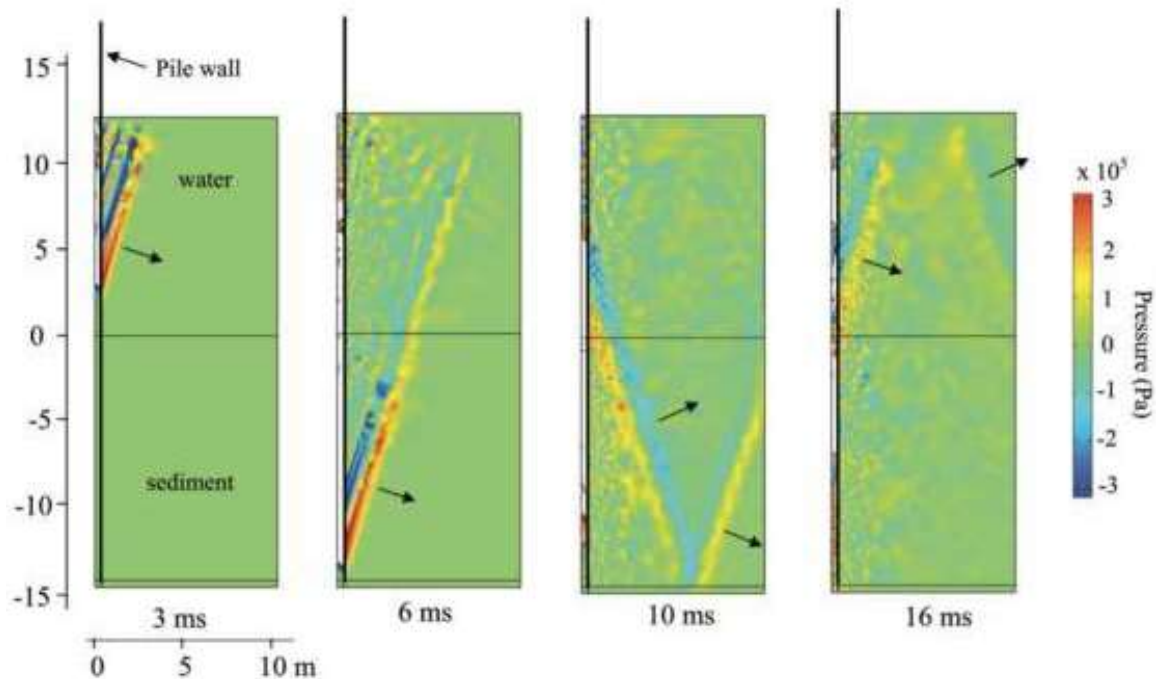


Figure 8. Reinhall Dahl (2011) modeled the creation of an acoustic wave in the water from a vertical pile. The speed of the compressional wave in the pile is about 5015 m/s and much greater than the water sound speed of about 1500 m/s. This creates a Mach wave which propagates at an angle of about 17° from the vertical.

Kim et al (2013) and Kim (2014) modeled the effect of the pile driving in an elastic seabed. The higher the angle of the Mach wave, the more energy is absorbed by the seafloor. But the Block Island Wind Farm piles are not vertical but are raked at an angle of 13.27° . Acoustic energy will be very dependent on direction and 3-dimensional modeling of that effect is ongoing in

collaboration with Sandia National Laboratory. **Figure 9** shows Kim's results and the resultant compressional wave in the water and the bottom, shear wave in the bottom and interface wave at the seafloor.

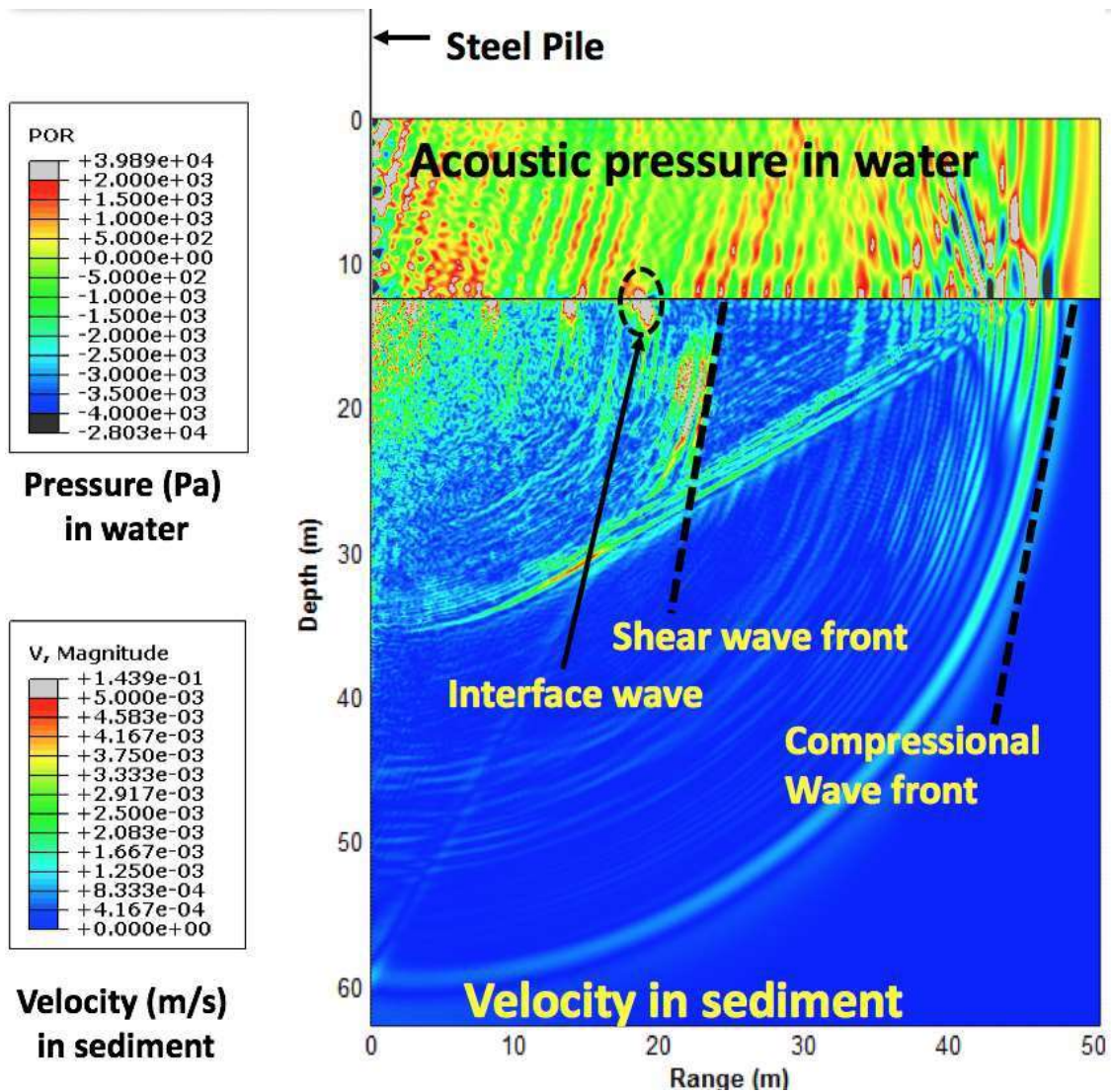


Figure 9. A finite element simulation using ABAQUS of the acoustic effects of impact pile driving into an elastic sea bottom is shown. The water depth is about 12 m and chosen to match the scenario modeled in Reinhall and Dahl (2011). The y-axis is depth below the water. The x-axis is range in meters. The pressure field is plotted in the water between -4 and +2 kPa. Pressures above 2 kPa are shown in gray and pressures below -4 kPa are shown in black. The magnitude of the particle velocity in sediment is shown between 0 and 0.005 m/s. Particle velocity magnitudes greater than 0.005 m/s is shown in gray.

This page intentionally left blank.

2. Monitoring Construction of the Block Island Wind Farm

Construction on the Block Island Wind Farm was conducted in the summer and fall of 2015.

Table 2 shows the days in which pile driving occurred and the various monitoring efforts. **Table 3** shows the location and depths of moorings. This report documents the results of the Towed Hydrophone Array led by Marine Acoustics, Inc. and the Geophysical Sled and Vertical Array Moorings led by the University of Rhode Island and Woods Hole Oceanographic Institution.

Table 2. Pile driving activities and associated monitoring efforts are shown. This report documents the results of the Towed Hydrophone Array led by Marine Acoustics, Inc. and the Geophysical Sled and Vertical Array Moorings led by the University of Rhode Island and Woods Hole Oceanographic Institution. Note that 14 of 16 days when pile driving occurred had acoustic monitoring.

Activity	Lead Organization	18-Aug-15	30-Aug-15	1-Sep-15	2-Sep-15	3-Sep-15	17-Sep-15	18-Sep-15	19-Sep-15	1-Sep-15	10-Oct-15	12-Oct-15	17-Oct-15	19-Oct-15	21-Oct-15	25-Oct-15	26-Oct-15	
		X	X	X	X	X	X	X	X	X	X	X	X	X	X	X	X	X
Pile driving	Deepwater Wind	X	X	X	X	X	X	X	X	X	X	X	X	X	X	X	X	X
Towed Hydrophone Array	MAI				✓		✓											
Geophysical Sled/Moorings	URI/WHOI											✓	✓	✓	✓	✓	✓	
Hydrophones	Subacoustech	✓	✓				✓	✓	✓	✓								
Hydrophones	Tetrattech		✓	✓	✓			✓	✓			✓	✓	✓	✓	✓	✓	✓

Figure 10 shows the locations of the Geophysical Sled, the Vertical Array Moorings and the tracks of the Towed Hydrophone Array.



Figure 10. Locations of the Geophysical Sled 500 meters from wind turbines 3 and 4, the Vertical Hydrophone Arrays at 7.5 and 15 km distance and the Towed Hydrophone Array tracks.

Table 3. Locations and depths of the acoustic moorings.

Mooring	Latitude (Degrees N)	Longitude (Degrees W)	Depth (m)
Geophone 917	41.1110	71.5225	26
Tetrahedral 918	41.1110	71.5225	26
SHRU 913	41.0127	71.4044	40
SHRU 919	41.0664	71.4590	41

Figure 11 shows a graphic illustrating the equipment and positions used to monitor the sound from pile driving during the construction of the BIWF. A geophysical sled with tetrahedral hydrophone array was placed 500 meters from WTG#3 and WTG#4. A towed hydrophone array was used to monitor the sound from about 1 km from the pile driving out to about 7.5 km. Two vertical hydrophone arrays were placed at 7.5 and 15 km from the wind farm. In addition to these systems, Subacoustech Environmental, LTD of the UK deployed hydrophones and particle velocity sensors at various positions around the wind farm and those results are described in a separate document.

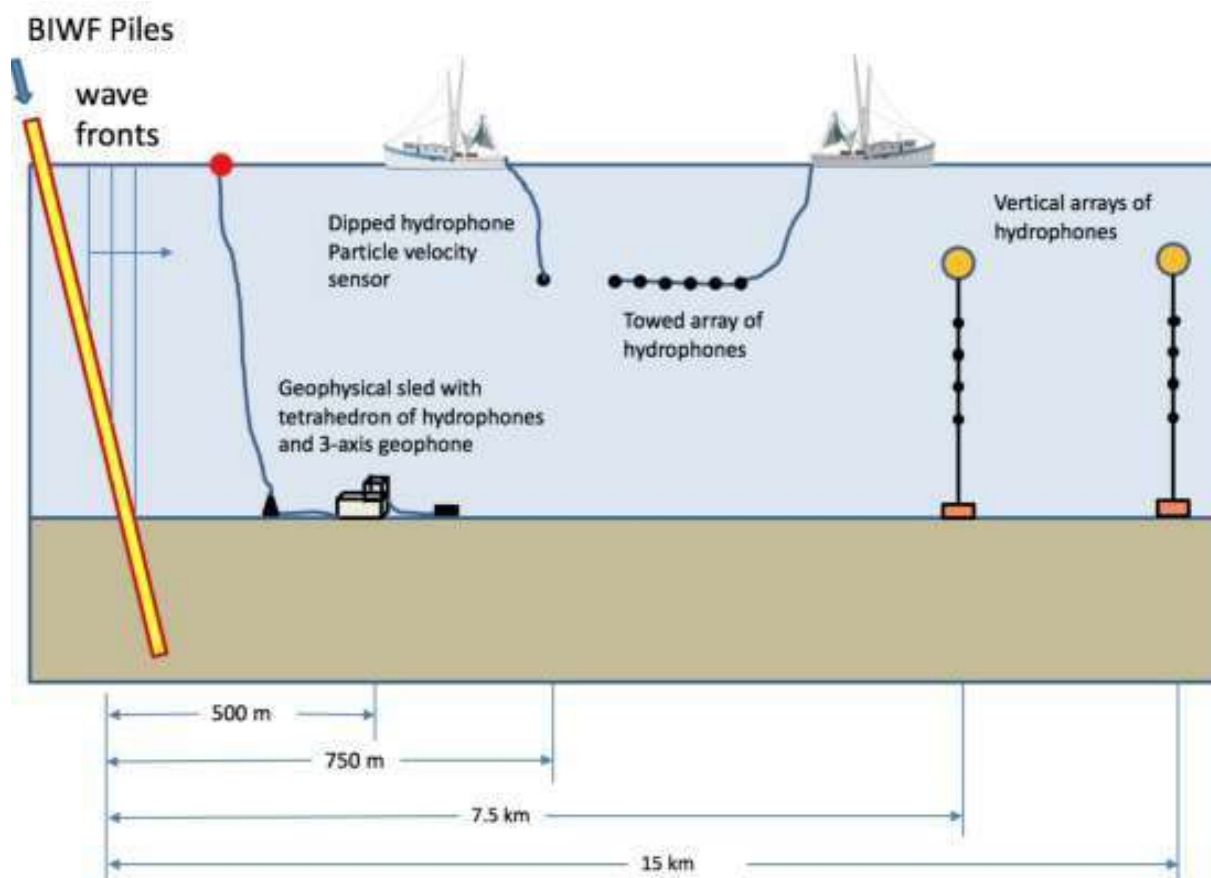


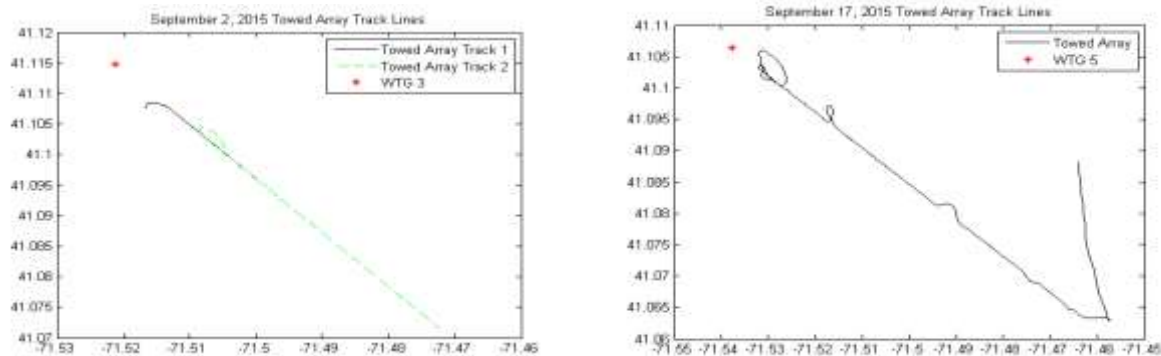
Figure 11. A graphic illustrating the equipment used to monitor sounds from pile driving during the construction of the Block Island Wind Farm.

2.1 Towed Hydrophone Array Results

On September 2, 2015, the towed array system recorded two separate pile-driving events on WTG #3 (**Figure 12**). The first event was the piling of the P1 segment of the B2 leg and the second event was the piling of the P1 segment of the A2 leg. The array was towed along a track, at ranges from 1 km out to 6 km from the piles. On September 17, 2015, the towed array system recorded the pile driving sounds of the P1 segment of leg A1 on WTG #5 from a range of 1 km out to 8 km from the pile. The tracks (**Figure 13**) on both days were in a southeast direction from the WTG location.



Figure 12. The left photo shows the towed array trailing aft of the Research Vessel Shanna Rose and the data collection equipment in the lab of the vessel is shown on the right photo.



Note: Track 1 relates to the first pile driving event on this day and Track 2 relates to the second event. Decimal degrees of latitude and longitude correspond to the vertical and horizontal axes respectively.

Figure 13. (Left) Track lines from September 2, 2015. (Right) Track lines from September 17, 2015.

Data were monitored in real-time using Raven 1.5 and recorded as consecutive 30 second duration files that were later processed on shore. On the first pile driving day 145 data files were collected, a total of 4.08 GB of data. On the second pile driving day 342 files were collected, culminating in 9.76 GB of data. Representative time series and spectrogram displays in **Figure 14** show a series of hammer strikes recorded 5.25 km from leg A2 on WTG #3 on

September 2, 2015. The majority of the energy in the hammer strikes is below 5 kHz and the signal to noise ratio is high.

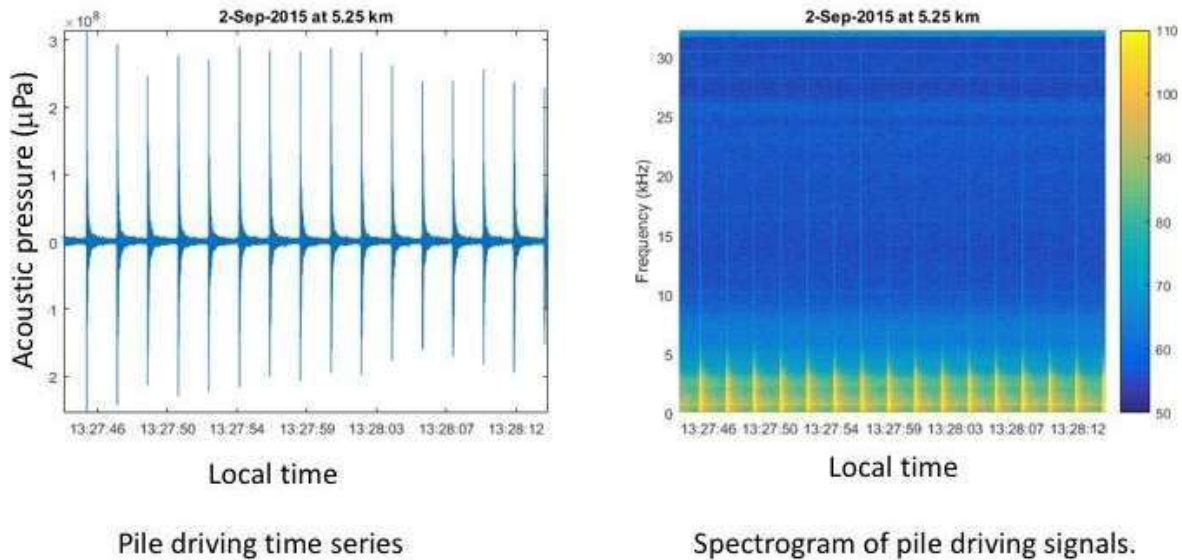


Figure 14. Time series (left) and spectrogram (right) taken from a 30-second file when the vessel was 5.25 km from pile driving of leg A2 on WTG 3 on September 2, 2015

The peak-to-peak received sound pressure level (SPL) and kurtosis values were determined for each hammer strike. These metrics were plotted against range to examine how the values changed with distance from the pile driving location. Each pile driving event was analyzed separately and then compared.

Post event analysis revealed that all channels on the hydrophone array functioned as expected and collected data for the entire deployment. **Figure 15** presents the preliminary calculations of the peak to peak received level for all of the hammer strikes from the three pile driving events. **Figure 16** presents the preliminary calculations of kurtosis for the pile driving of segment P1 on leg A1 from WTG#5 that was recorded on September 17, 2015. The trend toward decreased kurtosis with range is suggestive that this metric can be applied successfully to field data to better characterize the temporal nature of the received signals. However, further analyses and replication are needed. All of the analysis presented is preliminary and still in the working phase. Updated and finalized results will be presented in a peer reviewed paper that will be released at a future date. Please consult with the authors of this report before utilizing these calculations or for any comments or questions related to this analysis.

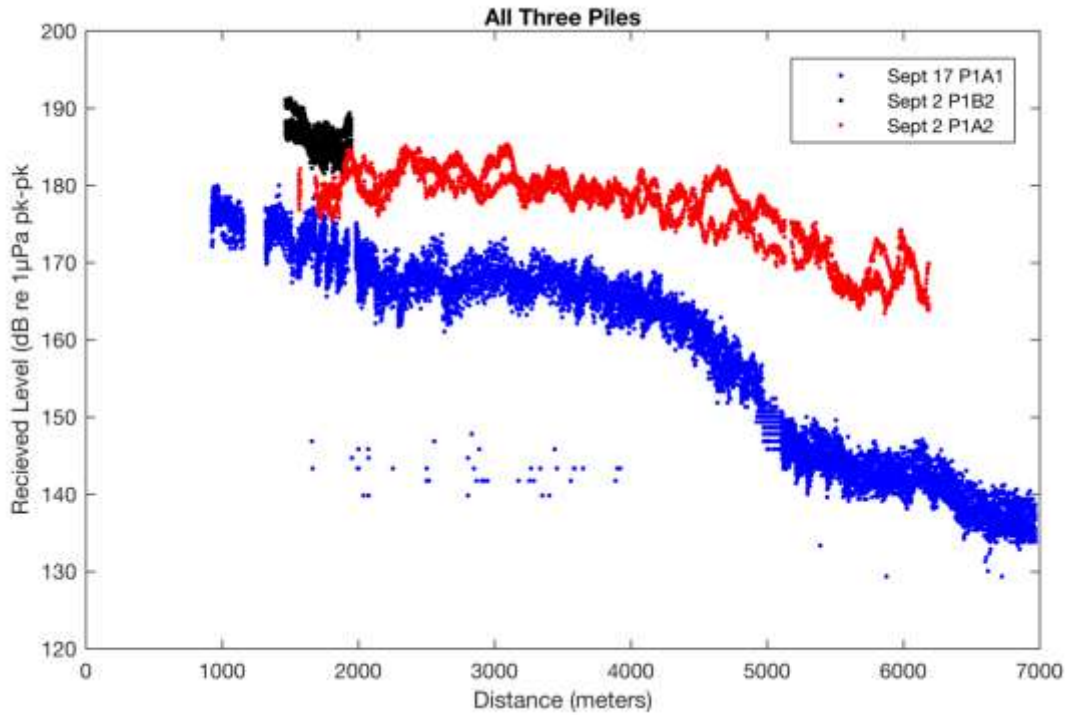


Figure 15. Peak to peak received level calculated on all of the hammer strikes from the three different pile driving events plotted over distance of the array from the turbine being worked on.

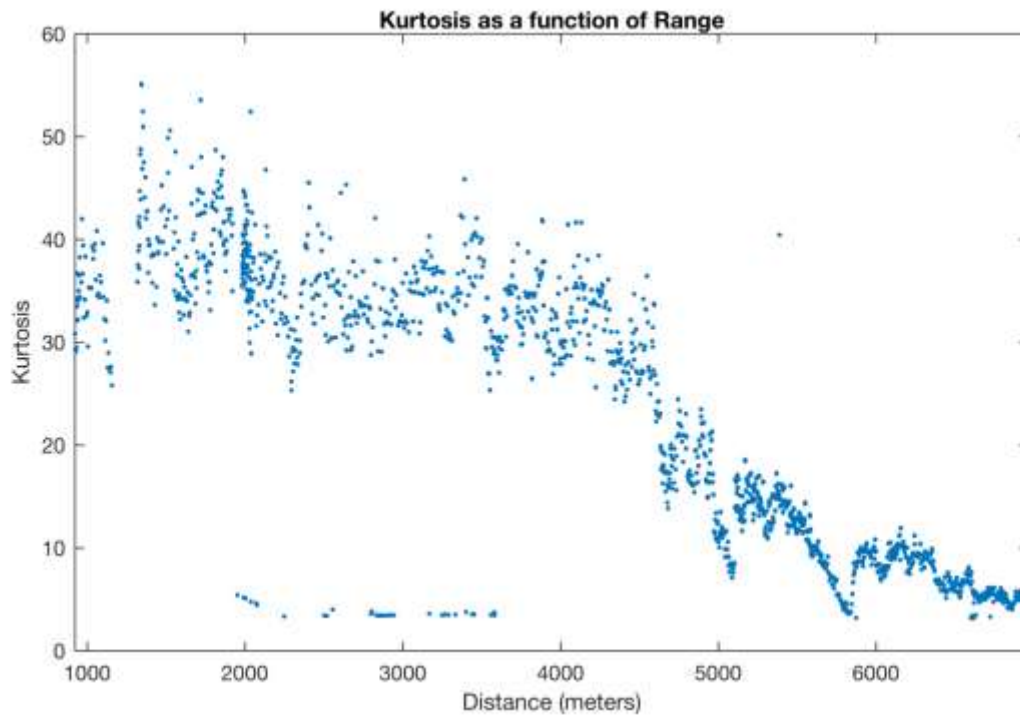


Figure 16. Kurtosis calculated using September 17, 2015 data, presented as a function of distance from WTG #5.

2.2 Preliminary Results for the Geophysical Sled

A geophysical sled with a 4-hydrophone tetrahedral array (for measurement of acoustic pressure and particle velocity) and a 3-axis geophone with low sensitivity hydrophone (for the measurement of sediment motion and acoustic pressure on the seabed) was deployed about 500 meters from WTG #3 and #4 at $41^{\circ} 6' 39.7152''$ N latitude $71^{\circ} 31' 21.0258''$ W longitude in about 26 meters of water. On the right in **Figure 17** is a photo of the surface floats for the sled with WTG#4 under construction in the background. The leftmost and center photos in **Figure 17** are pictures of the sled before deployment. These photos show the tetrahedral array of hydrophones with a spacing of 0.5 m.



Figure 17. (Left and Center) Images of the geophysical sled before deployment. These two photos show the tetrahedral array of hydrophones with a spacing of 0.5 m. (Right) photo of the surface floats for the sled with WTG#4 in the background.

When the sled was deployed, it landed on its side as shown in **Figure 18**. However, the photo taken by a GoPro camera mounted on the bow of the sled showed that the hydrophone array maintained its tetrahedral shape.

2.2.1 Tetrahedral Array Results

The geophysical sled has a four-hydrophone tetrahedral array installed for the estimation of acoustic particle velocity near the seabed. An example spectrogram of the data collected on one of the channels of the tetrahedral array is shown in the left panel of **Figure 18**. The x-axis for both plots is referenced to an arbitrary start time. The peak-to-peak received SPL for these signals was approximately 185 dB re 1 μ Pa. The array was deployed about 500 m from WTG #3 and #4 in approximately 26 m of water. Pile-driving signals from October 25 from all four hydrophones of the tetrahedral array are shown in the right panel. Data from tetrahedral array 500 meters from pile driving is be used to calculate particle velocity for fish studies. (Potty et al, 2017).

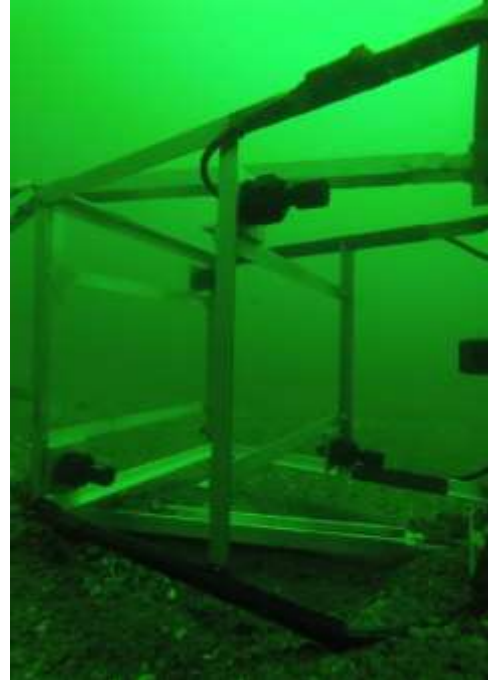


Figure 18. An underwater photo taken by a GoPro camera mounted on the bow of the sled shows the tetrahedral array of hydrophones is maintained despite the sled landing on its side.

As noted earlier, for the hammer strike data shown in **Figure 19**, the peak-to-peak received SPL at the sled was found to be about 185 dB re 1 μ Pa. Assuming spherical spreading, source level of the pile driving signal was estimated to be about 239 dB re 1 μ Pa at 1 m. The acoustic particle accelerations can be computed from the gradient of the acoustic pressures using the following:

$$-\nabla p = \rho \frac{\partial \bar{u}}{\partial t}$$

p acoustic pressure

\bar{u} acoustic particle velocity

ρ density

The particle velocity can be calculated from the above Equation by numerically integrating the particle accelerations. An example of the particle acceleration and velocity calculated for a hammer strike event is shown in **Figure 20**.

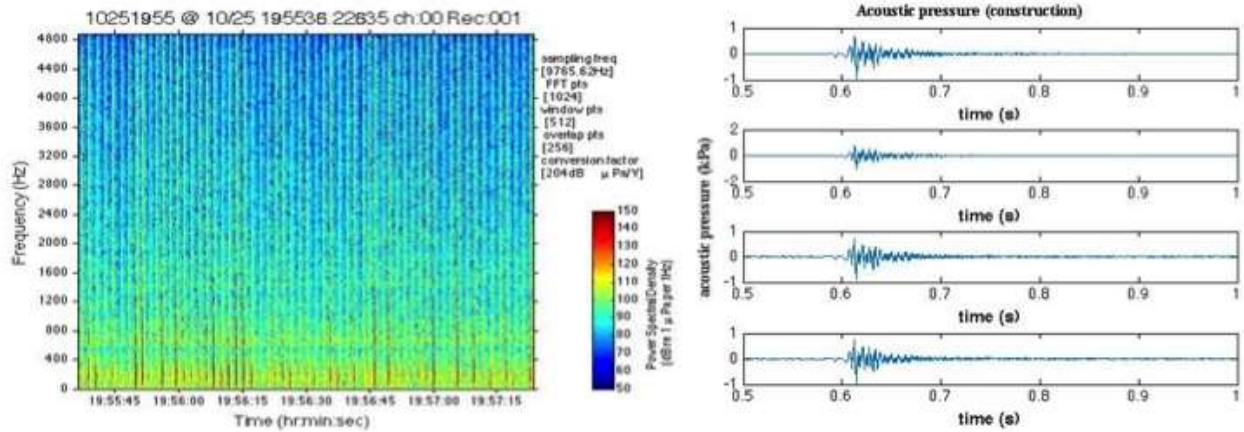


Figure 19. (Left) Spectrogram of data from a single tetrahedral array hydrophone and (Right) acoustic pressure signals on the four channels of the tetrahedral array collected on October 25, 2015.

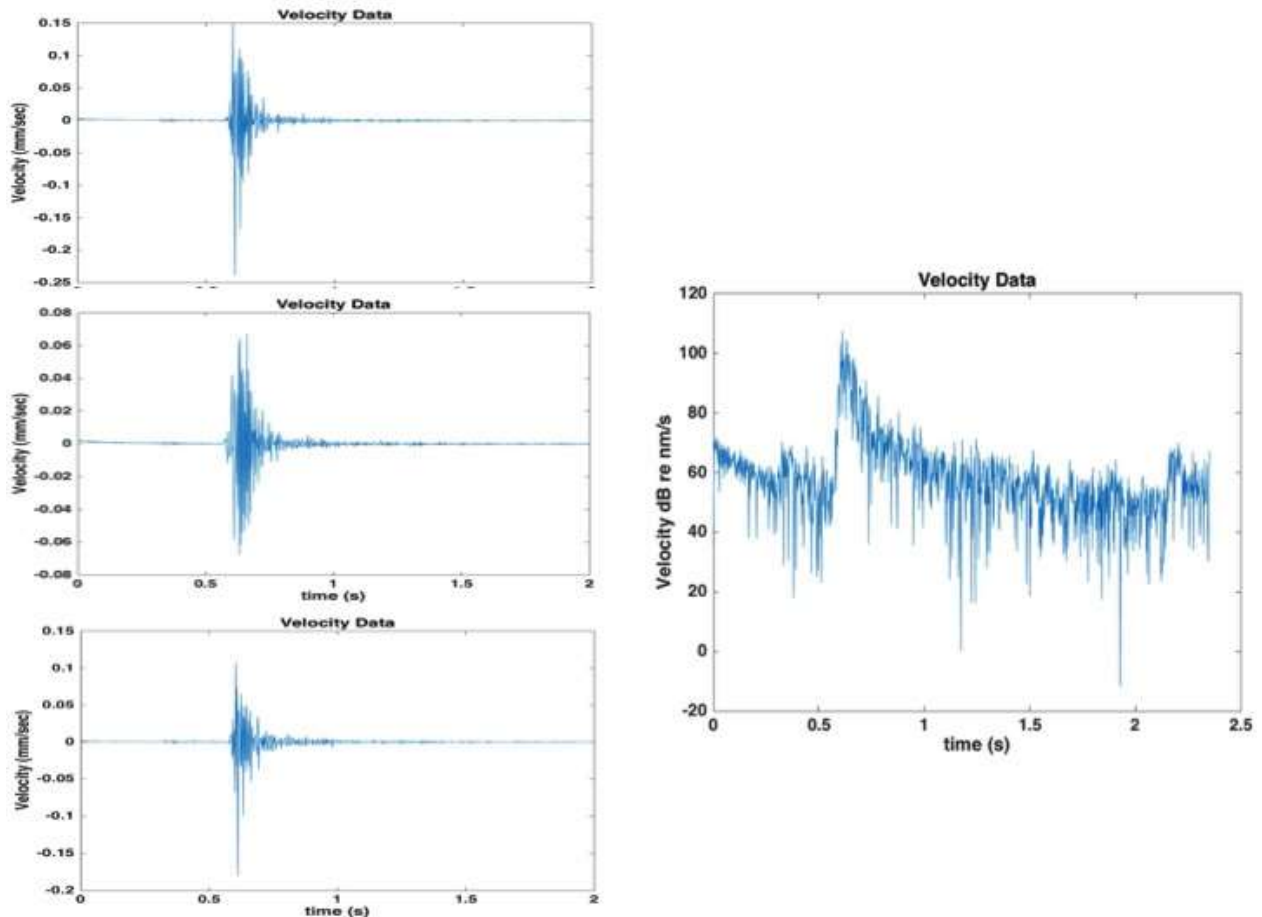


Figure 20. Particle velocity calculated for one hammer strike. Left panel shows the values in mm/s and the right panel shows the magnitude of the total velocity (vector sum) in dB re nm/s

2.2.2 Geophone Results

An example of the data from the 3-axis geophone deployed off the geophysical sled is shown in **Figure 21**. The figure shows the particle velocity along vertical and two horizontal directions (left panel) and pressure (right panel) generated by a single impact pile driving at a range of 500 meters from WTG #3 and #4. This data was recorded on October 25, 2015 around 2:58 UTC. The seismic signals from the pile driving had very high signal-to-noise ratio, no clipping, and the time series has complexity that may be ascribed to the pile driving mechanisms. The velocities are shown in mm/sec and the pressure in kPa. The peak – to – peak sound pressure levels are comparable to the levels measured (described previously) in the hydrophones in the tetrahedral array. The velocity magnitudes are higher compared to values calculated using the tetrahedral array data. This will be discussed later in this Section.

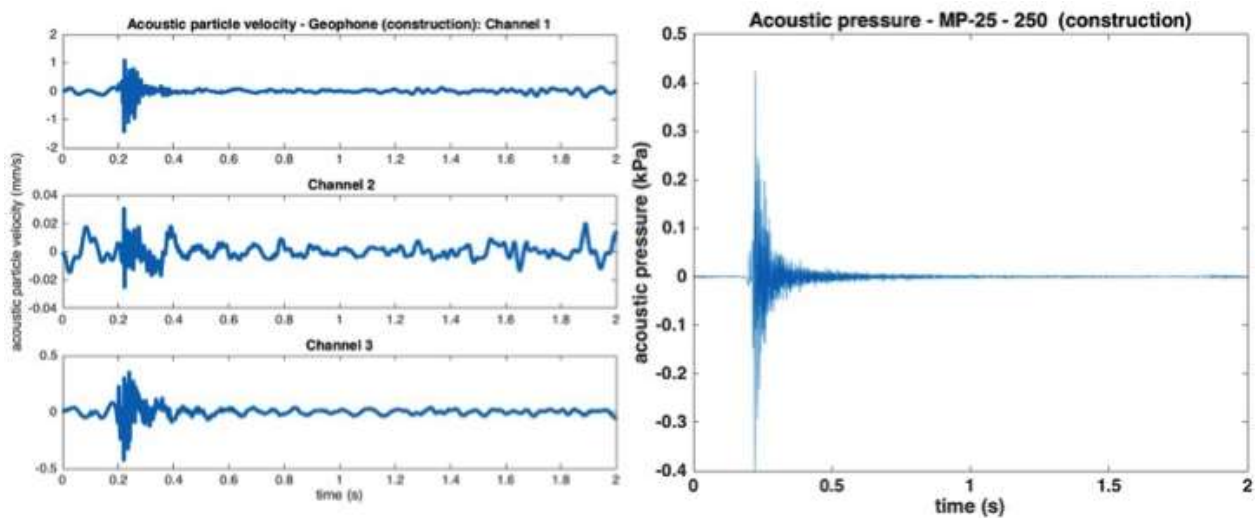


Figure 21. An example of the particle velocity data (in mm/s in three mutually perpendicular directions) from the 3-axis geophone deployed off the geophysical sled (left panel). Right panel shows the acoustic pressure measured by the hydrophone co-located with the geophone.

Figure 22 shows the particle velocities magnitude of the total velocity (vector sum) in dB re nm/s measured at the seabed using the geophone (left panel). Right panel shows the particle velocity in the water column (same units), 1 m from the seabed, calculated using the tetrahedral array data. There is a ~10 dB difference in peak velocities (dB re nm/s). The spectral distribution of the energy in the geophone and co-located hydrophone is shown in **Figure 23**. The difference in frequency content between the hydrophone and geophone response is apparent in the figure. This indicates that the response of the geophone and hydrophone are possibly dominated by different wave types. The geophones measure the ground motions whereas the tetrahedral array measures the particle velocities above the ground in the water column (approximately 1 m from the bottom). The hydrophone measures the compressional waves in the water whereas the geophone measures shear and interface (Scholte) waves in addition to compressional waves. Particle motions produced by interface waves (Scholte waves) are likely to dominate the geophone signal. These motions decay exponentially away from the interface (seabed). Previous studies have shown that signals recorded on seismic sensors on the seafloor are found to be more complicated than on co-located hydrophones (Bibee, 1991). The

differences were attributed to the response of the seismometer sensors to shear waves in the seafloor and interface waves at the water-sediment boundary. We hypothesize that differences between particle velocities measured at the bottom and in the water column can be different since shear and interface waves can contribute (in addition to compressional waves) in the sediment medium as opposed to compressional waves alone in the water medium.

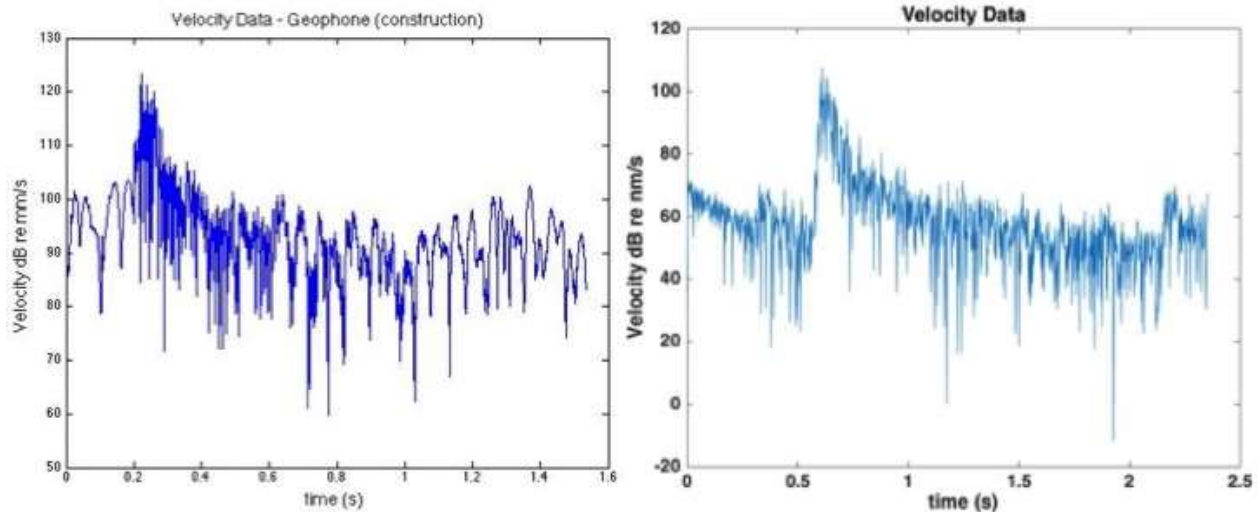


Figure 22. Particle velocity magnitude of the total velocity (vector sum) in dB re nm/s measured by the geophone (left panel). Right panel shows the magnitude of the total velocity (vector sum) calculated from the tetrahedral array data. Note that the start times (x-axis) are arbitrary.

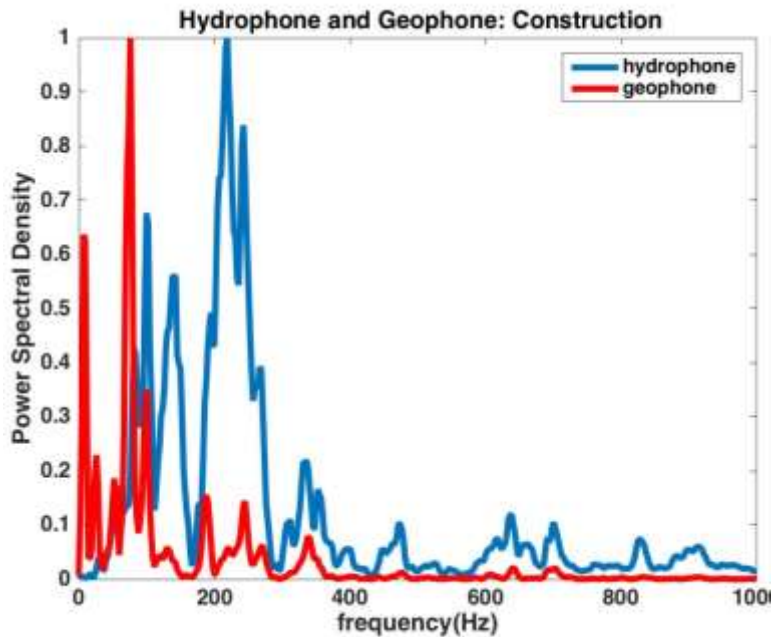


Figure 23. Spectra of the particle velocity (red) and acoustic pressure (blue) measured on the seabed using the co-located geophone and hydrophone. Note that the amplitudes are normalized using the peak values. The difference in frequency content between the hydrophone and geophone response is apparent.

2.2.3 Fish Hearing and Effect of Noise and Particle Motion

Fishes show extensive variability in their behavior, ecology, and physiology. Moreover, fishes vary in their abilities to detect and utilize sounds, and very likely also vary in their potential susceptibility to damage by sound. Particle motion plays a very important role in the fish sensory mechanism. Auditory portions of the fish ears are the “otolithic organs”. Each otolithic organ consists of a dense calcareous mass contacting a sensory epithelium. Otolithic organs of all fishes respond to particle motion of the surrounding fluid. Many fishes are also able to detect sound pressure via the gas bladder or other gas-filled structures that re-radiate energy, in the form of particle motion, to the otolithic organs. Fish with gas-filled structures near the ear and/or extensions of the swim bladder respond to fluctuating sound pressure, generating particle motion. The ability to detect sound pressure in addition to particle motion serves to increase hearing sensitivity and broaden the hearing bandwidth. Hence, fishes with gas filled structures have lower sound pressure thresholds and wider frequency ranges of hearing than do the purely particle motion sensitive species.

Hearing range and sensitivity varies considerably among species. Behavioral audiograms have been published for only a few species of fish and there are concerns about the usefulness of many of these. This is due to poorly monitored acoustic conditions and difficulty in determining whether the fish were responding to sound pressure or particle motion. Noise can result in the audiograms being masked so that the full hearing sensitivity of the animal cannot be determined. Auditory evoked potentials may not fully reflect the hearing capabilities of animals - do not include signal processing by the brain. (Popper et al., 2014).

There are no standards that exist which specify the criteria for mortality, injury and behavioral changes when fishes are exposed to sound. The technical report prepared by ANSI-Accredited Standards Committee S3/SC1 (Popper et al., 2014) provides some very useful sound exposure guidelines for fishes and sea turtles. The guidelines for acoustic pressure exposure specify the maximum peak levels as 213 dB_{peak} (fish without swim bladder) and 207 dB_{peak} (other types fishes) to avoid mortality and recoverable injury. The peak sound pressure levels measured in this study at 500 m are less than that will cause mortality or injury as per this guideline.

Figure 24 compares particle accelerations calculated from measurements with published behavioral audiograms for some of the fishes. The behavior audiograms shown in the figure are from: Atlantic salmon (Hawkins and Johnstone, 1978), Plaice and Dab (Chapman and Sand, 1974), Atlantic cod (Chapman and Hawkins, 1973). The left panel shows the frequency distribution of particle acceleration calculated using the tetrahedral array data and the right panel shows the geophone data. Particle accelerations are shown in dB re 1 $\mu\text{m}/\text{s}^2$.

Particle acceleration levels in water (left panel in **Figure 24**) are slightly above the behavioral sensitivity for the fishes considered in the frequency range 30 to 300 Hz. Hence, fishes may barely ‘feel’ the particle motion during construction at 500 m range. Note that the particle velocity levels measured on the seabed (right panel in **Figure 24**) are well above the behavioral sensitivity for all fishes shown in the figure up to a frequency of approximately 300 Hz. Based on the data it appears that the impact of construction will be more pronounced on fishes whose habitat is close to the seabed compared to fishes who spend most of their time in the water away from the seabed.

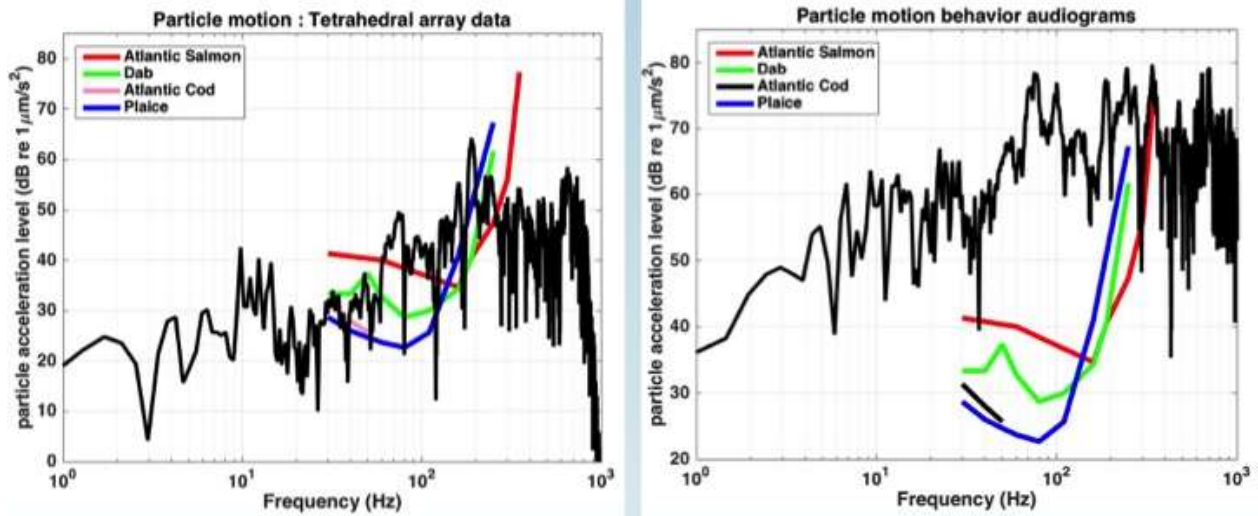


Figure 24. Spectra of the particle acceleration (black) in the water column estimated using the tetrahedral array (left panel) and measured on the seabed using the geophone (right panel). The acceleration levels are compared with published behavioral audiograms of some fishes. The audiogram data is from: Atlantic salmon (Hawkins & Johnstone, 1978), Plaice & Dab (Chapman and Sand, 1974), Atlantic cod (Chapman & Hawkins, 1973).

2.3 Vertical Hydrophone Array Results

Two vertical hydrophone array moorings with SHRUs (Several Hydrophone Receiving Units) were deployed at 7.5 and 15 km from the BIWF. The mooring configuration is shown in **Figure 25**. The top and third hydrophones had a normal gain of 26 dB while the second and bottom phones had a lower gain of 6 dB. The different gains were used to assure that the peak pressure from the pile driving would not clip the received signals.

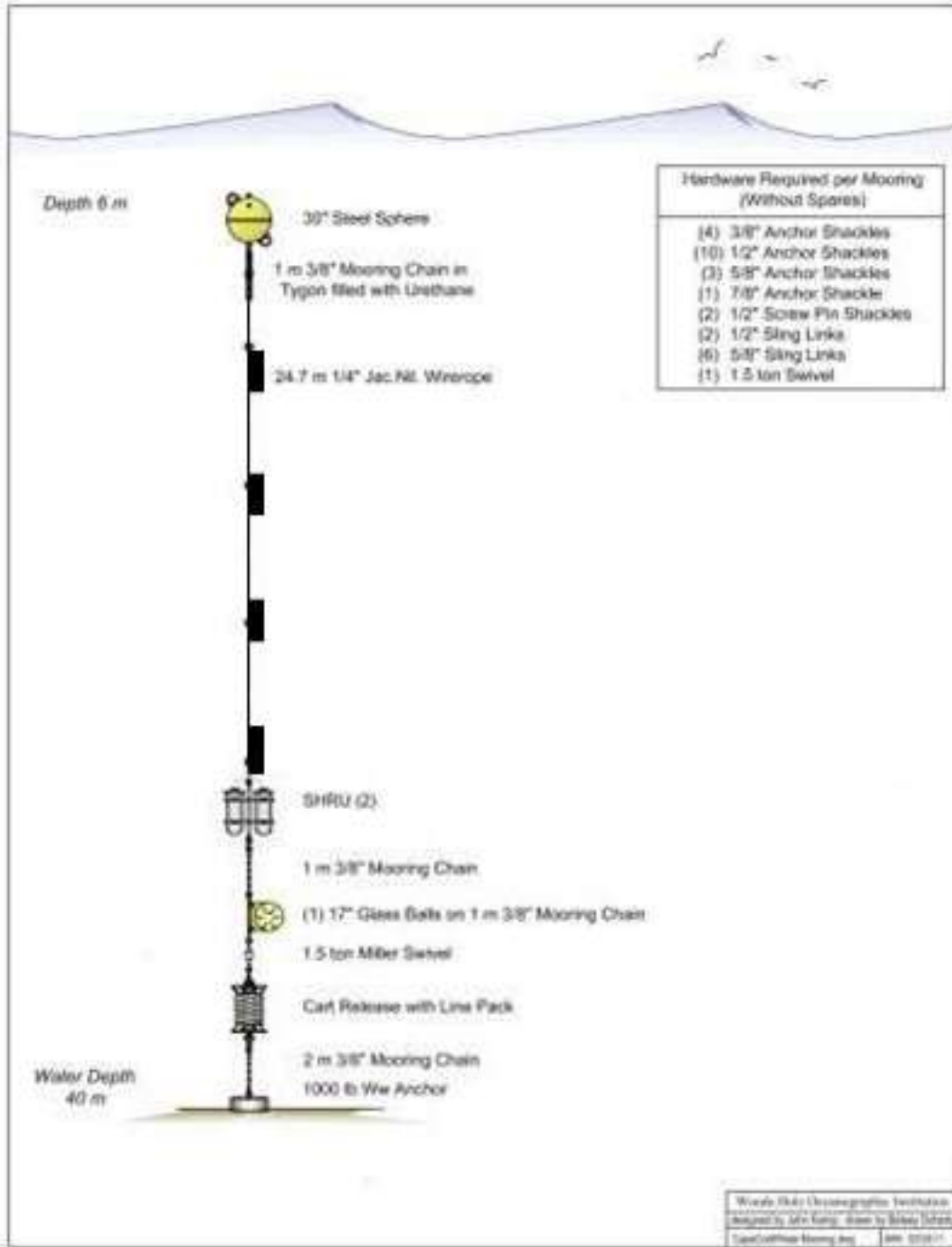


Figure 25. Vertical hydrophone array moorings with SHRUs were deployed at 7.5 and 15 km from the Block Island Wind Farm WTG#3

An example time series of the acoustic pile driving signal is shown in **Figure 26**. In the top panel, a single pile driving event is shown from SHRU 913 deployed at 7.5 km from WTG#3. While some clipping is evident in the high gain hydrophones, the low gain hydrophone shows no clipping.

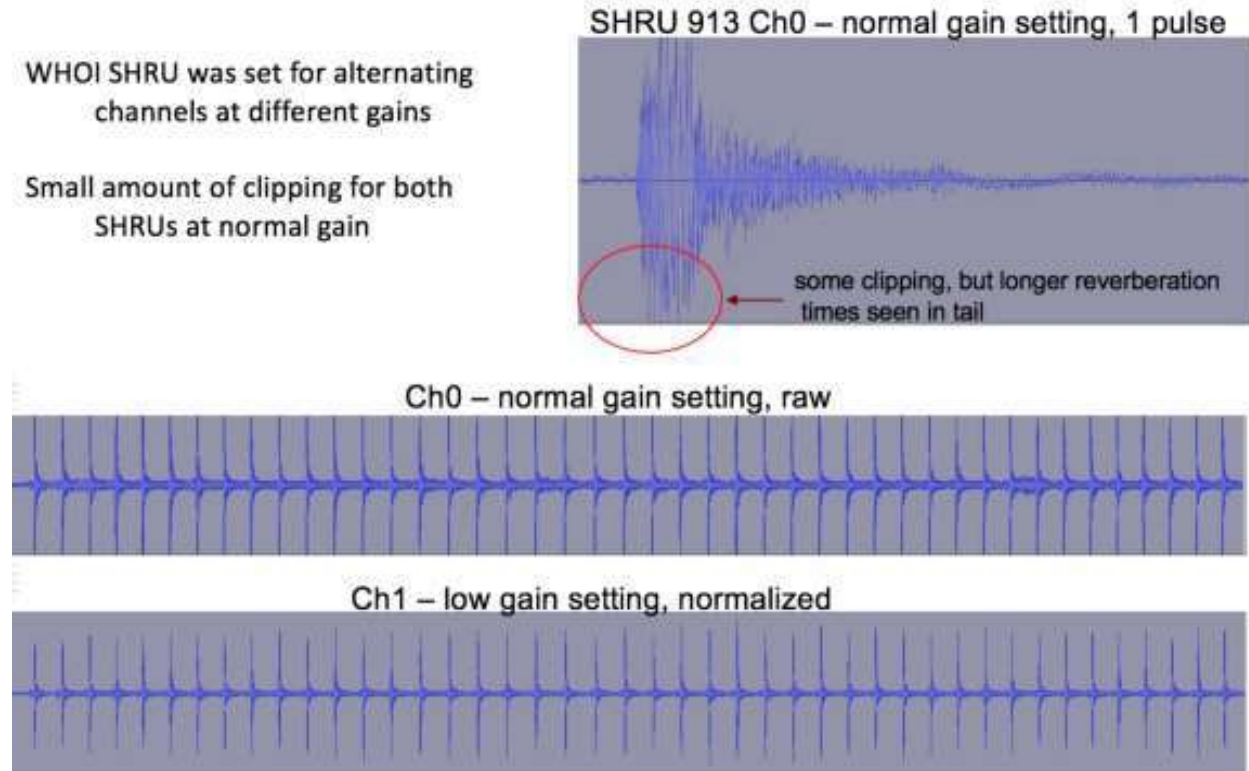


Figure 26. In the top panel, a signal pile driving event is shown from SHRU 913 deployed at 7.5 km from WTG#3. While some clipping is evident in the high gain hydrophones, the low gain hydrophone shows no clipping.

2.4 Summary of Measurements During Construction

Figure 27 shows a summary of the measurements on September 2 and 15, 2015 for the towed hydrophone array, measurements of the tetrahedral hydrophone array and vertical hydrophone arrays on October 25, 2015. There are significant differences between the sensors even at the same range. It is hypothesized that the varying pile rake causes the difference. The vertical axis of the graph is SPL peak-to-peak while the horizontal axis is range in km. The error bars show the data variability in terms of \pm two standard deviations. Note that all eight hydrophones of the towed array were used to calculate the mean (shown by the red and blue circles).

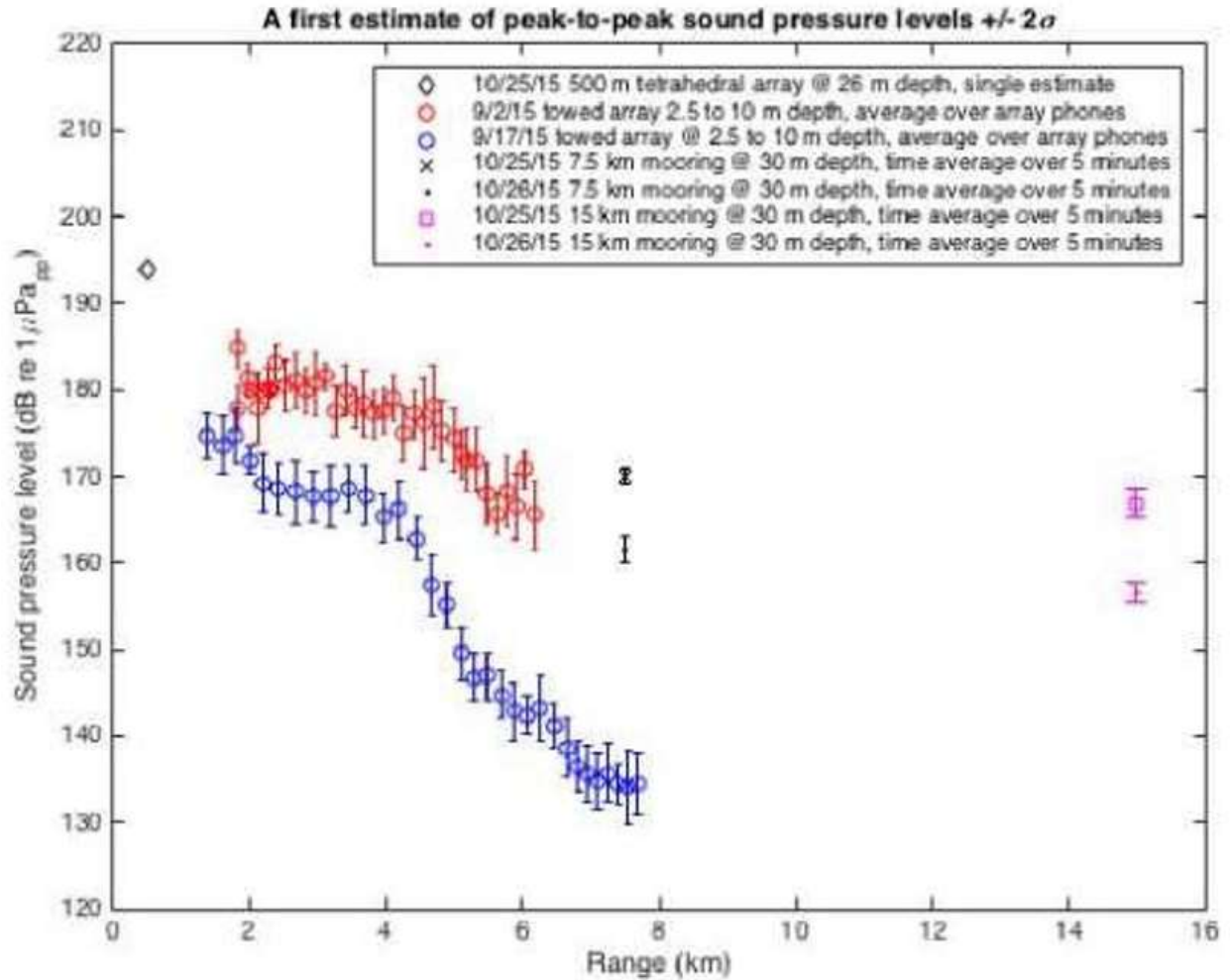
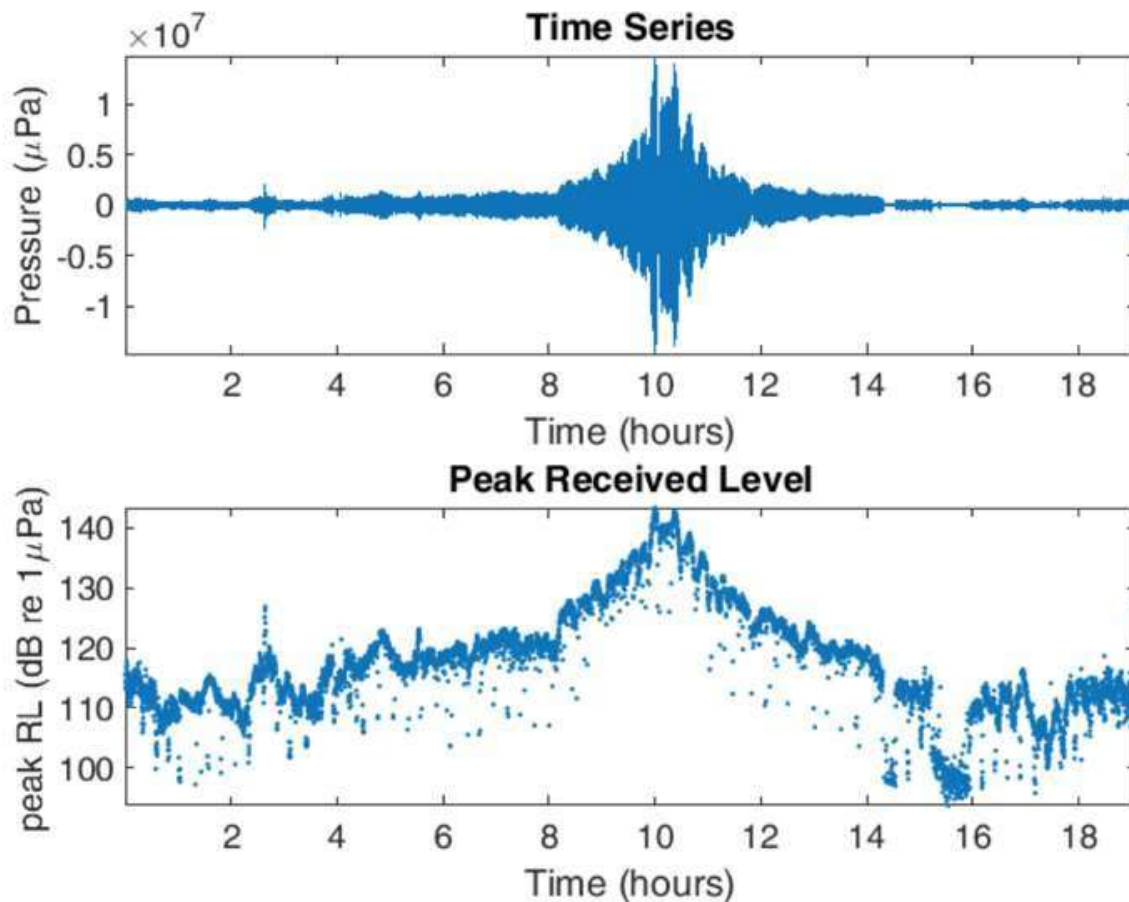


Figure 27. A summary of measurements on September 2 and 15, 2015 for the towed hydrophone array, measurements of the tetrahedral hydrophone array and vertical hydrophone arrays on October 25, 2015. There are significant differences between the sensors even at the same range. It is hypothesized that the varying pile rake causes the difference.

This page intentionally left blank.

3. Fin Whale Vocalizations

Fin whale vocalizations were detected during construction of the Block Island Wind Farm. Fin whale acoustic signals spanning about 20 hours are shown on the top panel of **Figure 28**. The approach, closest point of approach (CPA) around 10 hours and the departure of the whale are seen. In the bottom right panel, the peak SPL in dB re 1 μPa is shown as dots. A CPA range of 500 m and an 8 m/s speed for the whale seems to fit the data well. Source level is about 186 dB re 1 μPa at 1 m. Work on this data and localization technique is ongoing by J. Giard as part of her PhD dissertation. (Giard et al. 2017)



Note: Work on this data and localization technique is ongoing by J. Giard as part of her dissertation. (Giard et al. 2017). This data was collected at the 15 km SHRU vertical hydrophone array on November 4, 2015.

Figure 28. Fin whale acoustic signals spanning about 20 hours are shown on the top panel. The approach, closest point of approach (CPA) around 10 hours and the departure of the whale are seen. In the bottom right panel, the peak SPL in dB re 1 μPa is shown as dots. A CPA range of 500 m and an 8 m/s speed for the whale seems to fit the data well. Source level is about 186 dB re 1 μPa at 1 m.

Figure 29 shows a Parabolic Equation prediction of transmission loss in a waveguide of depth 50 meters.

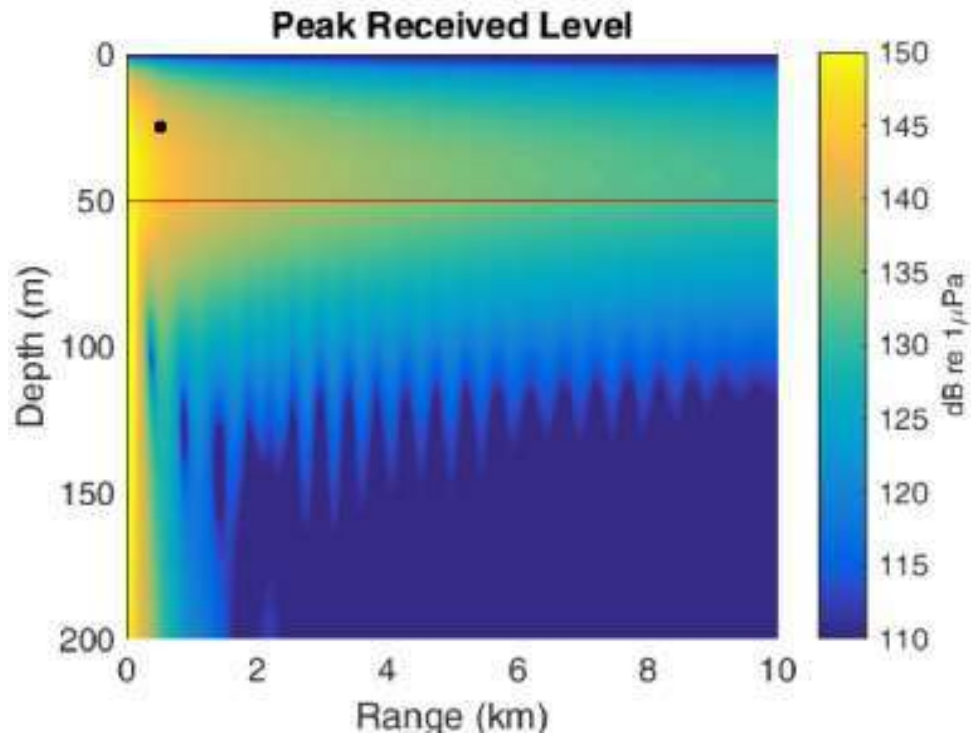


Figure 29. Transmission loss vs. range for a 20 Hz signal in a waveguide of depth 50 meters and a source depth of 25 m.

4. Conclusions and Recommended Next Steps

This report documented the preliminary findings of the acoustic and seismic monitoring of the construction of the Block Island Wind Farm done by the RODEO program. These measurements included quick look estimates of particle motion obtained using a tetrahedral hydrophone array, snapshots of acoustic pressure measurements from the same tetrahedral hydrophone array, a towed hydrophone array, two vertical multiple-hydrophone arrays, and a 3-axis 4- element geophone array. A preliminary numerical model of the three-dimensional underwater sound propagation in the Block Island Wind Farm area was presented. In addition, analysis of fin whale vocalizations south of Rhode Island that were recorded during the monitoring effort was described.

We recommend that the data be fully analyzed at all locations and all pile driving events for Sound Pressure Level (SPL rms, SPL peak), Sound Exposure Level (SEL) and Kurtosis. Also, we should compute particle velocity using tetrahedral array and other sensors for studies on the impact of pile driving on fish. We have begun 3D Finite Element Modeling for the angled pile driving and we propose to couple the output of the FEM to long range 3D and 2D underwater acoustic propagation codes. We propose to investigate the surprisingly intense fin whale calls recorded on the 15 km vertical hydrophone array on same day as the WHOI-NMFS DMON system detections as well as during operational noise measurements.

This page intentionally left blank.

References

- Bailey, H.; Senior, B.; Simmons, D.; Rusin, J.; Picken, G., Thompson, P.M.; (2010). "Assessing underwater noise levels during pile-driving at an offshore windfarm and its potential effects on marine mammals," *Mar. Pollut. Bull.*, 60, pp. 888–897.
- Betke K (2006) Measurement of underwater noise emitted by an offshore wind turbine at Horns Rev. Report for Institut für technische und angewandte Physik GmbH (ITAP), Oldenburg, Germany.
- Betke K, Schultz-von Glahn M, Matuschek R (2004) Underwater noise emissions from offshore wind turbines. Proceedings of the Joint Congress CFA/DAGA'04, 22– 25 March 2004, Strasbourg, France, pp 591–592.
- Bibee, L. D., 2011. A comparison of seismometer and hydrophone recordings of VLF seismo-acoustic signals, *OCEANS 91 Proceedings*, Volume: 1, 93 – 96.
- Carstensen, J.;Henriksen, O.D.; J. Teilmann, J.; (2006) "Impacts of offshore wind farm construction on harbour porpoises: acoustic monitoring of echolocation activity using porpoise detectors (T-PODs)," *Mar. Ecol. Prog. Ser.*, 321 (2006), pp. 295–308.
- Chapman CJ, Sand O. 1974. Field studies of hearing in two species of flatfish, *Pleuronectes platessa* (L.) and *Limanda limanda* (L.) (Family *Pleuronectidae*), *Comp. Biochem. Physiol.*, 47A, 371–385.
- Chapman CJ, Hawkins AD. 1973. A field study of hearing in the cod, *Gadus morhua* L., *J Comp. Physiol*, 85, 147–167.
- Giard, Jennifer; Miller, James H.; Potty, Gopu R.; Newhall, Arthur; Lin, Ying-Tsong; Baumgartner, Mark F., "Analysis of fin whale vocalizations south of Rhode Island", *J. Acoust. Soc. Am.*, 141, 3941 (2017); abstract, doi: 10.1121/1.4988927.
- Hawkins AD, Johnstone ADF. 1978. The hearing of the Atlantic salmon, *Salmo salar* . *J. Fish. Biol.*, 13, 655–673.
- Kim, H.; (2014) Prediction of structure borne noise radiation and propagation from offshore impact pile driving, PhD Dissertation, University of Rhode Island.
- Kim, H; Potty, G.R.; Dossot, G.; Smith, K.B.; Miller, J.H. (2012) "Long range propagation modeling of offshore wind turbine construction noise using Finite Element and Parabolic Equation models," *IEEE OCEANS*, 2012 - Yeosu (1)5, 21-24 May.
- Lin, Ying-Tsong; Newhall, Arthur; Potty, Gopu R.; Miller, James H., "A preliminary numerical model of three-dimensional underwater sound propagation in the Block Island Wind Farm area", *J. Acoust. Soc. Am.*, 141, 3993 (2017); abstract, doi: 10.1121/1.4989146.
- Ma BB, Nystuen JA, Lien RC (2005) Prediction of underwater sound levels from rain and wind. *J Acoust Soc Am* 117:3555–3565.

- Miller JH, Bradley DL, Nystuen, JA (2008) Ocean noise budgets. *Bioacoustics* 17:133– 136.
- Miller, J.H.; Potty G.R.; Vigness Raposa, K.; Casagrande, D.; Miller, L.A.; Nystuen, J.A.; Scheifele, P.M.; Clark, J.G.; (2010) "Assessment of the acoustic effects on marine animals by an offshore wind farm," *Bioacoustics*.
- Miller, James H.; Potty, Gopu R.; Lin, Ying-Tsong; Newhall, Arthur; Vigness-Raposa, Kathleen J.; Giard, Jennifer,; and Mason, Tim, "Overview of underwater acoustic and seismic measurements of the construction and operation of the Block Island Wind Farm," *J. Acoust. Soc. Am.*, 141, 3993 (2017); abstract, doi: <http://dx.doi.org/10.1121/1.4989144>
- Nystuen JA, Amitai E, Anagnostou EN, Anagnostou MN (2008) Spatial averaging of oceanic rainfall variability using underwater sound: Ionian sea rainfall experiment 2004. *J Acoust Soc Am* 123:1952–1962.
- Nystuen JA, Howe BM (2005) Ambient sound budgets. *Proceedings of the Underwater Acoustics Measurements Conference, 28 June - 1 July, Heraklion, Crete.*
- Popper A. N. et al., *Sound Exposure Guidelines for Fishes and Sea Turtles: A Technical Report prepared by ANSI-Accredited Standards Committee S3/SC1 and registered with ANSI, Springer Briefs in Oceanography, ASA Press, 2014.*
- Potty, Gopu R.; Tazawa, Makio; Giard, Jennifer; Miller, James H; Lin, Ying-Tsong; Newhall, Arthur; Vigness-Raposa, Kathleen J., *J. Acoust. Soc. Am.*, 141, 3993 (2017); abstract, doi: 10.1121/1.4989145.
- Reinhall, P. G.; Dahl, P. H.; (2011) Underwater Mach wave radiation from impact pile driving: Theory and observation *J. Acoust. Soc. Am.*, 130, 1209-1216.
- Schneider JA, Senders M (2010) Foundation design: A comparison of oil and gas platforms with offshore wind turbines. *MTSJ* 44:32–51.
- Thompson, P.M.; Hastie, G.D. Nedwell, J.; Barham, R.; Brookes, K.L.; Cordes, L.S.; Bailey, H.; McLean, N.; (2013) "Framework for assessing impacts of pile-driving noise from offshore wind farm construction on a harbour seal population," *Environmental Impact Assessment Review*, (43) 73-85.
- Tougaard, J.; Carstensen, J.; Teilmann, J.; Skov, H.; Rasmussen, P.; (2009) Pile driving zone of responsiveness extends beyond 20 km for harbor porpoises (*Phocoena phocoena* (L.)), *J. Acoust. Soc. Am.*, 126 (2009), pp. 11–14.
- Vigness-Raposa, Kathleen J.; Giard, Jennifer; Frankel, Adam S.; Miller, James H.; Potty, Gopu R.; Lin, Ying-Tsong; Newhall, Arthur; Mason, Tim, "Variations in the acoustic field recorded during pile-driving construction of the Block Island Wind Farm," *J. Acoust. Soc. Am.*, 141, 3993 (2017); abstract, doi: 10.1121/1.4989147

Submitted to:

Randy Gallien
HDR, Inc.
300 North Madison Street
Athens
AL 35611
USA

Tel: +1 256 232 1863

E-mail: Dennis.Gallien@hdrinc.com

Website: www.hdrinc.com

Submitted by:

Tim Mason
Subacoustech Environmental Ltd
Chase Mill
Winchester Road
Bishop's Waltham
Hampshire
SO32 1AH

Tel: +44 (0)1489 892 881

E-mail: tim.mason@subacoustech.com

Website: www.subacoustech.com

Measurement and assessment of
underwater noise and vibration during
construction at the Block Island wind
farm, Rhode Island

A G Collett, T I Mason, R J Barham

February 23, 2016

**Subacoustech Environmental Report No.
E494R0102**



<i>Document No.</i>	<i>Date</i>	<i>Written</i>	<i>Approved</i>	<i>Distribution</i>
E494R0101	01/17/2016	A Collett	T Mason	Randy Gallien (HDR)
E494R0102	02/23/2016	R Barham	T Mason	Randy Gallien (HDR)

This report is a controlled document. The report documentation page lists the version number, record of changes, referencing information, abstract and other documentation details.

Executive Summary

As part of the Real-time Opportunity for Development of Environmental Observations (RODEO) program, Subacoustech Environmental Limited, under the team headed by HDR Inc., undertook a series of underwater noise and seabed vibration measurements during the installation of the foundations for the Block Island Wind Farm (BIWF).

Five jacket-type frame foundation structures were placed and fixed off the coast of Block Island, Rhode Island over August, September and October 2015. The frames were placed by crane onto the seabed after which long metal piles were inserted into the frame, which were then driven by impact piling – striking the top of the piles with a specialised piling hammer – to fix the frame in place. This process generates high noise levels both above and below the sea surface.

The underwater noise and seabed vibration produced during piling was measured under a series of environmental conditions over 14 separate piling events on five days. A fixed underwater noise monitor was deployed and anchored at a chosen range recording continuously over the day to capture the variation in piling noise before being recovered at the end of the day. Underwater noise measurements were sampled along transects at mid-depth and at one meter above the seabed. In addition, seabed vibration measurements were captured at locations along transects.

This report presents the results and analysis of measurements of underwater noise and seabed vibration produced during piling and its propagation into the surrounding waters.

List of contents

1	Introduction.....	1
1.1	Study overview and site description.....	1
1.2	Construction machinery and foundation design.....	2
1.3	Scope of work.....	4
2	Methodology.....	5
2.1	Measurement equipment.....	5
2.2	Measurement procedure.....	5
2.2.1	Transect measurements.....	5
2.2.2	Fixed monitor measurements.....	7
2.2.3	Vibration measurements.....	8
2.3	Estimation of Source Level.....	8
2.3.1	Inputs and Assumptions.....	8
2.3.2	Modelled Transmission Loss.....	9
3	Background noise measurements.....	10
3.1	Introduction.....	10
3.2	Background noise measurements.....	10
4	Piling noise measurements.....	12
4.1	Introduction.....	12
4.2	WTG2 – 18 August 2015.....	12
4.3	WTG2 – 03 September 2015.....	12
4.3.1	Overview.....	12
4.3.2	Pile 1 Northwest Transect – Mid-depth.....	14
4.3.3	Pile 1 Northwest Transect – 1 m above seabed.....	15
4.3.4	Pile 2 and 3 East Transect – Mid-depth.....	16
4.3.5	Pile 2 East Transect – 1 m above seabed.....	18
4.3.6	SPL and blow energy comparison.....	19
4.4	WTG5 – 17 September 2015.....	22
4.4.1	Overview.....	22
4.4.2	SPL and blow energy comparison.....	22
4.5	WTG3 – 18 September 2015.....	23
4.5.1	Pile 4 Southeast Transect – Mid-depth.....	24
4.5.2	SPL and blow energy comparison.....	26
4.6	WTG1 – 19 September 2015.....	28
4.6.1	Overview.....	28
4.6.2	Piles 1 to 4 North Transect – Mid-depth.....	29

4.6.3	SPL and blow energy comparison	30
4.7	Summary and comparisons	33
4.7.1	Summary	33
4.7.2	Comparison with measured data	33
4.7.3	Comparison with modelled data	34
4.7.4	Hammer type and SPL comparison	36
5	Piling seabed vibration measurements	37
5.1	Introduction.....	37
5.2	Vibration measurements	37
5.2.1	WTG5 Pile 2 Northwest transect.....	37
5.2.2	WTG5 Pile 3 Northwest transect.....	38
6	Summary and conclusions	40
7	References	41
Appendix A	Measurement of underwater sound	43
A.1	Units of measurement	43
A.1.1	Peak level.....	43
A.1.2	Peak-to-peak level.....	44
A.1.3	Sound pressure level	44
A.1.4	Sound exposure level.....	44
A.2	Source level.....	45
A.3	Sound propagation	45
Appendix B	Calibration certificates	46
Appendix C	Detailed results.....	50
	Report documentation page.....	51

1 Introduction

BOEM (Bureau of Ocean Energy Management) seeks to investigate the environmental impacts associated with the construction and operation of offshore wind farms sited. The Block Island Wind Farm (BIWF), situated off the coast of Rhode Island, is the first of its kind to be constructed in United States waters and provides an opportunity to directly observe and measure a variety of potential stressors on the local environment. The Real-time Opportunity for Development of Environmental Observations (RODEO) program was set up by BOEM to enable this.

The construction and operation of an offshore wind farm will necessarily generate noise. This noise will be produced from many sources, including those associated with the transportation of construction equipment and materials, the operation of construction equipment and the operation of the completed offshore wind turbines. As part of the RODEO program, Subacoustech Environmental Limited, as part of a team led by HDR Inc., planned and executed a survey around the construction site to measure the noise emitted both in the air and underwater.

This report has been prepared by Subacoustech Environmental Ltd for HDR, Inc. It presents the methodology and results of the underwater environmental noise and vibration survey undertaken during the installation of the first foundations for the BIWF offshore wind turbines in August and September 2015.

1.1 Study overview and site description

The Block Island Wind Farm is situated approximately three miles off the southeast coast of Block Island, and south of Point Judith, Rhode Island. The wind farm plan is comprised of five offshore wind turbines, each of a 6 MW output, to produce a 30 MW development designed to significantly reduce Block Island's reliance on diesel fuelled electricity. Figure 1-1 below shows the overview layout of BIWF relative to Block Island.

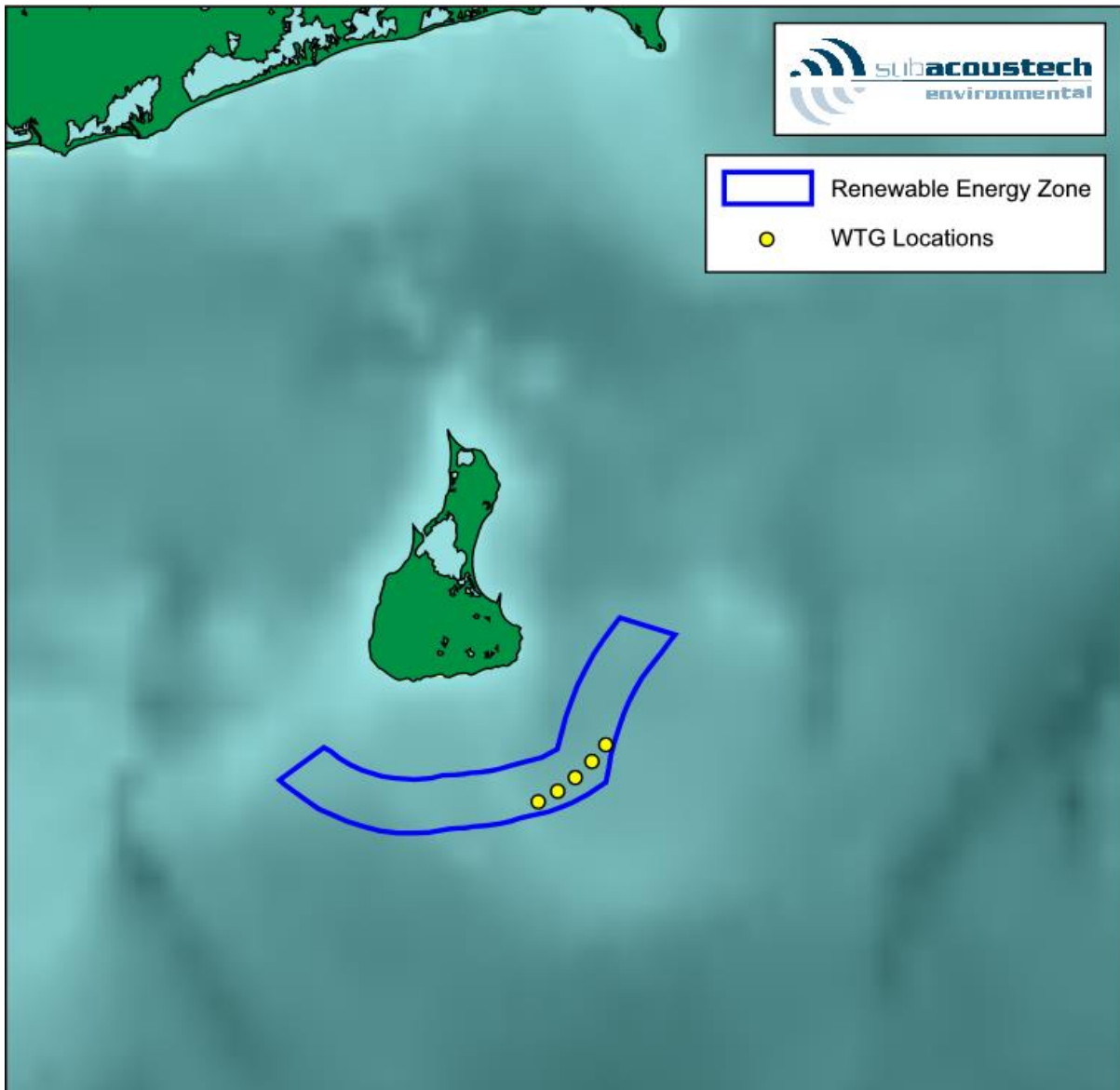


Figure 1-1 Location of the Block Island wind farm site

The wind turbines will each be situated on a 'jacket' frame foundation with a square profile. Each of the four corners is secured using a 1.372 m (54") diameter, steel tube, or 'pile', which is inserted by crane into each corner of the jacket and driven into the seabed using an impact pile driver supported by an adjacent barge.

The primary focus of this study was to observe and measure the levels of underwater noise and vibration produced during the installation of these piles. Underwater noise levels were sampled using a fixed monitor which was deployed prior to the pile driving and retrieved afterward. Measurements were also taken from a survey vessel along transects extending out from the turbine foundations.

1.2 Construction machinery and foundation design

The five wind turbine generators will be installed on jacket frames, fixed to the seabed by four piles using an impact (percussive) pile driving technique. Two barge designs were employed on the BIWF site: a floating barge (moored by a series of anchors during crane activity) and a jack-up barge (see Figure 1-3). Most piles were installed using the jack-up barge. Each jacket was lowered by crane into

the sea, and the piles lowered individually by crane into guide holes in each jacket corner. A hydraulic piling hammer was set onto the top of one of the piles and driven incrementally into the seabed by a series of strikes. Piling for each leg typically took approximately 30 minutes. The depth of the sea was approximately 30 m at the BIWF location.

Once the four piles were driven, a second stage of piles were welded on and driven using the same procedure.

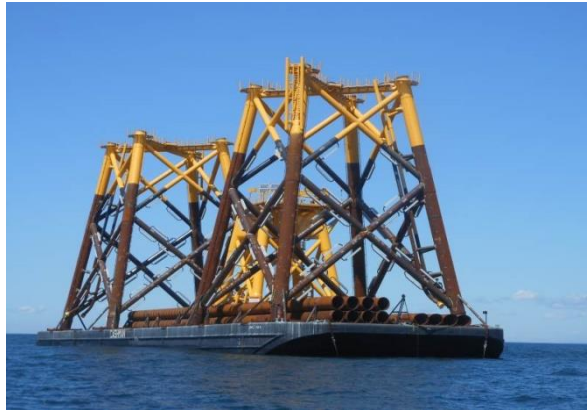


Figure 1-2 Jacket foundations and piles being transported by barge



Figure 1-3 Jack-up piling barge with four piles inserted, not driven, and hammer ready



Figure 1-4 Jacket with four driven piles

1.3 Scope of work

This report describes the results obtained from the underwater noise and vibration monitoring surveys for the jacket structure foundation WTG1, WTG2, WTG3 and WTG5. Also included within this report are descriptions of the methodology and data analysis performed. In summary, this report covers:

- Description of the methodology used to carry out the noise monitoring (Section 2);
- Measured background noise in and around the wind farm site (Section 3);
- Levels of noise measured during impact piling operations and estimated source levels (Section 4);
- Magnitude of vibration measured during impact piling operations (Section 5);
- Conclusions (Section 6);
- A review of background information on the units for measuring and assessing underwater noise (Appendix A).

2 Methodology

The section presents the processes completed in obtaining noise and vibration measurements at the BIWF site.

2.1 Measurement equipment

The following equipment was used on the survey:

- OceanSonics icListen HF-SB9 (Serial No. 1400) and icListen HF-X2 (Serial No. 1287) hydrophones;
- Reson TC4014 hydrophones (Serial No. #4005034 and #4005035);
- Brüel & Kjær type 8106 hydrophone (Serial No. #2575949);
- Custom built amplification, with variable 0 to 40 dB gain;
- National Instruments USB-6216 Data Acquisition hardware;
- A spar-buoy to suspend and stabilise the hydrophone in the water;
- Tri-axial Vibrock V901 geophone.

It should be noted that the Vibrock V901 geophone has a frequency range of 4 Hz to 200 Hz and the manufacturer states a useable peak particle velocity (PPV) range of 0.1 mm/s to 200 mm/s. Subacoustech have been informed that the lower limit of 0.1 mm/s is based upon the noise floor of the standard Vibrock processing electronics rather than the transducer itself. As Subacoustech Environmental use very low noise processing equipment (not the standard Vibrock system) it is possible to record levels significantly below 0.1 mm/s. However levels below 0.1 mm/s should be considered indicative.

Full calibration certification for the equipment is provided in Appendix B, for the complete frequency range of the hydrophones. Calibration was confirmed before departure using a pistonphone operating at 250 Hz.

The boat's position was recorded on the computer system by sending the output from a GPS receiver to a USB port on the logging computer, which was logged with the acoustic data. This was used to determine the range to the piling from the survey vessel.

2.2 Measurement procedure

2.2.1 Transect measurements

Measurements were taken from a single hydrophone deployed from the side of the survey vessel, the URI *R/V McMaster*, shown in Figure 2-1. The survey vessel's engines and other equipment which might have caused acoustic interference with the measurements were turned off and the boat was allowed to drift while measurements were taken. The hydrophone was attached to a spar-buoy to provide anti-heave whilst undertaking measurements, reducing the effect of surface waves. The hydrophone was allowed to float and drift freely from the vessel to minimise flow noise during measurements. Hydrophone drifts were generally 10 to 15 m from the start position, before the hydrophone was recovered and redeployed. The GPS position was logged at the start of the drift, at the closest point to the vessel (typically within five metres of the actual hydrophone position).



Figure 2-1 URI survey boat, R/V McMaster, used as the survey vessel for all transect measurements

At intervals starting at around 500 m and doubling in distance (500 m, 1 km, 2 km, 4 km, etc.) sound data was acquired on the computer, together with details of the boat’s position and other relevant information. In general, measurements were repeated in each location, taken in succession. For a number of transects measurements were taken at two depths, mid-depth and 1 m above the seabed. This was done by immediately recovering the hydrophone and changing the connection position of the spar-buoy in order to re-deploy the hydrophone at the second depth. A summary of the measurement details below is given in Table 2-1 and show which transects that measurements were taken at both depths.

Figure 2-2 provides an illustrative map of measurement transects taken from the various wind turbine foundations.

Transect ID	Date	Turbine Foundation	Direction	Ranges	Time (EST)	Water Depth	Hydrophone Depth
1	18 Aug 2015	WTG2 Stage 1 (1 pile)	Northwest	450 m – 725 m	15:53 – 16:11	20 – 25 m	Mid-depth (10 – 12 m)
2	03 Sep 2015	WTG2 Stage 2 (1 pile)	Northwest	550 m – 3.05 km	09:56 – 10:20	22 – 29 m	Mid-depth (11 – 14 m)
3	03 Sep 2015	WTG2 Stage 2 (1 pile)	Northwest	550 m – 3.05 km	09:58 – 10:17	22 – 29 m	1 m above seabed
4	03 Sep 2015	WTG2 Stage 2 (2 piles)	East	640 m – 20.0 km	11:14 – 15:11	10 – 53 m	Mid-depth (5 – 26 m)
5	03 Sep 2015	WTG2 Stage 2 (1 pile)	East	680 m – 4.05 km	11:18 – 11:34	10 – 27 m	1 m above seabed (9 – 26 m)
6	18 Sep 2015	WTG3 Stage 2 (1 pile)	Southeast	480 m – 6.41 km	14:20 – 15:07	25 – 27 m	Mid-depth (12 – 13 m)
7	19 Sep 2015	WTG1 Stage 1 (4 piles)	North	710 m – 24.0 km	08:37 – 15:11	10 – 40 m	Mid-depth (5 – 20 m)

Table 2-1 Summary of underwater noise transect measurements of impact piling

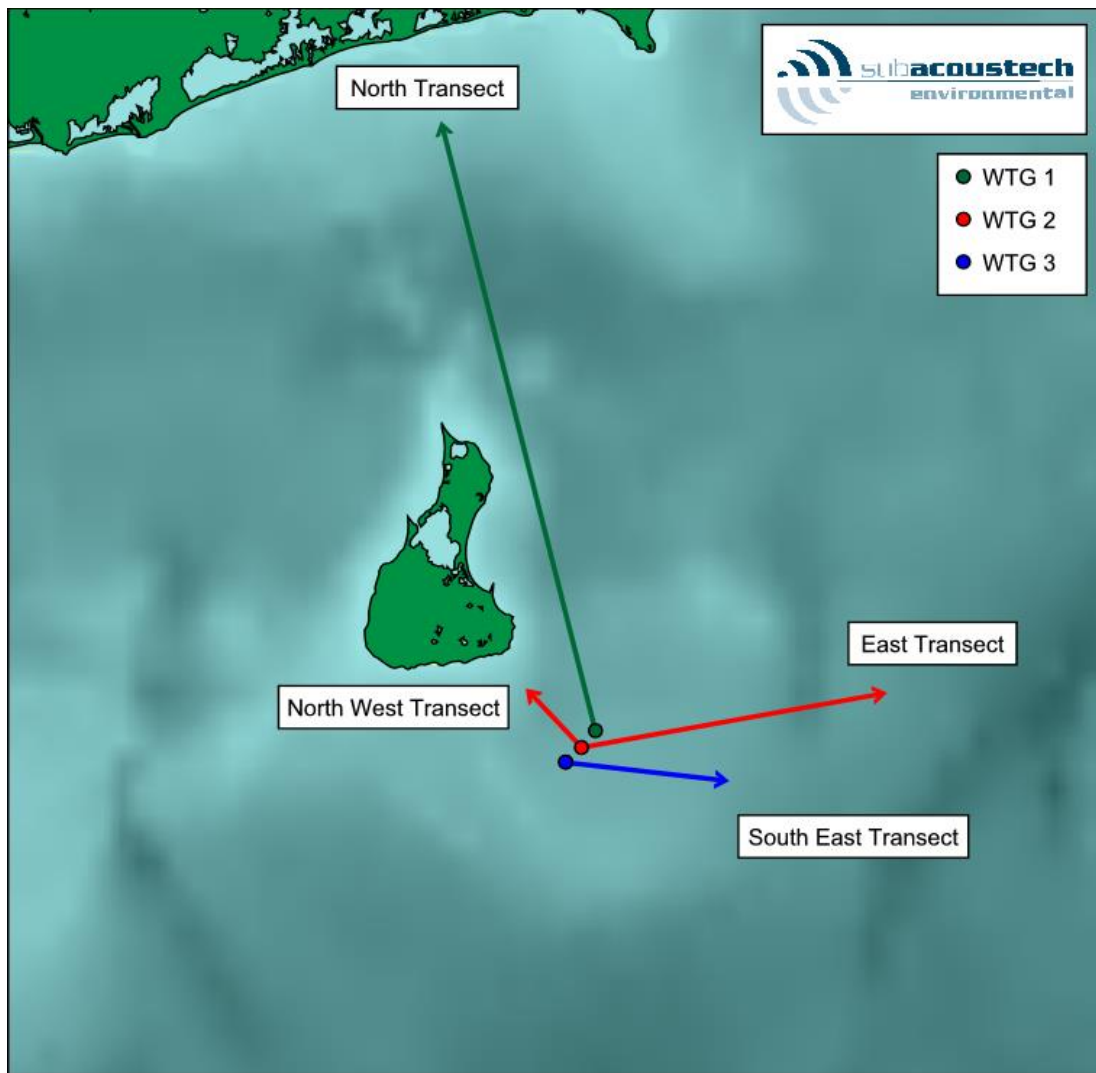


Figure 2-2 Sketch map showing the approximate transects measured during the survey

2.2.2 Fixed monitor measurements

An OceanSonics icListen hydrophone was deployed at a fixed location for each measurement day listed in Table 2-2. The hydrophone was fixed at mid-depth at approximately 750 m from the location of the piling, except on 19 September 2015 where the hydrophone was fixed at 1 m above the seabed at 5.93 km north of the piling.

Date	Turbine Foundation	Direction	Range
03 Sep 2015	WTG2 Stage 2 (4 piles)	Northwest	750 m
17 Sep 2015	WTG2 Stage 2 (3 piles)	Northwest	790 m
18 Sep 2015	WTG3 Stage 2 (4 piles)	South East	840 m
19 Sep 2015	WTG1 Stage 1 (4 piles)	North	5.93 km

Table 2-2 Summary of date and location of underwater noise fixed monitor measurements of impact piling

2.2.3 Vibration measurements

The vibration measurements were carried out on transects following a similar procedure to the underwater noise transect measurements. The geophone assembly is lowered onto the seabed using second line to maintain orientation and allowed to settle in the sediment. The geophone was oriented such that the longitudinal axis was in line with the direction of the transect. Once the geophone was deployed and as each measurement was started, the cable was fed out and allowed to drift with the flow to minimise the effect of additional vibration induced by the current on the cable (cable strum). Each measurement lasted for approximately 30 seconds and once complete, the cable is retrieved to remove any slack and the measurement repeated.

2.3 Estimation of Source Level

Estimates of source level (SL) have been undertaken from the measured levels of the pile strikes. A simple method for determining the SL is by using the transmission loss to extrapolate back from a measured received level. SL is usually expressed as dB re 1 μ Pa at 1 meter, where 1 μ Pa is the standard reference pressure used underwater.

In shallow water, estimating SL effectively is not always simple because of the interaction of the propagating sound with the surface and seabed. For the purpose of determining 'first look' source levels based on the measured data presented in this report, the RAMSGeo propagation model was chosen.

RAMSGeo is based on the much used RAM (Range-dependent Acoustic Model) software (Collins, 1994; Collins *et al*, 1996). The implementation used by Subacoustech Environmental is AcTUP v2.2 for MATLAB published by Curtin University. This model was chosen since it is effective at modelling low frequency propagation, allows for variable bathymetry and the incorporation of complex bottom types.

2.3.1 Inputs and Assumptions

A number of assumptions have been made based on available data. It should be noted that the modelling is intended to provide an indication of the transmission loss and hence determine indicative source levels for the measured data presented in later sections.

- Frequency range and spectral input. The RAMSGeo model considers the noise propagation across several separate frequency bands before calculating the broadband unweighted noise level. In order to get these frequency bands, the noise measurements that were taken along each transect during the noise survey at BIWF have been used.
- Bathymetry data. Acoustic propagation is strongly influenced by the interaction of the sound with the seabed and surface, especially in shallow waters, such as those surrounding the study area. Bathymetry data from GEBCO for the region has been used for this modelling.
- Sound speed profiles in the water column. In shallow water the water column exhibits a great deal of mixing and a uniform temperature profile has been assumed for the purpose of this modelling. A representative speed of 1520 m/s has been used throughout the calculations, based on a water temperature of 20°C (Mackenzie, 1981). That there will be variations in the sound speed profile over the day is acknowledged, but at this stage more complex or accurate profiles for the area are not available.
- Sediment and seabed type. From this the compressive and sheer sound speed profile, density profile, and compressive and shear attenuation in the sediment can be determined (Jensen *et al*, 1994).

2.3.2 Modelled Transmission Loss

Figure 2-3 and Figure 2-4 show the RAMSGeo transmission loss data for the north transect (Figure 2-2), which extends 28 km from WTG1 towards the Rhode Island shoreline. Frequency data measured 710 m from piling events at WTG1 on 19th September 2015 were used to calculate these losses. Also, a silt/sand seabed has been assumed based on data from the Block Island Wind Farm and Block Island Transmission System Underwater Acoustic Report (Environmental Report Appendix N-2 by Deepwater Wind).

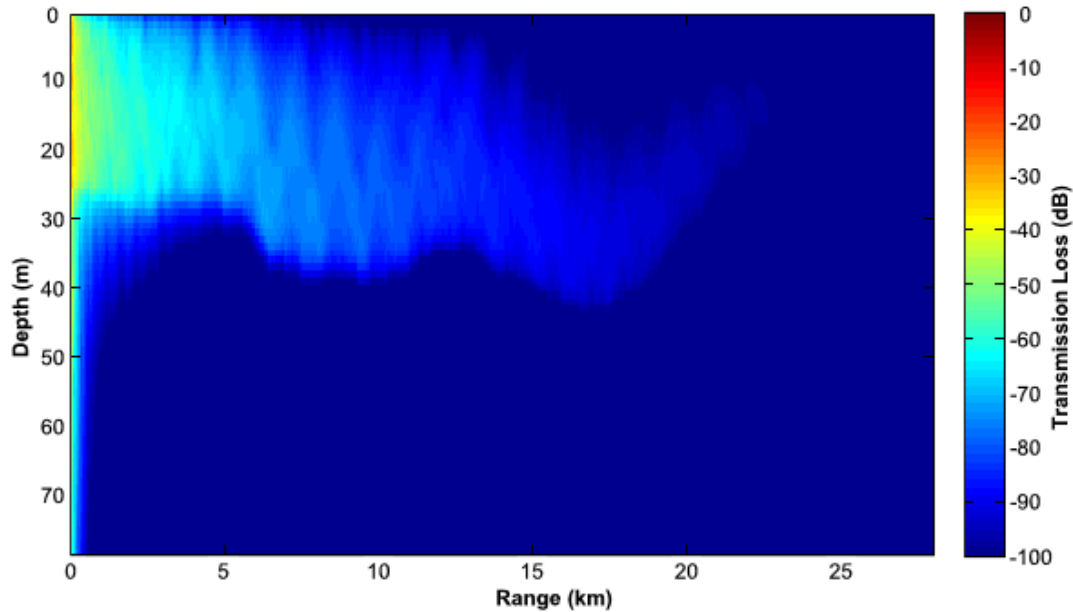


Figure 2-3 Temperature plot showing the predicted underwater noise propagation along the north transect

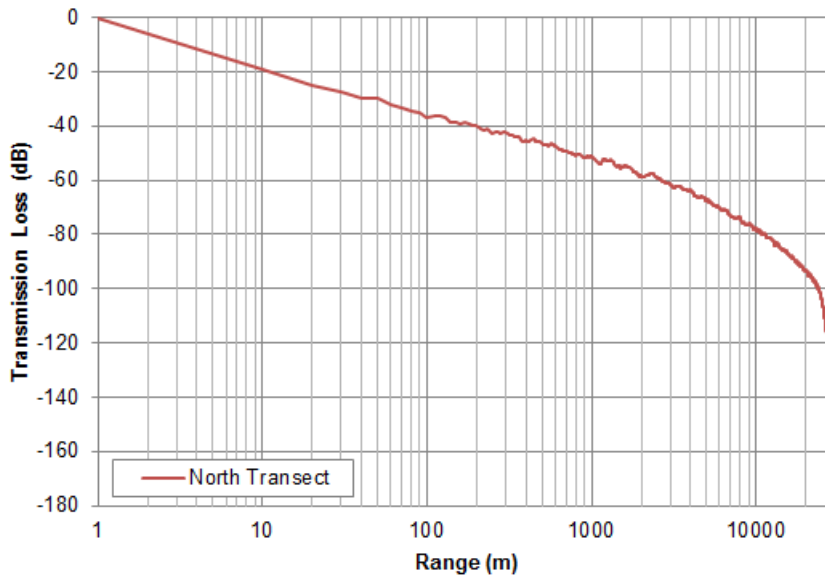


Figure 2-4 Level vs. range plot showing the predicted unweighted transmission loss along the north transect

3 Background noise measurements

3.1 Introduction

Background noise measurements were undertaken at opportune moments throughout the survey period when no piling activities occurred. As the focus of the survey was the observation and measurement of pile driving and installation of turbine foundations, the background noise measurements were considered secondary. Therefore the background measurements taken as part of this study only provide a snapshot of the ambient noise in and around BIWF.

A summary of the noise measurement terms are given in Appendix A.

Table 3-1 provides the details of the background measurements identifying the location and conditions.

Date	Location	Distance	Sea State (Beaufort scale)	Weather conditions
13 Aug 2015	Northwest transect	1.5 - 5.0 km Northwest of WTG2	2	Sunny, clear skies and light winds (2 m/s)
14 Aug 2015	South east transect	0.8 - 2.9 km South east of WTG3	3	Sunny, clear skies and gentle breeze (4 m/s)
23 Aug 2015	Northwest transect	1.0 - 1.14 km Northwest of WTG2	3	Sunny, clear skies and gentle breeze (4 m/s)
24 Aug 2015	North transect	0.9 - 4.0 km north of WTG1	3	Sunny spells, cloud 7/8 coverage, dry, gentle breeze (3.5 m/s)
03 Sep 2015	East transect	20.0 - 30.5 km east of WTG2	3	Dry, sunny, cloud light but clear 1/8, light breeze (3 m/s)

Table 3-1 Details of location and conditions of the background measurements

3.2 Background noise measurements

The maximum, minimum and mean measured background noise levels are presented in Table 3-2. The mean levels (SPL RMS) range from 107.4 dB re 1 μ Pa, for measurements taken up to 30 km east of the BIWF site, to 118.7 dB re 1 μ Pa, for measurements taken as close as 1.0 km from the site. The background noise levels measured near to the BIWF site were found to be higher due to the presence of construction vessels and also a greater number of small recreational vessels. The lowest levels were measured at a distance of 30 km east of the BIWF site away from vessel traffic and other anthropogenic noise sources. The power spectral density of this measurement is presented in Figure 3-1 showing the level across the frequency range is less than that of the measurements from other locations. The other power spectral density plots show higher levels between 30 and 300 Hz mostly due to the presence of vessels associated with the BIWF construction operation.

The maximum and minimum noise levels are 1 second samples over the sampling period on that transect. The mean level is an arithmetic average accounting for all of the measurements over the transect.

Measurement and assessment of underwater noise and vibration during construction at the Block Island wind farm, Rhode Island

Date	Location	Max level (dB re 1 μ Pa)	Min Level (dB re 1 μ Pa)	Mean Level (dB re 1 μ Pa)	Comments
13-Aug-15	Northwest transect	123.7	104.2	115.3	Noise from small vessels and construction barge
14-Aug-15	Southeast transect	124.7	96.0	112.4	Some noise from construction barge
23-Aug-15	Northwest transect	129.7	111.1	118.7	Machinery noise from construction barge and passing vessels
24-Aug-15	North transect	119.7	103.2	112.1	Noise from construction barge and from ferry
03-Sep-15	East transect	125.7	97.7	107.4	Vessel traffic contributes at 20 km, very quiet at 30 km

Table 3-2 Summary of SPL RMS background noise measurements taken in the vicinity of Block Island Wind Farm site

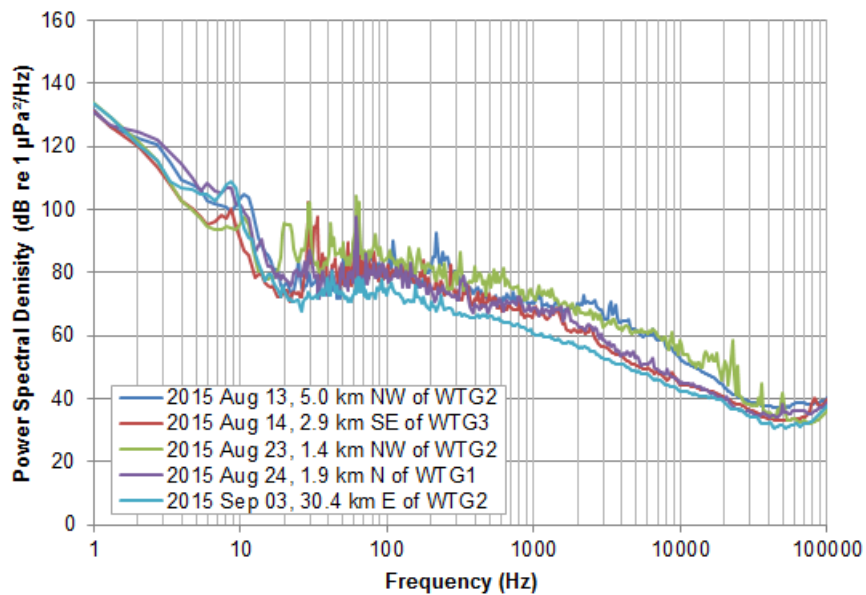


Figure 3-1 Power spectral density plots of noise measurements taken in the vicinity of Block Island Wind Farm site

4 Piling noise measurements

4.1 Introduction

Underwater noise measurements of impact piling were taken along transects from three WTG locations at the Block Island wind farm; WTG1, WTG2 and WTG3. A fixed monitor was used to measure the underwater noise of impact piling at approximately 750 m on four of the WTG locations; WTG1, WTG2, WTG3 and WTG5. The unweighted measurements from these locations are presented in the following sections in the order they were collected. A summary of the noise measurement terms is given in Appendix A.

A series of data sheets giving detailed results and conditions for all measurement days and piling events is given in Appendix C.

4.2 WTG2 – 18 August 2015

The first measurements of underwater noise from the piling operation were measured on 18 August 2015 on WTG2 foundation. The jacket structure had previously been placed and the first stage piles had been ‘stabbed’ (i.e. positioned in the frame) ready to be driven. It was thought that piling operation would occur though out the day but it appeared that the construction crew ran into technical difficulties leading to only a short amount of time spent piling. The short period of sustained piling that did occur happened between 15:53 and 16:11. The hammer used on 18 August 2015 was a Bauer-Pileco Inc Model D280-22 diesel piling hammer, different to the Menck hydraulic hammer used for all the subsequent piling measurements presented in the following sections. Comparisons of the SPLs recorded for the two hammers found that there is little difference for equivalent levels (see section 4.7.4).

Measurements were taken on a transect to the northwest of the turbine foundation towards Block Island. Due to the short time of piling, measurements were only taken between 450 m and 725 m.

A summary of the measurements is given in Table 4-1 showing the maximum and mean peak to peak SPLs recorded at each distance from the piling. All the measurements were taken with the hydrophone positioned at mid-depth, with the exception of measurement at 700 m which was taken at 1 m above the seabed. Blow energies were not available for the diesel hammer.

Distance (m)	No. of strikes recorded	Blow energy	Maximum level (dB re 1 μ Pa)	Mean level (dB re 1 μ Pa)
450	8	Not available	191.2	186.0
500	2	-	186.0	185.1
700	20	-	188.4*	186.4*
710	21	-	188.1	184.1
725	24	-	187.6	184.8

Table 4-1 Measured peak-to-peak SPLs taken along a northwest transect at mid-depth (* Indicates measurements that were taken at a depth of 1 m above the seabed)

4.3 WTG2 – 03 September 2015

4.3.1 Overview

Underwater noise measurements took place during the second stage of pile driving for the foundation WTG2 on 3rd September 2015. The jacket foundation had previously been set and the first stage of pile driving had occurred. All four of the second stage piles were driven starting at 09:56.

The fixed monitor was deployed at 750 m from WTG2 prior to the start of piling. During the first piling event, measurements were undertaken along a transect to the northwest starting at 550 m from

WTG2 and heading towards the Southeast Light on Block Island. Measurements were taken out to 3.05 km before piling stopped on the first pile. At each measurement position samples were recorded at two depths, mid-depth and 1 m above the seabed, one after the other.

Throughout the driving of the second pile, measurements were carried out along an eastern transect between 640 m and 4.05 km. The second piling event began at 11:14 and ceased at 11:35. As with the first piling event, measurements were taken at the two depths.

In between driving the second and third piles the survey vessel moved out to 7.6 km to continue measurements along the east transect. On commencement of piling for the third pile measurements were taken at mid-depth between 7.6 km and 20 km.

The survey vessel continued to a distance of 30 km in between driving the third and fourth piles. At 30 km the survey vessel was unable to communicate with the observation vessel, which was near the piling, or listen in on the radio chatter of the construction crew due to being out of range. As a result of being unable to know for certain whether the fourth pile was to be driven, after a period of waiting and listening for piling noise underwater with the monitoring equipment it was decided to transit back towards the piling operation. When back in range of radio signal and cell coverage it was learned that the fourth pile had been driven whilst the survey vessel was transiting back. The fixed monitor was then recovered before heading back to port.

Figure 4-1 shows the SPL RMS time history data captured by the fixed monitor located 750 m from WTG2. The graph clearly displays four 'blocks' which correspond to the four piling events during the day, with a short gap occurring during the piling of pile 3. Each pile took between 25 and 35 minutes to be installed after which the noise returned to background level. The background SPLs are dominated by construction activity and vessel movements related to BIWF. The shortest break in piling of approximately 50 minutes is seen to have occurred between pile 1 and 2. It is seen that greatest levels were recorded when the second pile was driven.

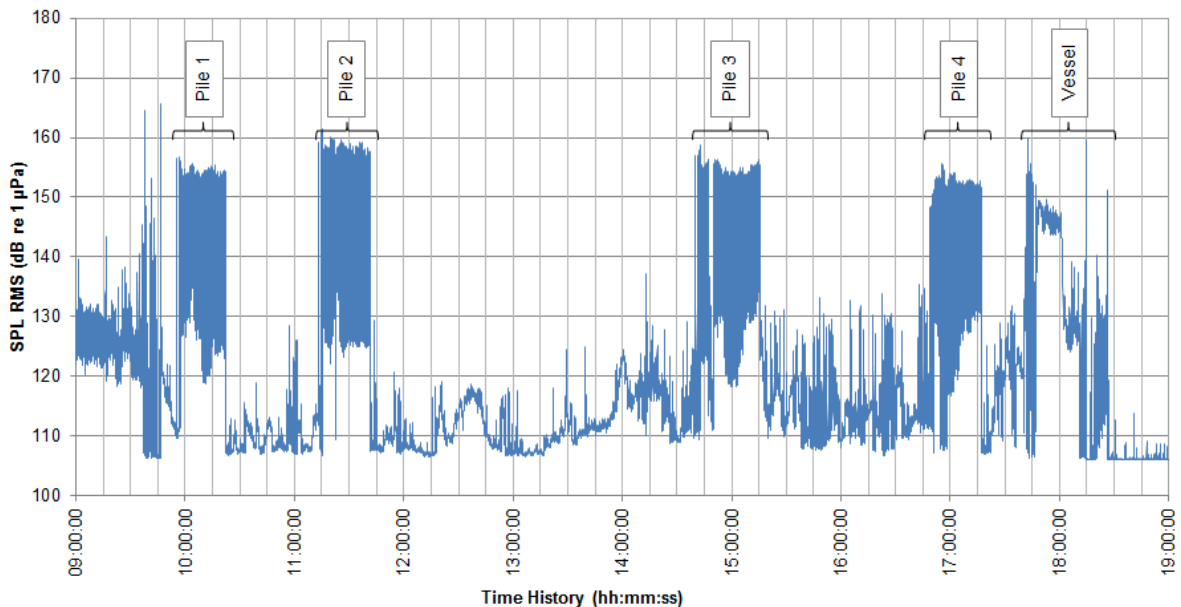


Figure 4-1 Time history plot of 1 s SPL RMS recorded by the fixed monitor 750 m from WTG2 on 03 September 2015

Note that an insensitive hydrophone was used to sample the high levels of piling noise above and thus lower noise levels outside of the actual piling often fall below the noise floor of the instrument

(see the flat line between 18:30 and 19:00 above). This represents a limitation of the instrumentation and not the background noise level.

4.3.2 *Pile 1 Northwest Transect – Mid-depth*

Table 4-2 presents the peak-to-peak SPLs determined from measurements taken along the northwest transect at mid-depth. The table clearly shows a decrease in level as the distance increases and is further illustrated in Figure 4-2. All the pile strikes measured are plotted and transmission loss (TL) data calculated using the RAMSGeo acoustic model. For this transect, the extrapolated source level using the RAMSGeo transmission loss is estimated to be 234 dB re 1 μPa @ 1 m.

The data presented in Figure 4-3 show a clear reduction in PSD (Power Spectral Density) level with range, as would be expected for measurements taken successively further away from a noise source. It can also be seen that this reduction is evident over a very wide range of frequencies, from about 10 Hz up to 100 kHz indicating that the piling operation is generating underwater noise over this range. The maximum levels of underwater noise during these measurements were at frequencies between about 60 Hz up to about 400 Hz.

Distance (m)	No. of strikes recorded	Approx. blow energy (kJ)	Maximum level (dB re 1 μPa)	Mean level (dB re 1 μPa)
550	19	70	191.6	188.5
1000	36	80	181.8	180.3
2030	25	85	175.4	173.9
3050	29	75	171.6 </td <td>171.0</td>	171.0

Table 4-2 Measured peak-to-peak SPLs for the northwest transect taken at mid-depth

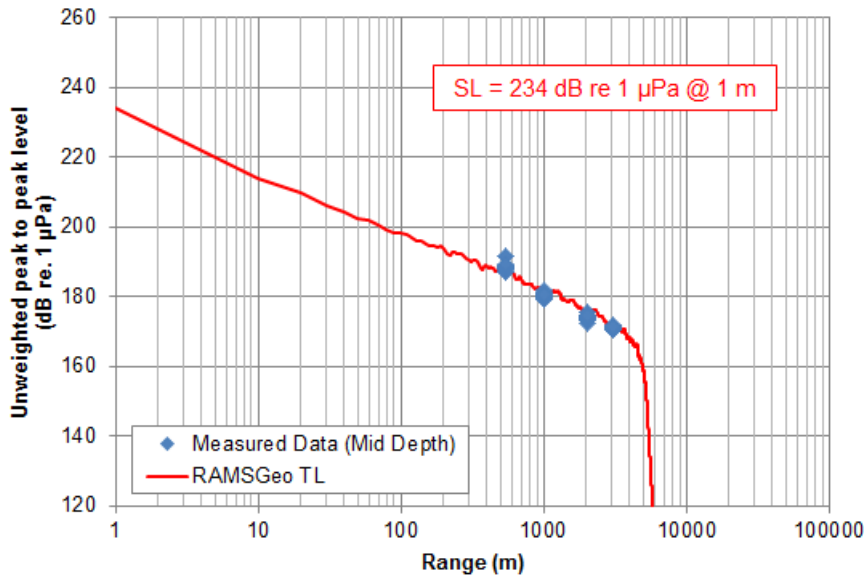


Figure 4-2 Level against range plot for the measured data taken along the northwest transect at mid-depth

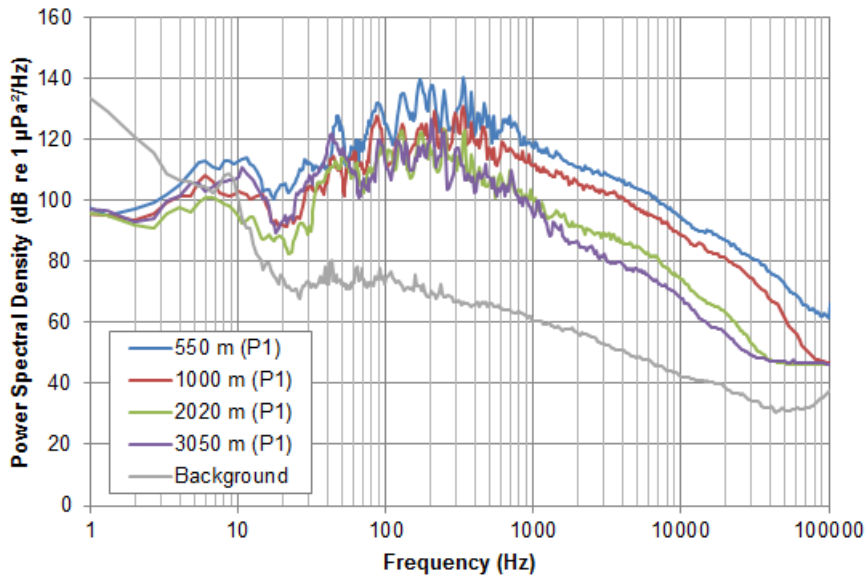


Figure 4-3 PSD levels of the measured data for the northwest transect at mid-depth

4.3.3 Pile 1 Northwest Transect – 1 m above seabed

Table 4-3 shows the data from measurements taken at 1 m above the seabed along the northwest transect. The peak-to-peak SPLs presented in Table 4-3 are seen to be higher than the SPLs measured at mid-depth and shown in Table 4-2, with the exception of the maximum peak-to-peak level measured at 550 m. Figure 4-4 provides a level range plot of the pile strikes measured close to the seabed. A RAMSGeo transmission loss fit has also been plotted which shows a 2 dB higher source level of 236 dB re 1 µPa @ 1 m compared to the data measured at mid-depth.

Distance (m)	No. of strikes recorded	Approx. blow energy (kJ)	Maximum level (dB re 1 µPa)	Mean level (dB re 1 µPa)
550	31	80	191.1	189.7
1000	43	80	183.4	182.5
2050	13	80	179.9	179.1
3050	28	80	173.8	173.2

Table 4-3 Measured peak-to-peak SPLs for the northwest transect taken 1 m above the seabed

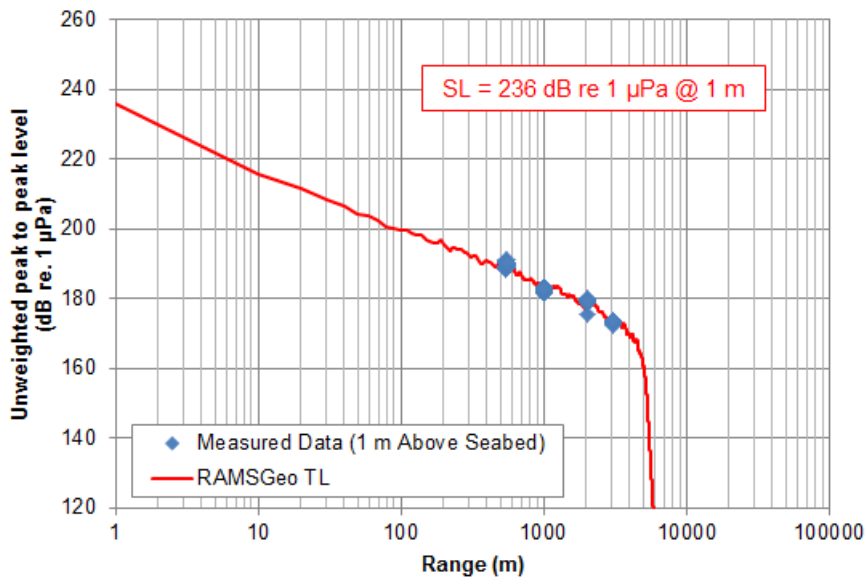


Figure 4-4 Level against range plot for measured data taken along the northwest transect 1 m above the seabed

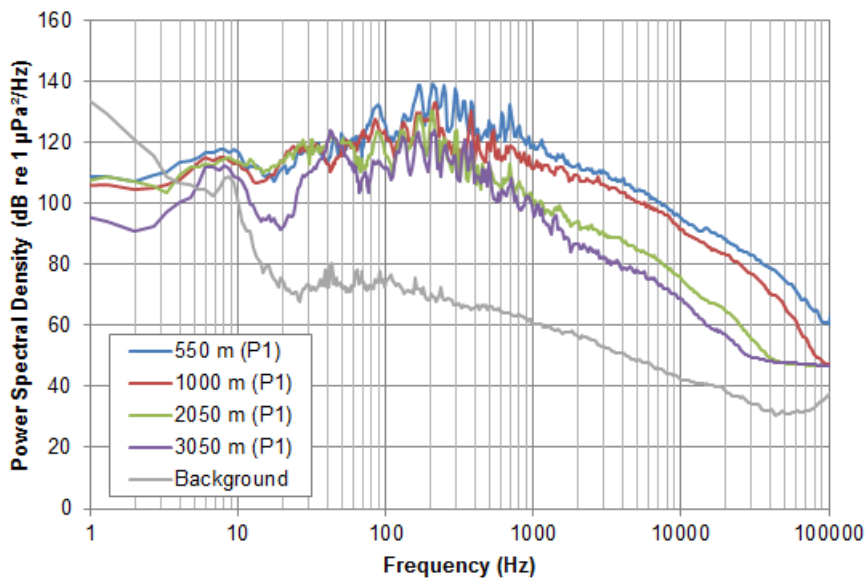


Figure 4-5 PSD levels of the measured data for the northwest transect 1 m above the seabed

4.3.4 Pile 2 and 3 East Transect – Mid-depth

Measurements were taken along an east transect at mid-depth for two piles. Table 4-4 presents a summary of the captured data at mid-depth along the east transect. Noise events of pile strikes were recorded up to 20 km from the piling.

Figure 4-6 shows a level vs range plot of the peak-to-peak SPLs with the RAMSGeo transmission loss fit for measurements taken along the east transect. The data from east transect provides an indication of the underwater noise propagation into deeper water.

Figure 4-7 displays the power spectral density level for a number of the measurements and shows how the transmission loss across the frequency range differs.

Distance (m)	No. of strikes Recorded	Approx. blow energy	Maximum levels (dB re 1 μ Pa)	Mean levels (dB re 1 μ Pa)
640 (P2)	35	70	188.2	184.9
1030 (P2)	20	80	183.2	182.5
2070 (P2)	15	75	176.2	175.2
4080 (P2)	29	80	168.8	167.4
7600 (P3)	18	70	162.8	158.8
12000 (P3)	42	80	156.8	155.7
20000 (P3)	41	160	147.8	140.0

Table 4-4 Measured peak-to-peak SPLs for the east transect taken at mid-depth

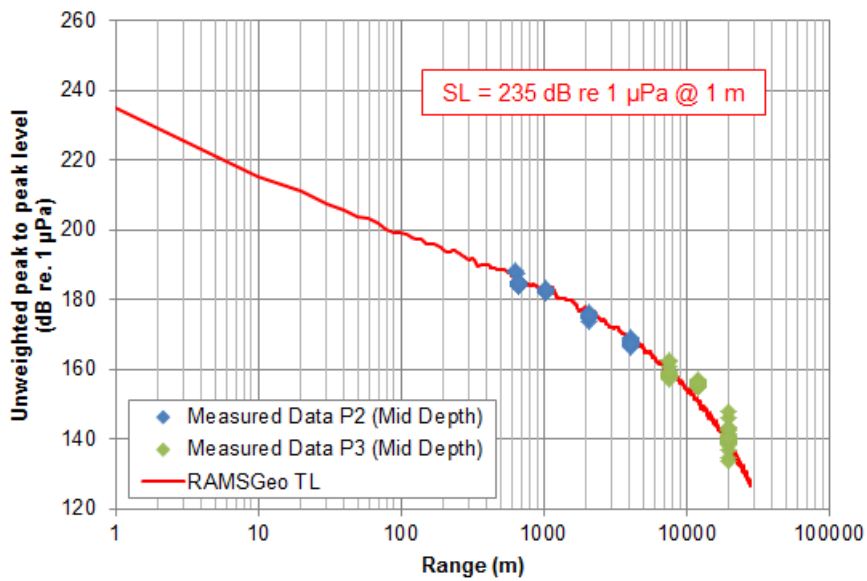


Figure 4-6 Level vs. range plot for measured data taken along the east transect at mid-depth

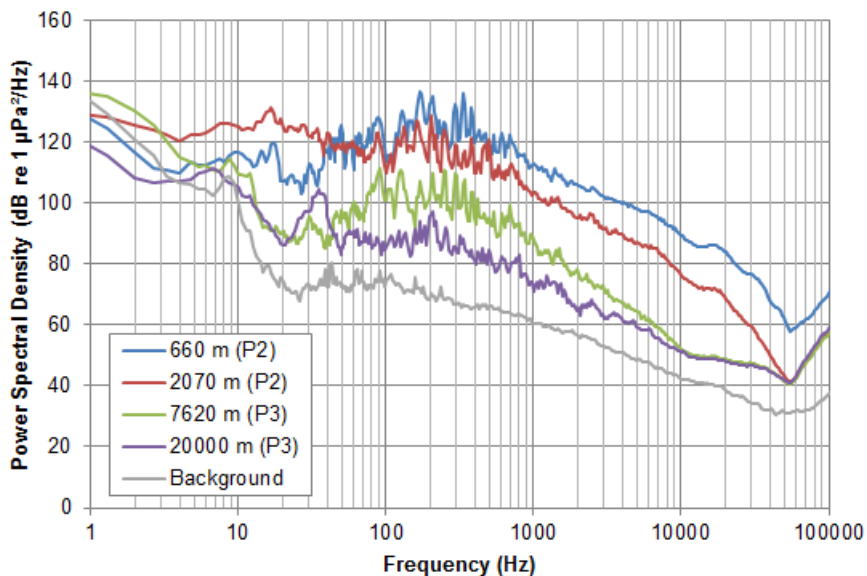


Figure 4-7 PSD levels of the measured data for the east transect taken at mid-depth

4.3.5 *Pile 2 East Transect – 1 m above seabed*

Underwater noise measurements of pile strikes were taken on an east transect 1 m above the seabed between 680 m and 4.05 km. Table 4-5 presents a summary of the measured peak to peak SPLs. A brief comparison of the levels measured at mid-depth presented in Table 4-4 shows the levels measured near the seabed to be greater when the distance from the piling is equivalent.

Figure 4-8 shows the measured data plotted on a level vs. range chart. The apparent source level, found by fitting transmission loss data from RAMSGeo to the data, was estimated to be 237 dB re 1 µPa @ 1 m which is 2 dB higher than calculated for the measured data taken at mid-depth.

The power spectral density levels are displayed in Figure 4-9 and show the broadband (i.e. covering a wide frequency range) nature of the measured noise. It also shows the transmission loss at higher frequencies to be greater with increasing range than for lower frequencies of the noise.

Distance (m)	No. of strikes Recorded	Approx. blow energy (kJ)	Maximum levels (dB re 1 µPa)	Mean levels (dB re 1 µPa)
680	31	80	188.3	187.4
1010	18	85	185.1	184.1
2080	15	75	179.6	178.5
4050	14	80	173.8	173.1

Table 4-5 Measured peak-to-peak SPLs for the east transect taken 1 m above the seabed

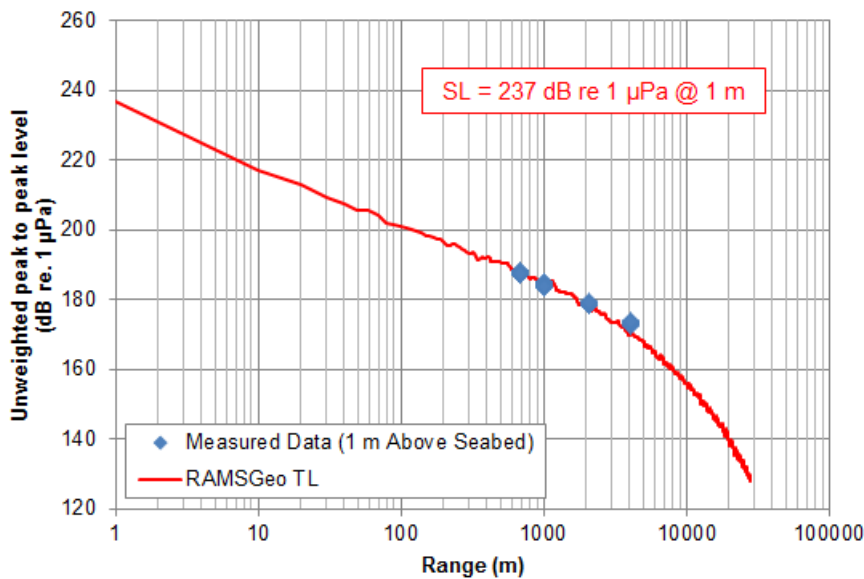


Figure 4-8 Level vs. range plot for measured data taken along the east transect 1 m above the seabed

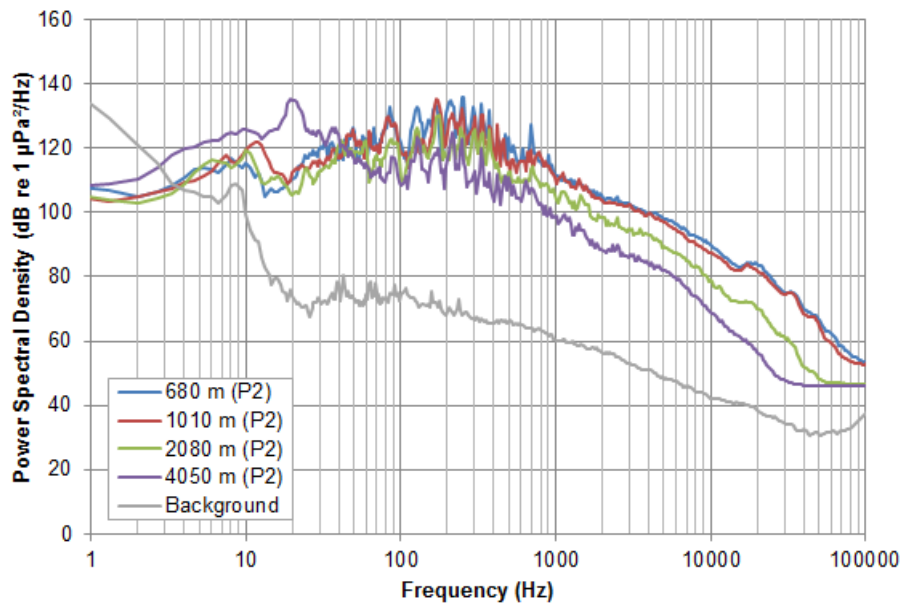


Figure 4-9 PSD levels of the measured data for the east transect taken 1 m above the seabed

4.3.6 SPL and blow energy comparison

The SPL RMS time history recorded by the fixed monitor, as shown in Figure 4-1, has been plotted along with the record of blow energy of the impact piling hammer for each of the four piles driven on 03 September 2015 and can be seen in Figure 4-10 to Figure 4-13.

In Figure 4-10 the SPL RMS level for the installation of the first pile on WTG2 follows the general trend of the blow energy, which varies between 60 and 100 kJ. Figure 4-11 and Figure 4-13 show that the blow energy for the installation of the second and fourth piles also consistently varied between 60 and 100 kJ with the maximum SPL RMS varying by 3 to 5 dB. Figure 4-12 shows the blow energy more than doubles from around 75 kJ to over 150 kJ for the last 5 minutes of piling for pile 3 of WTG2. The effect of the doubling the blow energy appears to increase the SPL RMS level by 2 to 3 dB to around 155 dB re 1 μ Pa, although this level was reached early on in the piling at a lower blow energy. It should be noted that, in theory, a doubling of energy or power equates to a 3 dB increase in level.

Measurement and assessment of underwater noise and vibration during construction at the Block Island wind farm, Rhode Island

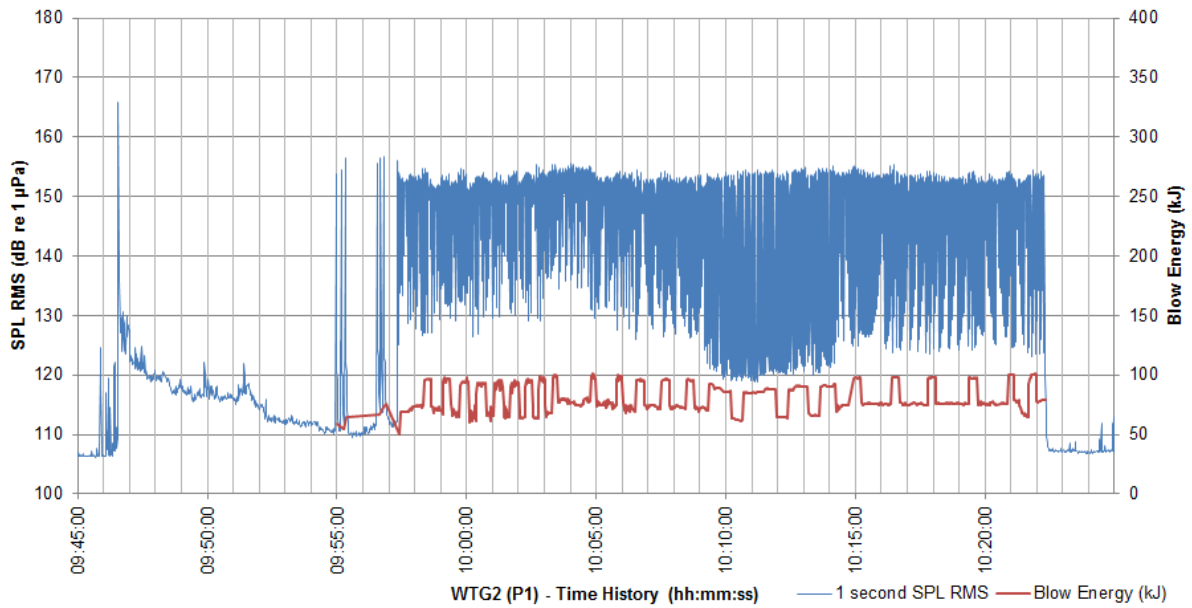


Figure 4-10 Time history of SPL RMS recorded by the fixed monitor 750 m from WTG2 and blow energy of hammer used to install pile 1 on 03 September 2015

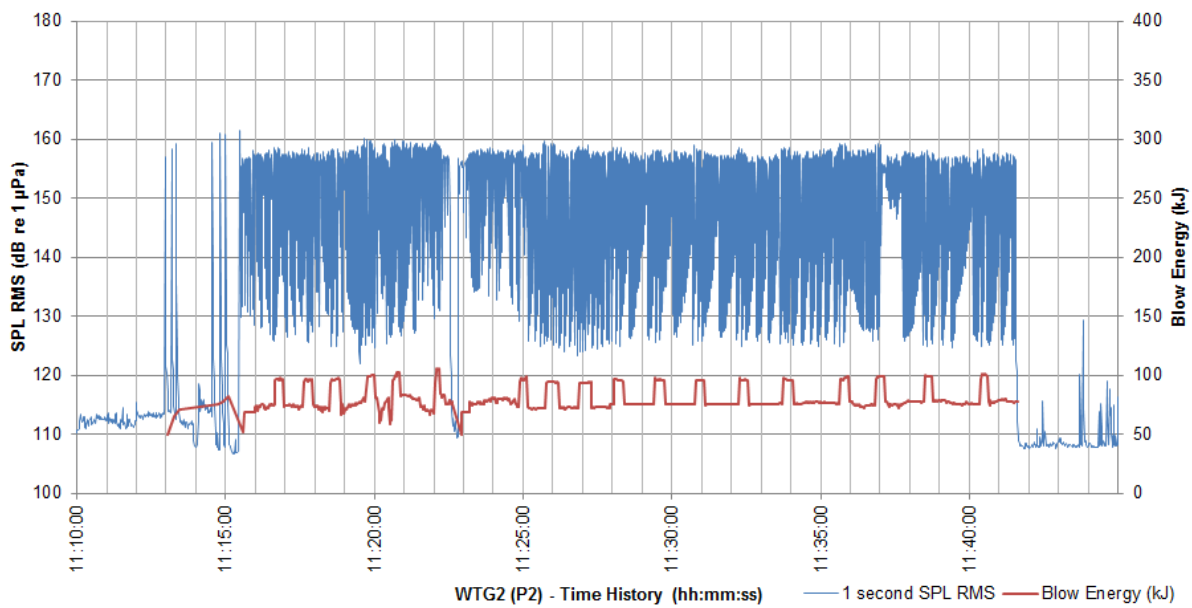


Figure 4-11 Time history of SPL RMS recorded by the fixed monitor 750 m from WTG2 and blow energy of hammer used to install pile 2 on 03 September 2015

Measurement and assessment of underwater noise and vibration during construction at the Block Island wind farm, Rhode Island

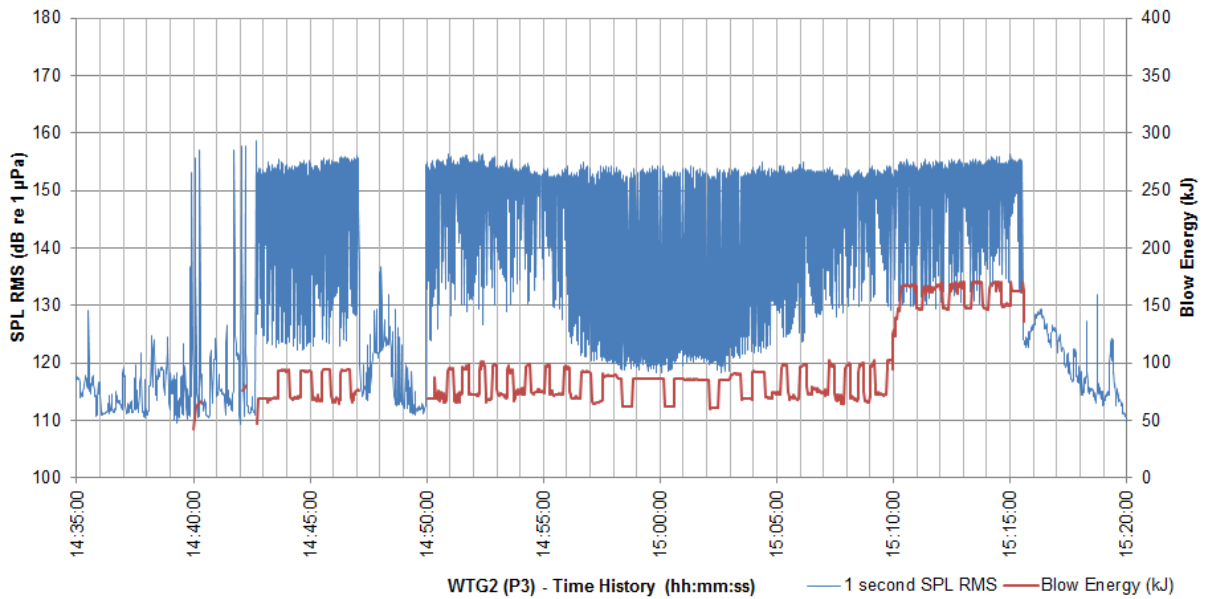


Figure 4-12 Time history of SPL RMS recorded by the fixed monitor 750 m from WTG2 and blow energy of hammer used to install pile 3 on 03 September 2015

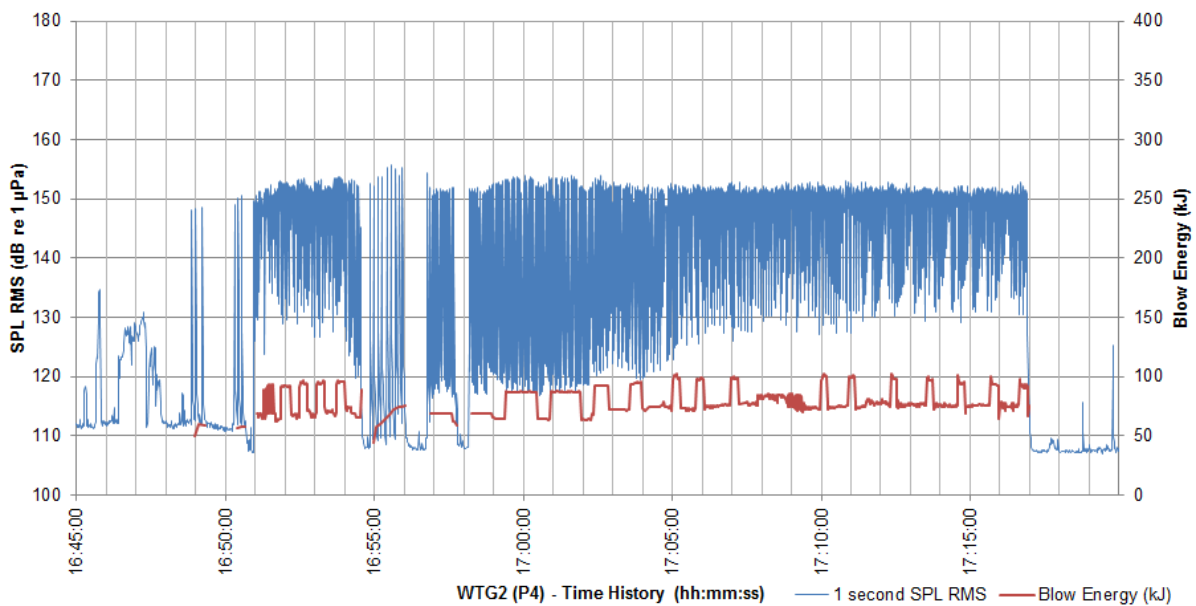


Figure 4-13 Time history of SPL RMS recorded by the fixed monitor 750 m from WTG2 and blow energy of hammer used to install pile 4 on 03 September 2015

4.4 WTG5 – 17 September 2015

4.4.1 Overview

Underwater noise measurements were undertaken on 17 September 2015 at a fixed location. At the same time, measurements of seabed vibration were undertaken; these are reported in section 5. The pile driving was carried out on WTG5 foundation. The jacket structure of the foundation had been placed and the first stage of the four piles had been placed into the jacket.

Prior to the start of piling the fixed monitor was deployed and anchored 790 m from WTG5. Figure 4-14 shows the SPL RMS time history data recorded by the fixed monitor. The plot shows the three piling events that occurred with the second pile producing slightly lower levels of underwater noise compared to pile 1 and 3. Each of the piles took between 45 and 80 minutes to install including the small breaks in piling at the start, most notably for pile 1 and 3. The noise level between piling is seen to be similar to the mean background levels presented in section 3.2, although will not reach the lowest levels due to the noise floor of the instrument mentioned in section 4.3.1.

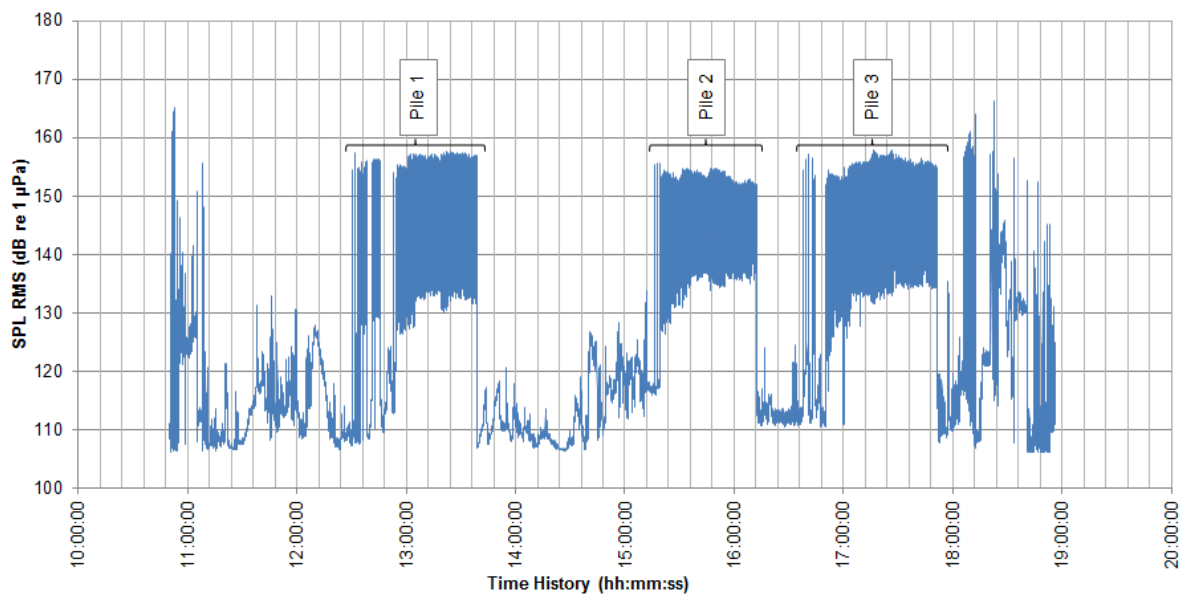


Figure 4-14 Time history plot of SPL RMS recorded by the fixed monitor 790 m from WTG5 on 17 September 2015

4.4.2 SPL and blow energy comparison

The SPL RMS time history recorded by the fixed monitor, as shown in Figure 4-14, has been plotted along with the record of blow energy of the impact piling hammer for the first and third piles driven on 17 September 2015 and can be seen in Figure 4-15 and 4-16.

Figure 4-15 and 4-16 both show step increases in the blow energy during the piling of the first and third piles. The effect of the step increases in blow energy in regards to the SPL can be seen in Figure 4-15 where resultant level is slightly higher following the increase. The smaller variations in blow energy also appear to affect the variation in the maximum levels in the time history. Slight increases in the SPL are also seen for the first two step increases in blow energy in Figure 4-16 for pile 3.

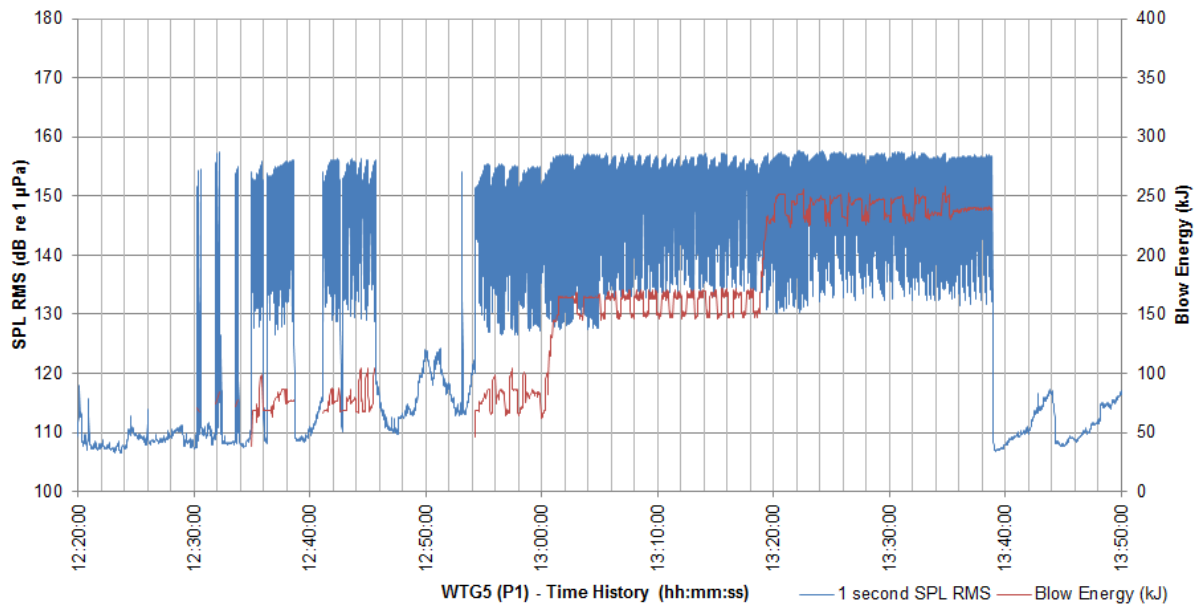


Figure 4-15 Time history of SPL RMS recorded by the fixed monitor 790 m from WTG5 and blow energy of hammer used to install pile 1 on 17 September 2015

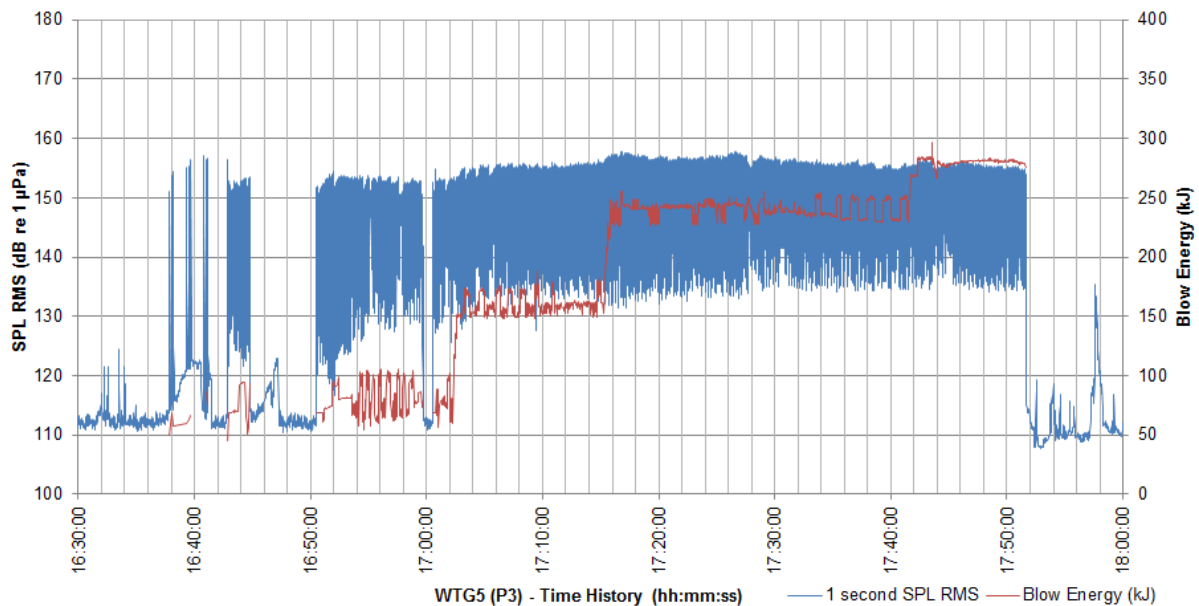


Figure 4-16 Time history of SPL RMS recorded by the fixed monitor 790 m from WTG5 and blow energy of hammer used to install pile 3 on 17 September 2015

4.5 WTG3 – 18 September 2015

Underwater noise measurements took place during the second stage of pile driving for the foundation WTG3 which took place on 18 September 2015. The jacket foundation had been set and the first stage of pile driving had occurred.

The fixed monitor was deployed at 840 m from WTG3, slightly further than the intended 750 m due to vessel drift, at mid-depth prior to the start of piling and captured the underwater noise of all four of the driven piles. Underwater noise transect measurements were carried out during the pile driving of the fourth pile along a transect to the southeast from WTG3, out into deeper waters.

Figure 4-17 presents a plot of SPL RMS recorded by the fixed monitor. The four piling events are clearly evident. The first two piles that were driven appear to have produced higher levels of underwater noise than the third and fourth piles. Each of the four piles took between 45 and 65 minutes to install with short breaks of 20 to 30 minutes between piles 1 and 2 and piles 3 and 4.

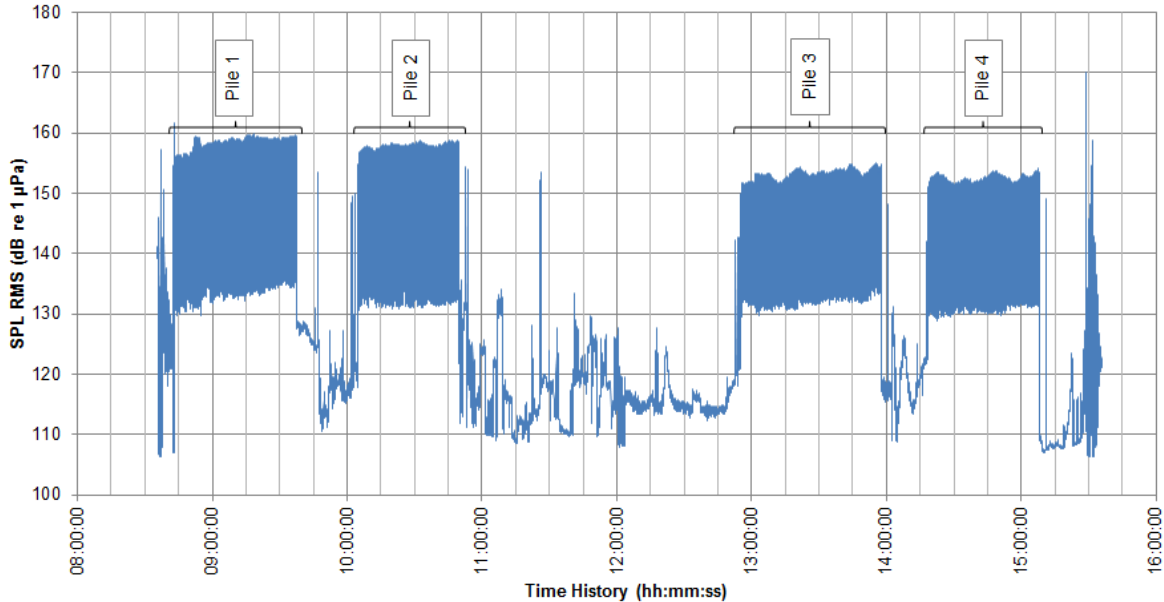


Figure 4-17 Time history plot of SPL RMS recorded by the fixed monitor 840 m from WTG2 on 18 September 2015

4.5.1 Pile 4 Southeast Transect – Mid-depth

Table 4-6 presents a summary of the measurements undertaken on the southeast transect at mid-depth from WTG3. The table shows maximum and mean peak to peak SPLs of pile strikes measured between 480 m and 6.41 km.

The measured peak-to-peak levels of the pile strikes for the southeast transect have been plotted and can be seen in Figure 4-18. A RAMSGeo transmission loss fit has been applied to the data to determine the apparent source level of 242 dB re 1 µPa @ 1 m. It is of note that the measured data points fall slightly faster than the RAMSGeo fit suggests. Measurements were taken on a progressively closer transect (rather than moving away with time) and the measurements at closer range were at a higher blow energy.

Figure 4-19 displays the power spectral density level for a number of the measurements and shows how the transmission losses across the frequency range change.

Distance (m)	No. of strikes recorded	Approx. blow energy (kJ)	Maximum level (dB re 1 μ Pa)	Mean level (dB re 1 μ Pa)
480	12	300	196.4	196.1
730	30	300	195.3	193.3
1620	24	300	186.0	185.0
2060	12	300	182.6	182.3
3040	18	300	179.3	178.8
6410	28	300	168.7	166.9

Table 4-6 Measured peak-to-peak SPLs for the south east transect taken at mid-depth

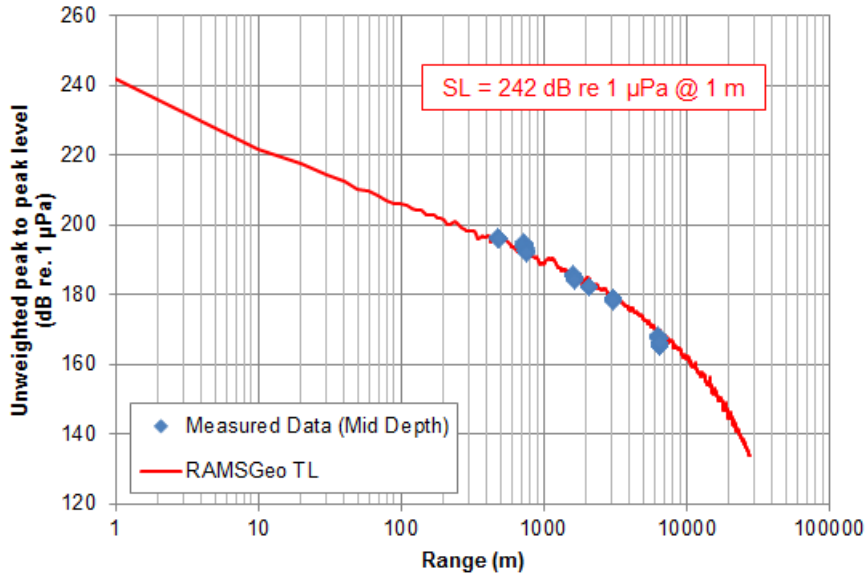


Figure 4-18 Level vs. range plot for measured data taken along the southeast transect at mid-depth

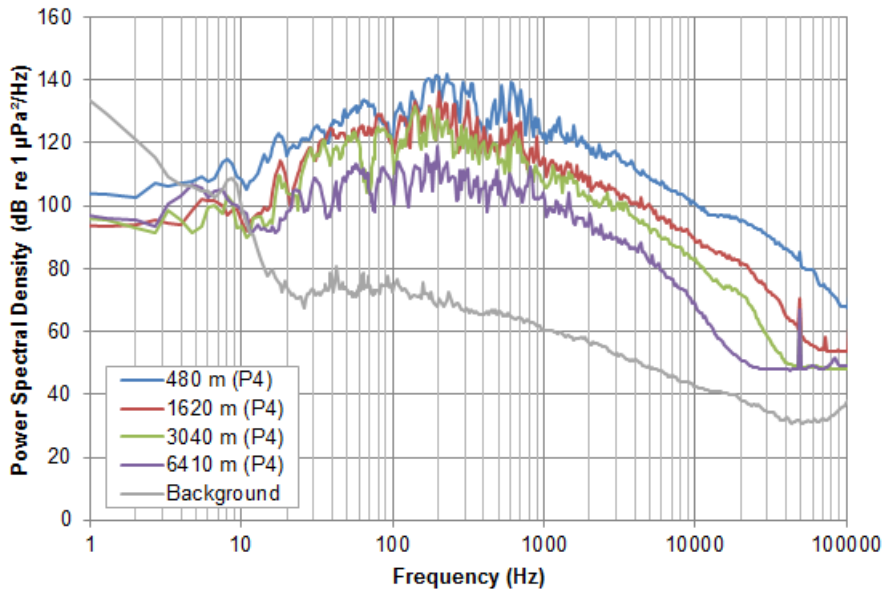


Figure 4-19 PSD levels of the measured data for the southeast transect taken at mid-depth

4.5.2 SPL and blow energy comparison

The SPL RMS time history recorded by the fixed monitor, as shown in Figure 4-17, has been plotted along with the record of blow energy of the impact piling hammer for each of the four piles driven on 18 September 2015 and can be seen in Figure 4-20 to Figure 4-23.

The blow energy used to install each of the four piles on 18 September 2015 was higher than during samples presented on the other days. On further investigation it was found that for the piling of the second stage section of a pile, in general a greater blow energy is used. Given that the pile, during the second stage, consists of two piles welded together and hence a greater mass suggests that a higher blow energy is required to install the pile at an equivalent rate.

Increases in blow energy are again seen to cause slight increases in SPL, most notably for the first pile shown in Figure 4-20 when the blow energy almost reached 600 kJ for a short duration. Figure 4-21 and Figure 4-23 shows the blow energy remains consistent at around 300 kJ for the whole duration of piling for pile 2 and 4. The maximum SPLs for installation of pile 2 are approximately 5 dB higher than they are for pile 4, ruling out blow energy as the reason for difference in SPL.

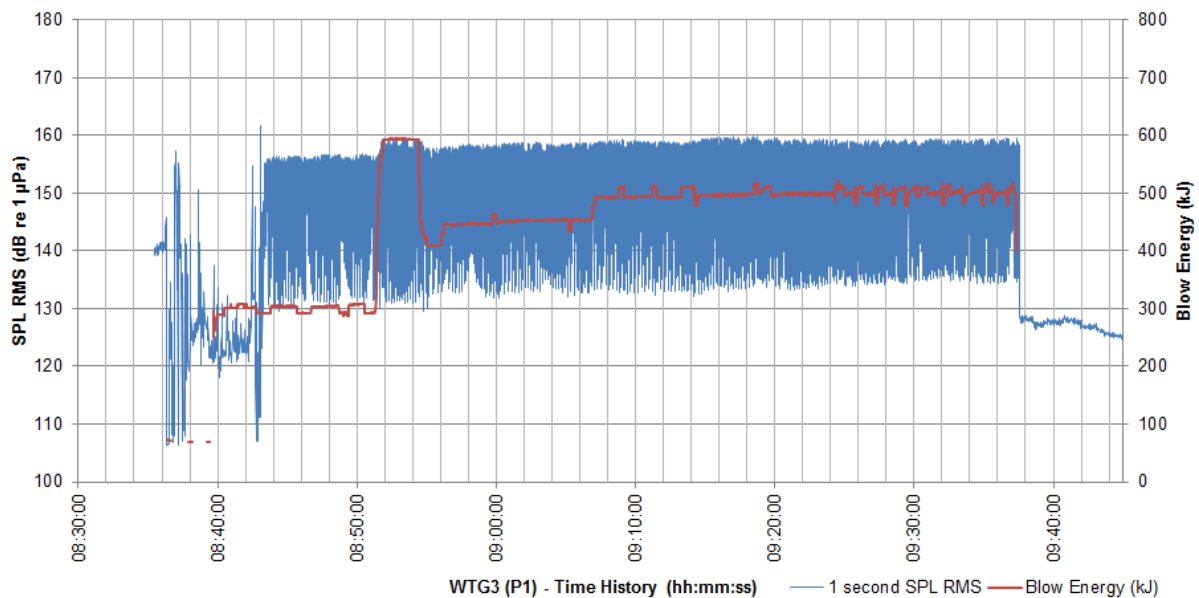


Figure 4-20 Time history of SPL RMS recorded by the fixed monitor 840 m from WTG3 and blow energy of hammer used to install pile 1 on 18 September 2015

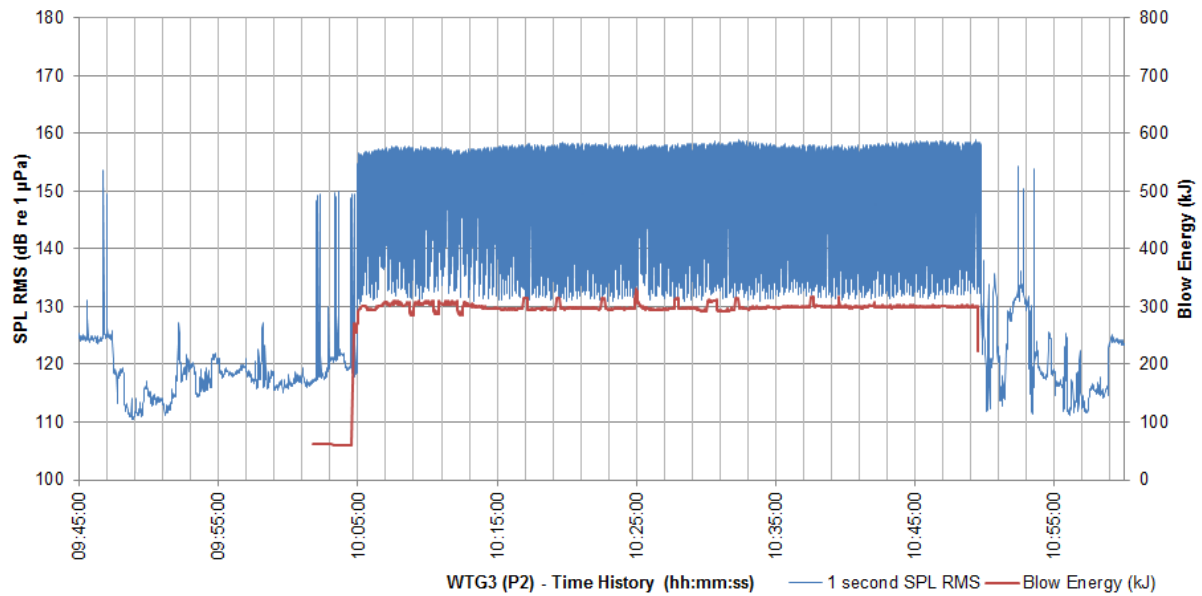


Figure 4-21 Time history of SPL RMS recorded by the fixed monitor 840 m from WTG3 and blow energy of hammer used to install pile 2 on 18 September 2015

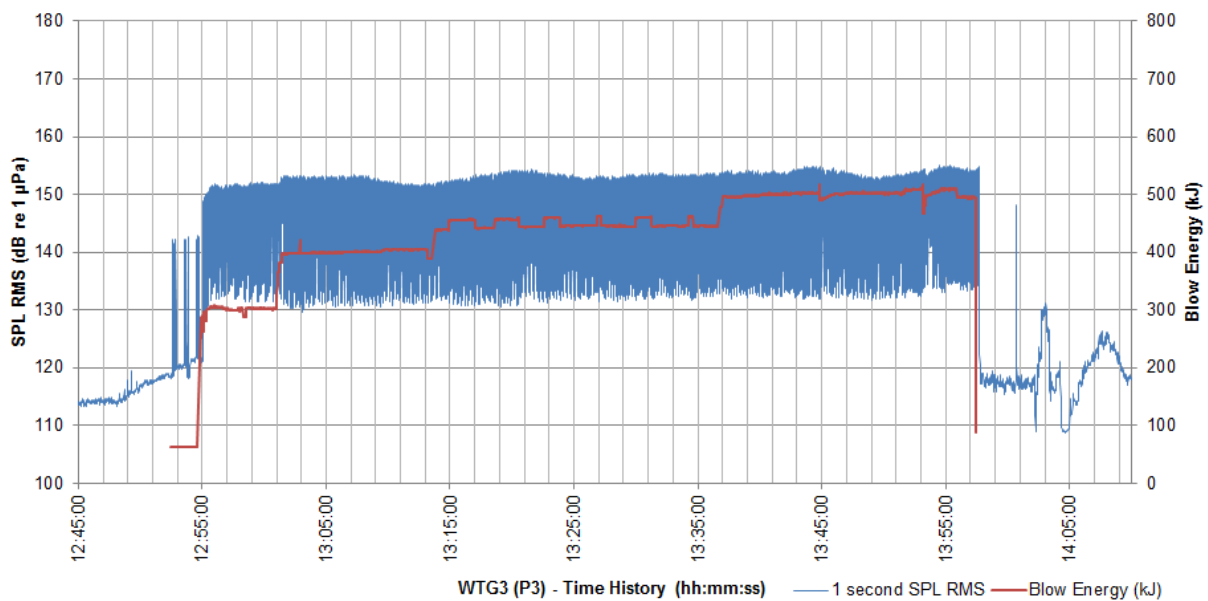


Figure 4-22 Time history of SPL RMS recorded by the fixed monitor 840 m from WTG3 and blow energy of hammer used to install pile 3 on 18 September 2015

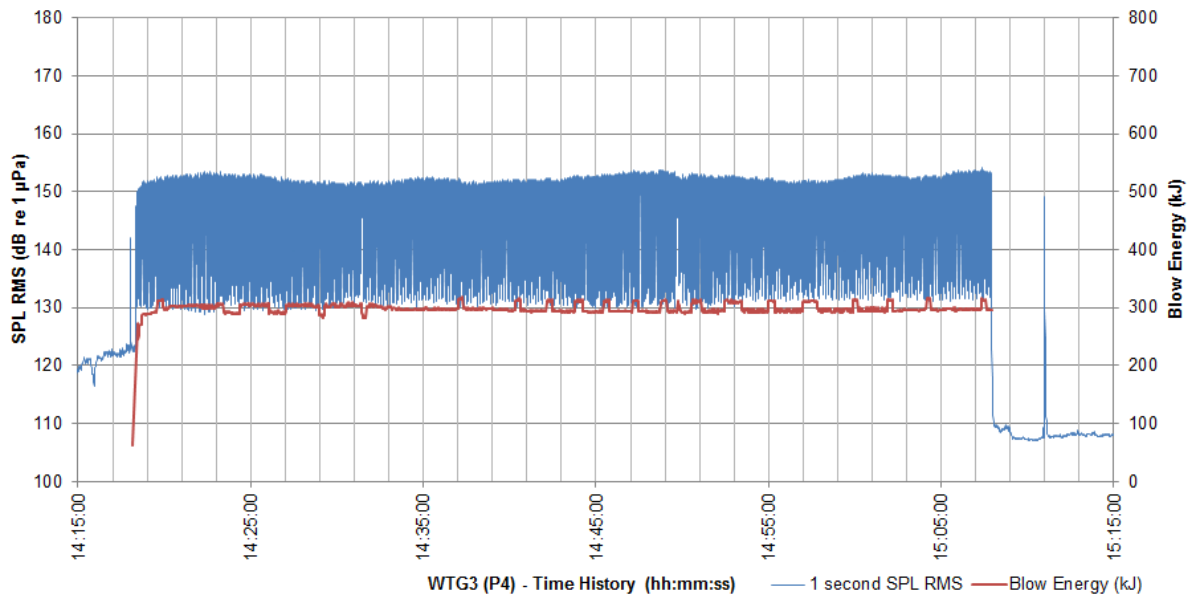


Figure 4-23 Time history of SPL RMS recorded by the fixed monitor 840 m from WTG3 and blow energy of hammer used to install pile 4 on 18 September 2015

4.6 WTG1 – 19 September 2015

4.6.1 Overview

Pile driving for the first stage of the WTG1 foundation was carried out on 19 September 2015. Piling began at 8:30, earlier than expected, and transect measurements were started immediately before the fixed monitor was installed. Measurements were taken along a north transect towards Point Judith starting at 710 m from WTG1. Once there was a break in piling the fixed monitor was deployed at a distance of 5.93 km and a depth of 1 m above the seabed. The piling resumed on pile 1 at 12:25, and measurements were taken from the survey vessel at 12.4 km. The survey vessel then continued on the north transect in order to take measurements further out for the second pile. Pile strikes were recorded out to 24 km during installation of the second pile. Measurements were attempted at a greater range of 27 km but due to the presence of several vessels in the vicinity and coastal noise, pile strikes were not clearly detected. For the installation of the third and fourth piles the survey vessel moved back toward WTG1 foundation and measurements were undertaken at distances where measurements were not previously taken during the first and second pile installations.

Figure 4-24 shows a graph of time history vs. SPL RMS recorded by the fixed monitor. The fixed monitor captured all the piling events except for the first piling at the start of the day between 08:30 and 08:56. The breaks between piling events, following the completion of the first pile, are 20 to 25 minutes. It can be seen that the underwater noise measured for the final part of the first pile appears to be 10 dB greater than the levels recorded for the following three piles. This increase has not been explained at the time of writing.

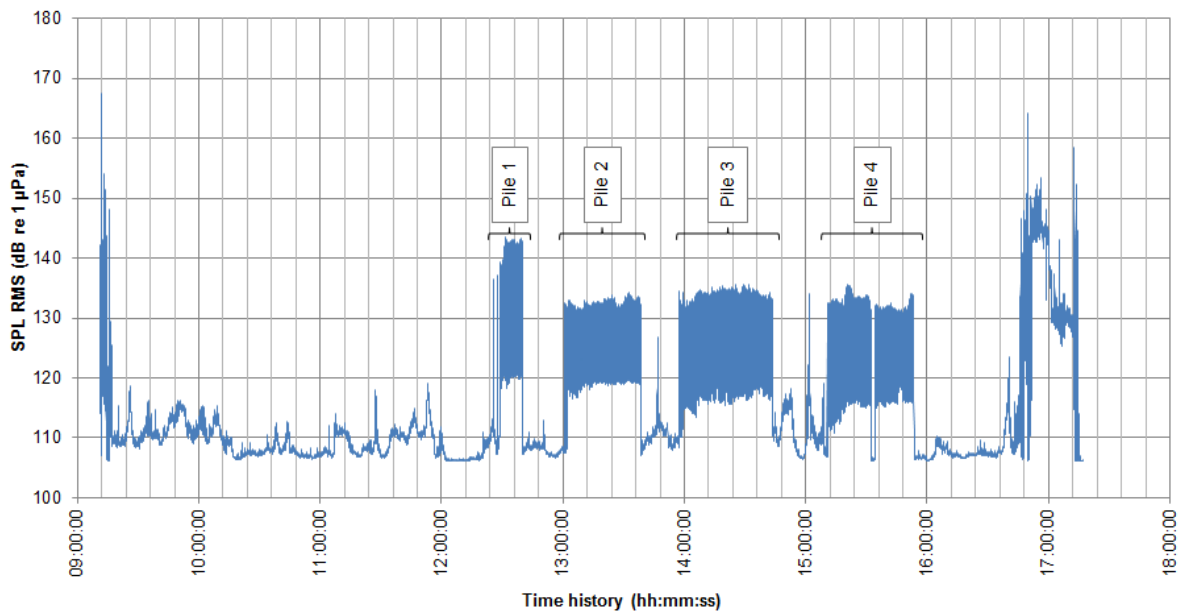


Figure 4-24 Time history plot of SPL RMS recorded by the fixed monitor 5.93 km from WTG1 1 m above the seabed on 19 September 2015

4.6.2 Piles 1 to 4 North Transect – Mid-depth

Table 4-7 provides a summary of the measured peak-to-peak SPLs for the pile strikes recorded on the north transect. The table shows measurements of the pile strikes for the four different piles. On the whole it is seen that with increasing distance the SPLs decrease as expected. However the levels measured at 12.4 km when pile 1 was being driven are higher than those measured at 6.14 km for pile 4. The most likely reason for the measured level to be higher at a greater distance is that the source level was significantly greater, which is evidenced in Figure 4-24. It does not appear to be possible to attribute this to higher blow energies (see section 4.6.3).

Figure 4-25 illustrates the measured data on a level range plot. RAMSGeo propagation loss curves have been fit to the data. It was seen as necessary to fit two separate curves because of the difference level between pile 1 and the rest previously highlighted in Figure 4-24.

Figure 4-26 presents power spectral density levels of the measured data.

Distance (m)	No. of strikes recorded	Blow energy	Maximum level (dB re 1 µPa)	Mean level (dB re 1 µPa)
710 (P1)	25	-	196.7	194.6
1560 (P1)	32	-	188.5	187.2
3990 (P1)	20	-	183.3	182.3
6140 (P4)	24	80	163.7	162.2
12400 (P1)	69	105	166.8	163.2
15300 (P3)	37	160	146.1	143.6
18100 (P2)	34	75	145.8	142.4
20000 (P3)	57	120	142.1	138.8
24000 (P2)	8	165	140.9	138.6

Table 4-7 Measured peak-to-peak SPLs for the north transect taken at mid-depth

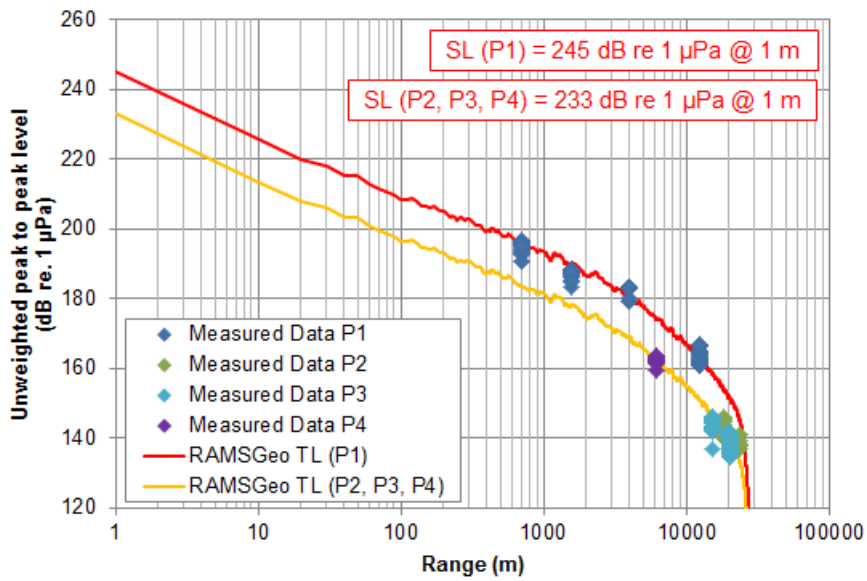


Figure 4-25 Level vs. range plot for measured data taken along the north transect at mid-depth

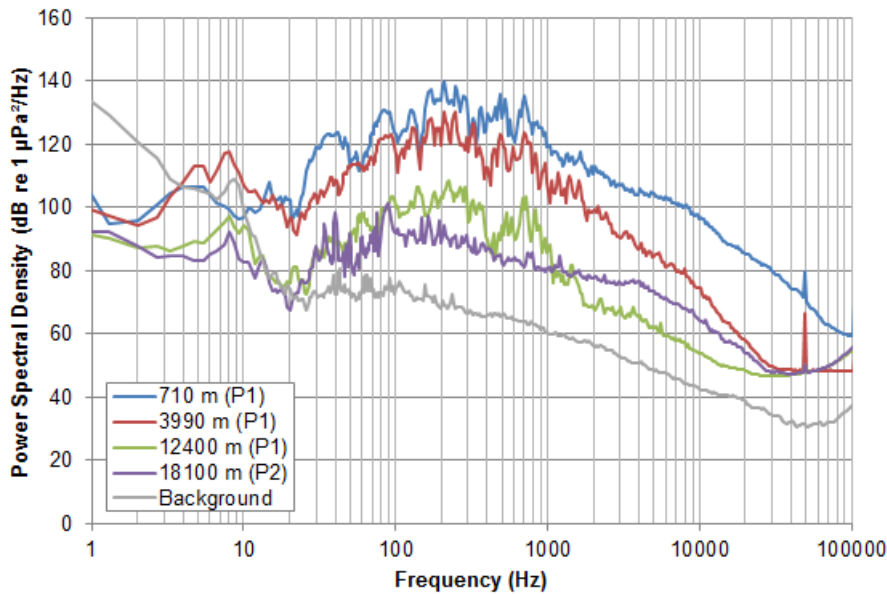


Figure 4-26 PSD levels of the measured data for the southeast transect taken at mid-depth

4.6.3 SPL and blow energy comparison

The SPL RMS time history recorded by the fixed monitor, as shown in Figure 4-24, has been plotted along with the record of blow energy of the impact piling hammer for each of the four piles driven on 03 September 2015 and can be seen in Figure 4-27 to Figure 4-30.

It was noted at the beginning of section 4.6 that SPL during the installation of pile 1 was 10 dB higher than for the subsequent three piles. Figure 4-27 to Figure 4-30 show the blow energies are comparable for all four piles driven, therefore, the higher SPL is not caused by a greater blow energy used on pile 1.

Measurement and assessment of underwater noise and vibration during construction at the Block Island wind farm, Rhode Island

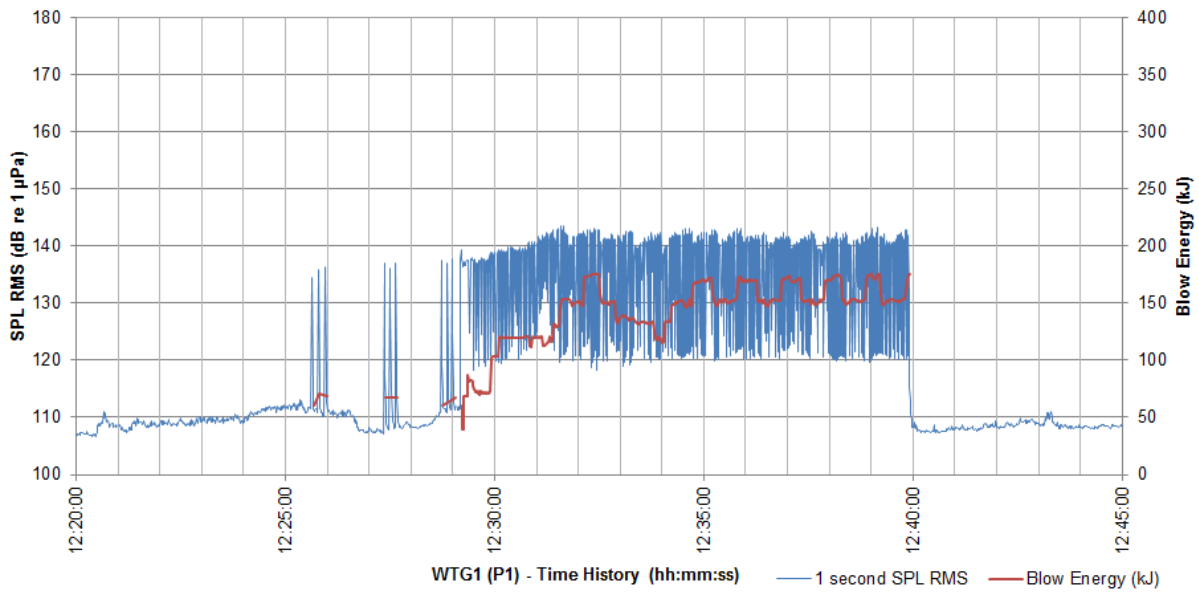


Figure 4-27 Time history of SPL RMS recorded by the fixed monitor 5.93 km from WTG3 and blow energy of hammer used to install pile 1 on 19 September 2015

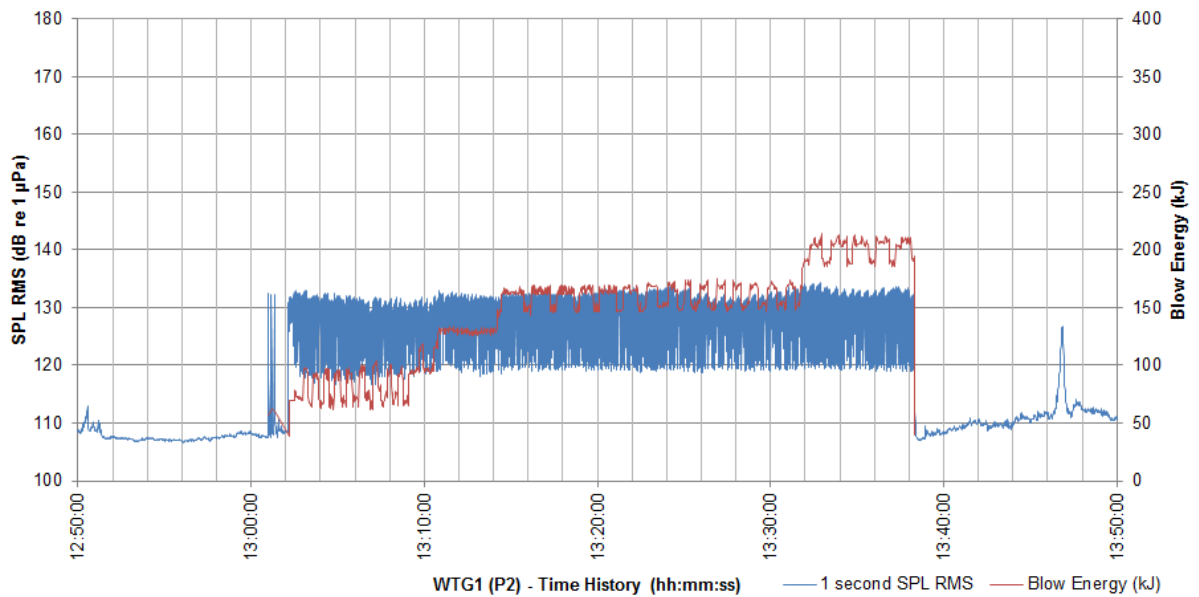


Figure 4-28 Time history of SPL RMS recorded by the fixed monitor 5.93 km from WTG3 and blow energy of hammer used to install pile 2 on 19 September 2015

Measurement and assessment of underwater noise and vibration during construction at the Block Island wind farm, Rhode Island

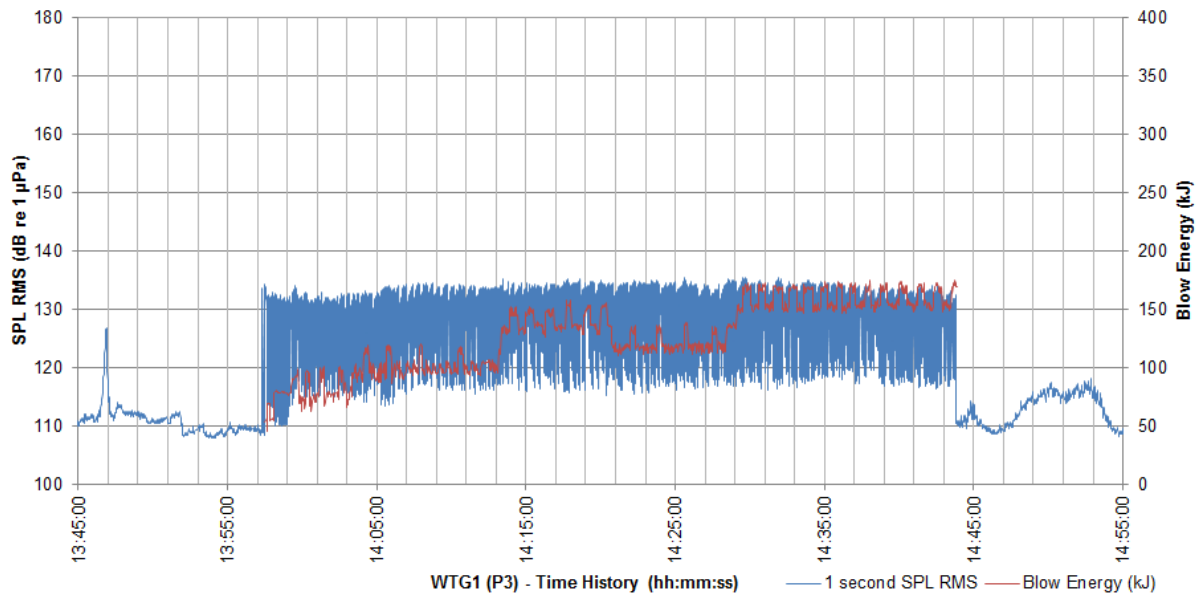


Figure 4-29 Time history of SPL RMS recorded by the fixed monitor 5.93 km from WTG3 and blow energy of hammer used to install pile 3 on 19 September 2015

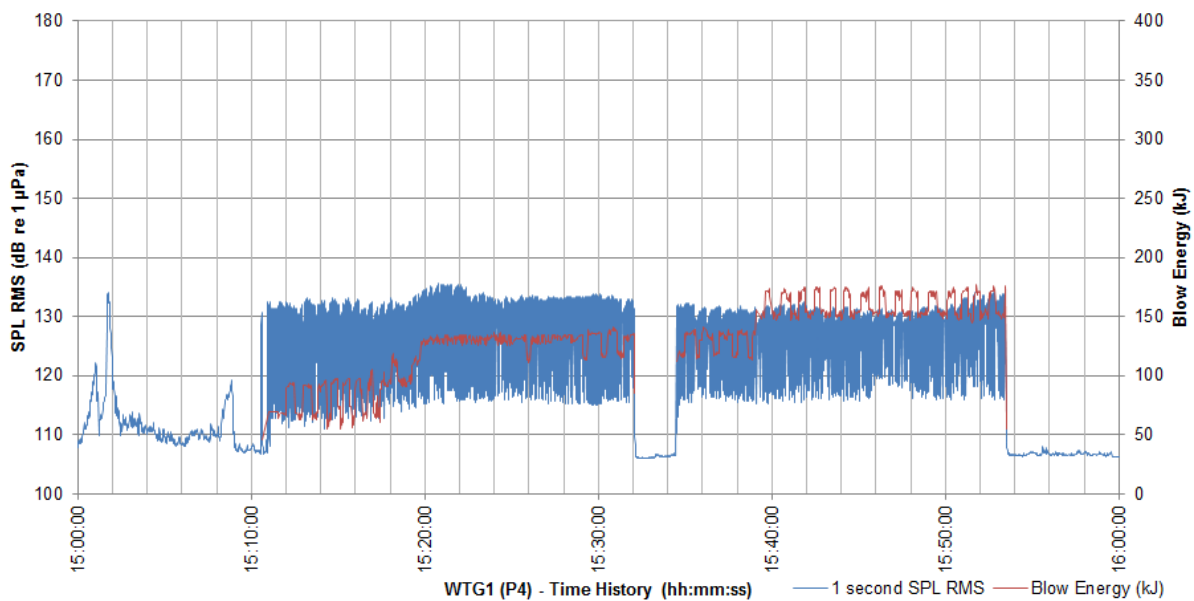


Figure 4-30 Time history of SPL RMS recorded by the fixed monitor 5.93 km from WTG3 and blow energy of hammer used to install pile 4 on 19 September 2015

4.7 Summary and comparisons

4.7.1 Summary

A summary of the estimated source levels for each measurement transect has been collated in Table 4-8. The estimated peak-to-peak source levels, using transmission losses calculated in RAMSGeo, are between 233 and 245 dB re 1 μ Pa @ 1 m.

Transect ID	Transect direction	Hydrophone depth	SL	Figure reference
1	Northwest	Mid	-	-
2	Northwest	Mid	234	Figure 4-2
3	Northwest	Seabed	236	Figure 4-4
4	East	Mid	235	Figure 4-6
5	East	Seabed	237	Figure 4-8
6	South East	Mid	242	Figure 4-18
7 (Pile 1)	North	Mid	245	Figure 4-25
7 (Piles 2-4)	North	Mid	233	Figure 4-25

Table 4-8 Estimates of source level (SL) based on fits to the measurement transects from the piling operations

4.7.2 Comparison with measured data

In order to make a comparison with the levels measured at the BIWF site, the noise levels recorded at a range of 750 m have been compared with similar projects measured by Subacoustech Environmental at wind farm sites in the EU. Where measurements were not taken at the exact range of 750 m, the transmission losses estimated using RAMSGeo have been used. Table 4-9 summarises both the peak-to-peak levels and single strike SEL values for the measurements.

It can be seen that the levels measured at BIWF (with 1.372 m diameter piles) are in line with what would be expected, with levels for smaller piles (North Sea, 1.067 m) being lower and the majority of levels for the larger piles (East Irish Sea and Moray Firth) being higher. As with all measurements like this, there will be complications when comparing sites as there are so many different parameters involved. For example, these basic comparisons do not take into account changes in bathymetry, sediment type, or temperature data etc.

BIWF Transect ID	Level at 750m (pk-pk)	Level at 750m (SEL _{ss})	EU Windfarm site	Level at 750m (pk-pk)	Level at 750m (SEL _{ss})
2	184	160	UK east coast (1.372m)	182	158
3	185	161	North Sea (1.829m)	193	165
4	185	161	North Sea (1.067m)	185	158
5	187	162	East Irish Sea (1.830m)	191	163
6	191	166	East Irish Sea (1.830m)	192	164
7 (Pile 1)	195	168	East Irish Sea (1.830m)	192	166
7 (Piles 2-4)	183	159	East Irish Sea (1.830m)	192	164
			Moray Firth (1.830m)	194	165

Table 4-9 Comparison of measured noise levels at a range of 750 m at the BIWF site (with pile diameters of 1.372 m) and other measurements undertaken in the EU

4.7.3 *Comparison with modelled data*

Underwater noise modelling for impact piling at the Block Island site was carried out by Deepwater Wind using the RAMGeo acoustic model, as reported in the Block Island Wind Farm and Block Island Transmission System, Environmental Report Appendix N-2 Underwater Acoustic Report (Deepwater Wind, May 2012). The modelling was carried out over eight equally spaced transects (one every 45°) for two pile hammer energies; 200 kJ and 600 kJ. The ranges to three thresholds were presented:

- 180 dB re 1 µPa (RMS) – MMPA Level A harassment threshold, where noise has the potential to injure a receptor.
- 160 dB re 1 µPa (RMS) – MMPA Level B harassment threshold, where noise has the potential to disturb a receptor. This threshold is specifically for impulsive noise sources.
- 120 dB re 1 µPa (RMS) – MMPA Level B harassment threshold; as above. This threshold is for a continuous noise source or an intermittent non-pulsed source; this is not specifically relevant to impact piling, however it has been included to aid comparisons to the modelling undertaken by Deepwater Wind.

The measured data along with the RAMSGeo transmission losses (Section 2.3.2) are presented alongside the modelled data from Deepwater Wind below. Table 4-10 and Table 4-11 show the closest modelled transects to those measured at BIWF and the difference in range between the modelled and measured disturbance thresholds. These results are shown as level against range plots in Figure 4-31 to Figure 4-34.

These results show that the modelling gives a conservative prediction of the measured noise, with almost all the measured levels being lower than those predicted by Deepwater Wind using RAMGeo. Also, it can be seen that, for the majority of the transects, the difference between the measured and modelled levels becomes greater with range.

BIWF Transect ID	Approx. measured bearing	Closest modelled bearing	Closest modelled blow energy	Range to 180 dB _{RMS}	Range to 160 dB _{RMS}	Range to 120 dB _{RMS}
2 (Northwest)	316°	315°	200 kJ	61 m	3.1 km	5.75 km
3 (Northwest)						
4 (East)	80°	90°	200 kJ	60 m	2.7 km	30.6 km
5 (East)						
6 (Southeast)	97°	90°	600 kJ	382 m	4.6 km	37.5 km
7 (Pile 1) (North)	346°	0°	200 kJ	61 m	2.8 km	27.4 km
7 (Piles 2-4) (North)						

Table 4-10 Summary of the measured transects and the modelling parameters from Deepwater Wind that correspond closest to them

BIWF Transect ID	Difference in range between the measured and modelled disturbance threshold levels		
	180 dB _{RMS}	160 dB _{RMS}	120 dB _{RMS}
2 (Northwest)	+ 21 m	+ 2.4 km	+ 0.35 km
3 (Northwest)	+ 11 m	+ 2.1 km	+ 0.31 km
4 (East)	+ 2 m	+ 1.8 km	+ 14.2 km
5 (East)	0 m	+ 1.5 km	+ 13.8 km
6 (Southeast)	+ 270 m	+ 2.8 km	+ 16.7 km
7 (Pile 1) (North)	- 69 m	+ 0.88 km	+ 4.5 km
7 (Piles 2-4) (North)	+ 30 m	+ 2.1 km	+ 10.8 km

Table 4-11 Summary of the difference in range, between the measured and modelled noise levels for the three disturbance thresholds

Measurement and assessment of underwater noise and vibration during construction at the Block Island wind farm, Rhode Island

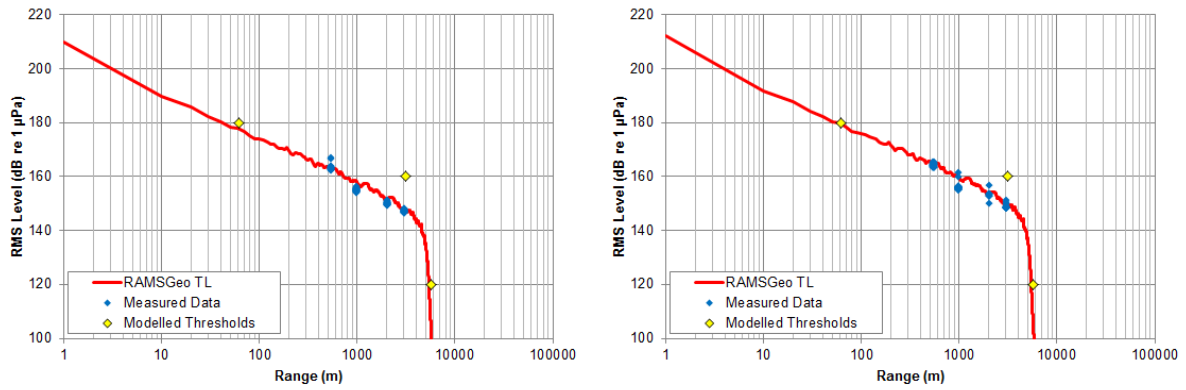


Figure 4-31 Comparison between measured data and modelled thresholds for transects 2 (left) and 3 (right) using the modelled data from the 315° transect using a 200 kJ blow energy

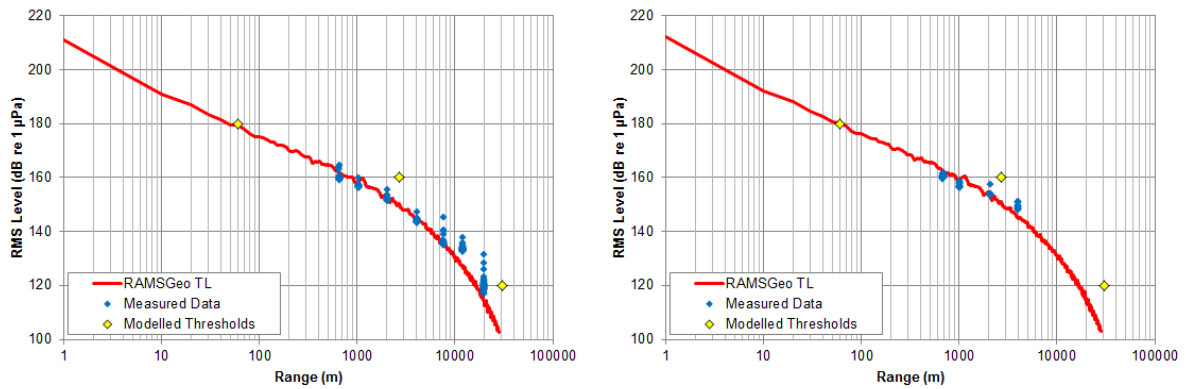


Figure 4-32 Comparison between measured data and modelled thresholds for transects 4 (left) and 5 (right) using the modelled data from the 90° transect using a 200 kJ blow energy

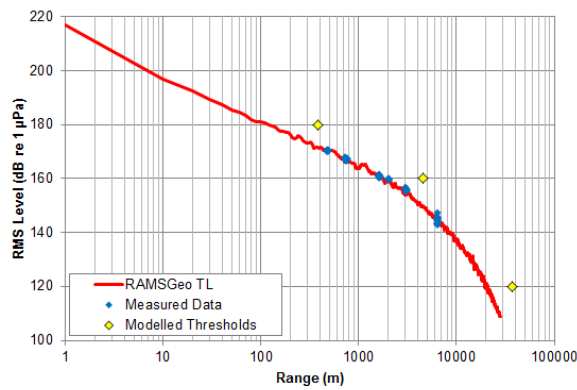


Figure 4-33 Comparison between measured data and modelled thresholds for transect 6 using the modelled data from the 90° transect using a 600 kJ blow energy

Measurement and assessment of underwater noise and vibration during construction at the Block Island wind farm, Rhode Island

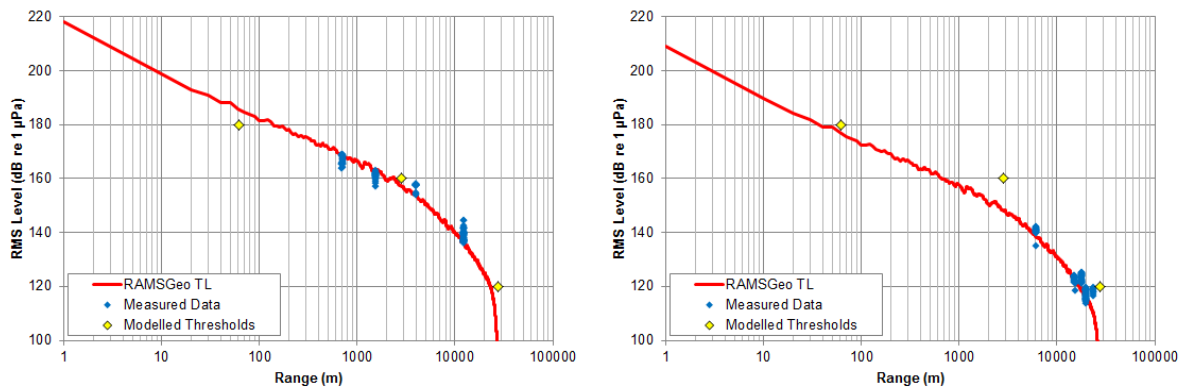


Figure 4-34 Comparison between measured data and modelled thresholds for transect 7 (pile 1, left, and piles 2-4, right) using the modelled data from the 0° transect using a 200 kJ blow energy

4.7.4 Hammer type and SPL comparison

A comparison of the unweighted peak-to-peak sound pressure levels, at a range less than 1200 m to piling, for two different hammer types is presented in Figure 4-35. The levels measured for the Bauer-Pileco Inc Model D280-22 diesel hammer are seen to be of the same order for the levels measured for the Menck hydraulic hammer on 03 September 2015 and follow the same trend. The higher levels recorded on 18 and 19 September 2015 are linked to higher blow energies at least when compared with the levels measured on 03 September. The blow energies for the diesel hammer were not available for comparison, although specifications for it state that its available blow energy range is much greater than that of the Menck.

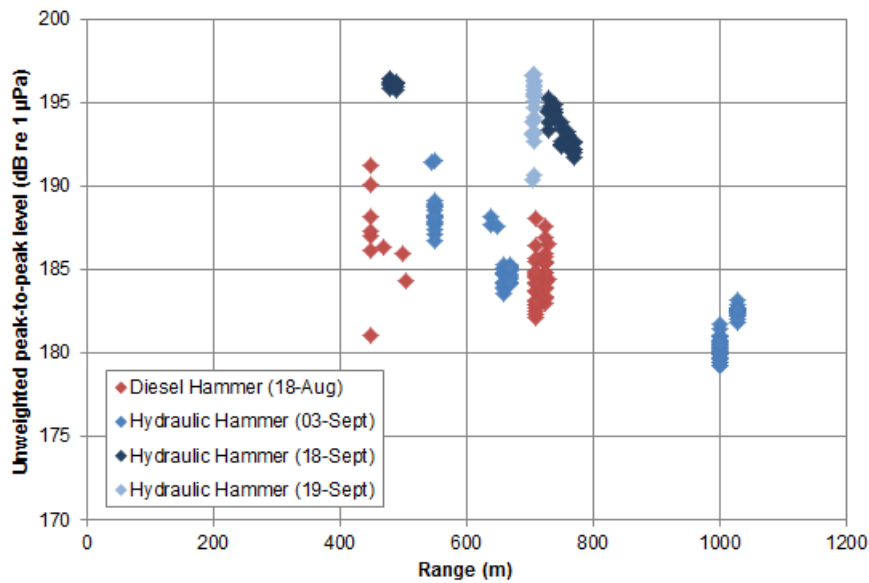


Figure 4-35 Comparison of unweighted peak-to-peak sound pressure levels between a Diesel Hammer and a Hydraulic hammer

5 Piling seabed vibration measurements

5.1 Introduction

Seabed vibration measurements of impact piling were taken along transects from foundation WTG5 at BIWF during piling of the first stage piles, on 17 September 2015. The measurements from these transects are presented in the following section in the order they were collected.

5.2 Vibration measurements

Measurements of seabed vibration were carried out along a northwest transect from turbine foundation WTG5. The measurement transect was repeated two times, each time a different pile was driven. Measurements began at the edge of the exclusion zone and were then taken at increasing distance from the turbine foundation in steps of approximately 500 m. The axes were vertical (away from the seabed), longitudinal (toward piling) and transverse (perpendicular to piling).

The first transect measurement was carried out between 12:42 and 13:36 on 17 September 2015. On review of the data it was found that interference had occurred due to the survey vessel's engines not being turned off during the measurement. For the second and third transects, measurements were taken once the survey vessel's engines and electronic equipment was turned off.

5.2.1 WTG5 Pile 2 Northwest transect

Vibration measurements taken during the installation of pile 2 of WTG5 are presented in Table 5-1 in terms of peak particle velocity for the three axes. The greatest magnitudes of peak particle velocity are seen to be for the longitudinal axis which was deployed to line up with the transect direction. This data can be seen in graphical form in Figure 5-1.

Distance (m)	Approx. Blow Energy (kJ)	Vertical PPV Peak (mm/s)	Longitudinal PPV Peak (mm/s)	Transverse PPV Peak (mm/s)
550 (P2)	Not available	0.079	0.158	0.112
570 (P2)	-	0.100	0.177	0.112
590 (P2)	-	0.112	0.177	0.079
590 (P2)	-	0.100	0.177	0.079
1040 (P2)	-	0.040	0.079	0.063
1060 (P2)	-	0.071	0.112	0.100
1060 (P2)	-	0.050	0.100	0.079
1660 (P2)	-	0.032	0.063	0.028
1660 (P2)	-	0.028	0.063	-
2150 (P2)	-	0.020	0.040	0.020
2150 (P2)	-	0.021	0.050	0.020
2500 (P2)	-	0.018	-	-
3350 (P2)	-	0.011	0.016	0.013
3350 (P2)	-	-	0.018	-

Table 5-1 Measurements of the peak particle velocity (PPV) magnitudes taken along a northwest transect from WTG5 for the installation of pile 2

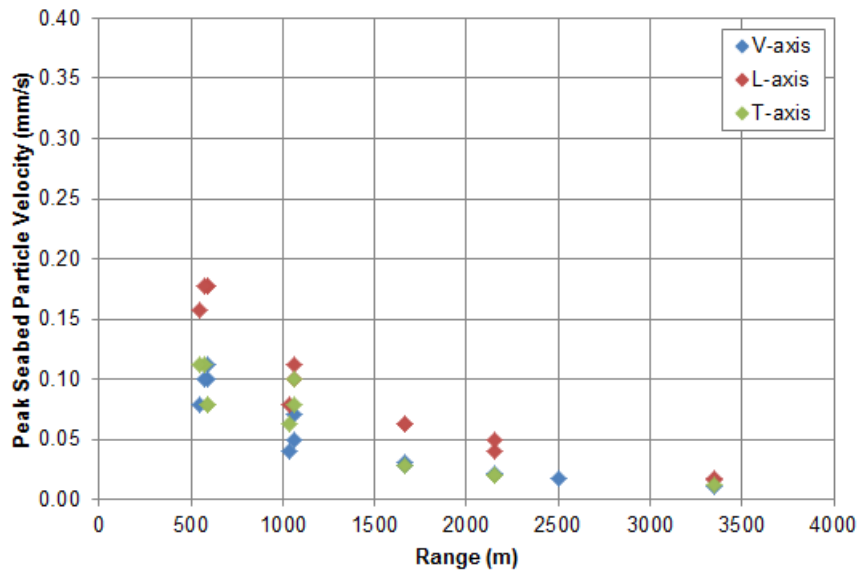


Figure 5-1 Peak particle velocity (PPV) magnitudes plotted against range for a northwest transect from WTG5 for the installation of pile 2

5.2.2 WTG5 Pile 3 Northwest transect

Vibration measurements taken during the installation of pile 3 of WTG5 are presented in Table 5-2 in terms of peak particle velocity for the three axes. The greatest magnitudes of peak particle velocity are again seen to be for the longitudinal axis 0.354 mm/s at 400 m. Magnitudes of peak particle velocity were measured in excess of 0.2 mm/s, at a range of 750 m, greater than the highest magnitude of peak particle velocity, measured at a closer range of 570 m, on the first transect. Figure 4-14 in section 4.4 shows the underwater noise time history for 17 September 2015 and indicates a greater vibration emission in the impact piling of pile 3 compared with pile 2, hence the higher magnitudes of peak particle velocity measured for pile 3. This data can be seen in graphical form in Figure 5-2.

Distance (m)	Approx. Blow Energy (kJ)	Vertical PPV Peak (mm/s)	Longitudinal PPV Peak (mm/s)	Transverse PPV Peak (mm/s)
400 (P3)	65	0.177	0.354	0.177
420 (P3)	70	0.188	0.281	0.186
710 (P3)	230	0.112	0.171	0.133
750 (P3)	70	0.071	0.126	0.092
750 (P3)	80	0.079	0.149	0.112
750 (P3)	235	0.119	0.199	0.112
750 (P3)	235	0.106	0.199	0.100
750 (P3)	235	0.100	0.211	0.094
780 (P3)	250	0.094	0.223	0.112
780 (P3)	230	0.106	0.164	0.089
1210 (P3)	80	0.035	0.133	0.040
1250 (P3)	70	0.050	0.100	0.045
2050 (P3)	240	-	0.028	-
3050 (P3)	240	0.014	0.021	0.019

Table 5-2 Measurements of the peak particle velocity (PPV) magnitudes taken along a northwest transect from WTG5 for the installation of pile 3

6 Summary and conclusions

This report describes a series of underwater noise and seabed vibration measurements that have been carried out during impact piling operations at the Block Island Wind Farm. Five turbine foundations were installed consisting of a jacket-structure with cylindrical piles, split into two or three sections, inserted into each corner of a jacket and impact driven. Underwater noise measurements from a fixed monitor captured 15 piling events in August and September 2015. Measurements of underwater noise were also undertaken from a survey vessel along transects, with a total of seven transects sampled. A further three transect measurements were undertaken to capture seabed vibration, of which two were deemed to have data of sufficient quality for analysis. The measurements were carried out during impact piling operations on foundations WTG1, WTG2, WTG3 and WTG5.

Background noise measurements were collected when no piling occurred predominantly in and around the wind farm site. Samples of background noise were taken at a distance of up to 30 km from the site in quieter waters. The mean RMS SPLs recorded ranged between 107.4 and 118.7 dB re 1 μ Pa. Higher levels of background noise were found closer to the wind farm site which can be attributed to construction vessels and also to recreational vessel traffic. The background noise measurements carried out as part of this survey only provide a snapshot of the levels at the locations and times they were taken.

The measured data from the fixed monitor captured the variation in the underwater noise level during pile driving operations over the period of a day. This data provided useful information for the analysis of the measured transect data, most notably for the north transect where measurements were taken during the piling of the four stage one piles for the WTG1 foundation.

All the transect measurements of underwater impact piling noise were seen to decrease in level with increasing distance as expected. A comparison of the underwater noise levels measured at mid-depth with those measured at one meter above the seabed showed noise levels were higher nearer the seabed.

For each transect, the transmission loss was calculated, using the RAMSGeo propagation model in order to determine the source levels. The estimated peak-to-peak source levels extrapolated from the measured data ranged between 233 and 245 dB re 1 μ Pa at 1 m.

Transect measurements of seabed vibration were also undertaken during impact piling operations on WTG5 using a tri-axial geophone. The measurements were repeated for subsequent piles on a northwest transect. The greatest magnitude of peak particle velocity was measured to be 0.354 mm/s on the longitudinal axis (towards piling) at a range of 400 m from the piling.

7 References

1. Bebb A H, Wright H C (1953). *Injury to animals from underwater explosions*. Medical Research Council, Royal Navy Physiological Report 53/732, Underwater Blast Report 31, January 1953.
2. Bebb A H, Wright H C (1954a). *Lethal conditions from underwater explosion blast*. Royal Navy Physiological Report 51/654, RNPL 3/51, National Archives reference ADM 298/109, March 1954.
3. Bebb A H, Wright H C (1954b). *Protection from underwater explosion blast – III. Animal experiments and physical measurements*. Royal Navy Physiological Report 54/792, RNPL 2/54, March 1954.
4. Bebb A H, Wright H C (1955). *Underwater explosion blast data from the Royal Navy Physiological Labs 1950/55*. Medical Research Council, April 1955.
5. Collins M D (1994). *Generalisation of the Split-Step Padé solution*. J. Acoust. Soc. Am. 96, 382-385.
6. Collins M D, Cederberg R J, King D B, Chin-Bing S A (1996). *Comparison of algorithms for solving parabolic wave equations*. J. Acoust. Soc. Am. 100, 178-182.
7. Cudahy E A, Parvin S J (2001). *The effects of underwater blast on divers*. Naval Submarine Research Laboratory Report 1218, Groton, CT 06349 62.
8. Goertner J F (1982). *Prediction of underwater explosion safe ranges for sea mammals*. NSWC/WOL TR-82-188. Naval Surface Weapons Centre, White Oak Laboratory, Silver Spring, MD, USA, NTIS AD-A 139823.
9. Hastings M C, Popper A N (2005). *Effects of sound on fish*, Report to the California Department of Transport, under contract no. 43A01392005, January 2005.
10. Hill S H (1978). *A guide to the effects of underwater shock waves in arctic marine mammals and fish*. Pacific Mar. Sci. Rep. 78-26. Inst. Ocean Sciences, Patricia Bay, Sidney B.C. 50pp.
11. Jensen F B, Kuperman W A, Porter M B, Schmidt H (1994). *Computational ocean acoustics*. AIP Press, Woodbury, NY, p38.
12. Mackenzie K V (1981). *Nine-term equation for the sound speed in the oceans*. J. Acoust. Soc. Am. 70(3), pp 807-812.
13. Nedwell J R, Langworthy J, Howell D (2003). *Assessment of sub-sea acoustic noise and vibration from offshore wind turbines and its impact on marine wildlife; initial measurements of underwater noise during construction of offshore wind farms, and comparison with background noise*. Subacoustech report no. 544R0423 to COWRIE, May 2003.
14. Rawlins J S P (1974). *Physical and patho-physiological effects of blast*. Joint Royal Navy Scientific service. Volume 29, No. 3 pp 124 – 129, May 1974.
15. Rawlins J S P (1987). *Problem in predicting safe ranges from underwater explosions*. Journal of Naval Science, Volume 14, No. 4 pp 235 – 246.
16. Richardson W J, Green C R, Malme C I, Thompson D H (1995). *Marine mammals and noise*. Academic Press Inc., San Diego, 1995.

17. Richmond D R, Yelverton J T, Fletcher E R (1973). *Far-field underwater blast injuries produced by small charges*. Defense Nuclear Agency, Department of Defense, Washington D.C. Technical Progress Report DNA 3081.
18. Yelverton J T, Richmond D R, Fletcher E R, Jones R K (1973). *Safe distances from underwater explosions for mammals and birds*. DNA 3114T, Lovelace Foundation for Medical Education and Research, Final Technical Report.
19. Yelverton J T, Richmond D R (1981). *Underwater explosion damage risk criteria for fish, birds and mammals*. J. Acoust. Soc. Am. 70, S84.

Appendix A Measurement of underwater sound

Sound travels much faster in water (approximately 1500 m/s) than in air (340 m/s). Since water is a relatively incompressible, dense medium the pressures associated with underwater sound tend to be much higher than in air. Background levels of about 130 dB re 1 μ Pa for coastal waters (Nedwell *et al*, 2003) and rivers are not uncommon. This level equates to about 100 dB re 20 μ Pa, using the units that would be used in air. Such levels in air would be considered to be hazardous, however, marine animals have evolved to live in this environment and thus the relatively high levels are not dangerous.

A.1 Units of measurement

Sound measurements underwater are usually expressed using the decibel (dB) scale, which is a logarithmic measure of sound. A logarithmic scale is used because rather than equal increments of sound having an equal increase in effect, typically a constant ratio is required for this to be the case, that is, each *doubling* of the sound level will cause a roughly equal increase in “loudness”.

Any quantity expressed in this scale is termed a “level”. If the unit is sound pressure, expressed on the dB scale, it will be termed a “Sound Pressure Level”. The fundamental definition of the dB scale is given by

$$Level = 10 \times \log_{10} \left(\frac{Q}{Q_{ref}} \right)$$

where Q is the quantity being expressed on the scale, and Q_{ref} is the reference quantity. The dB scale represents a ratio and, for instance, 6 dB really means “twice as much as...” It is therefore used with a reference unit, which expresses the base from which the ratio is expressed. The reference quantity is conventionally smaller than the smallest value to be expressed on the scale, so that any level quoted is positive. For instance, for sound in air a reference quantity of 20 μ Pa is usually used, since this is the threshold for human hearing.

A refinement is that the scale when used with sound pressure is applied to the pressure squared, rather than the pressure. If this was not the case, and the acoustic power level of a source rose by, say, 10 dB, the sound pressure level would rise by 20 dB. So that variations in the units agree, the sound pressure must be specified in units of Root Mean Square pressure (see Section A.1.3, below). This is equivalent to expressing the sound as

$$Sound\ Pressure\ Level = 20 \times \log_{10} \left(\frac{P_{RMS}}{P_{ref}} \right)$$

For underwater sound, typically a unit of one micropascal (μ Pa) is used as a reference unit; a Pascal is equal to the pressure exerted by one Newton over one square metre. One micropascal equals one-millionth of this.

A.1.1 Peak level

The peak sound pressure level is the maximum level of the acoustic pressure, usually a positive pressure. This form of measurement is often used to characterise underwater blasts where there is a clear positive peak following the detonation of explosives. Examples of this type of measurement used to define underwater blast waves can be found in Bebb and Wright (1953, 1955), Richmond *et al* (1973), Yelverton *et al* (1973), and Yelverton and Richmond (1981). The data from these studies have been widely interpreted in a number of reviews on the impact of high level underwater noise causing fatality and injury in human divers, marine mammals, and fish (see, for example, Rawlins, 1974; Hill, 1978; Goertner, 1982; Richardson *et al*, 1995; Cudahy and Parvin, 2011; Hastings and Popper, 2005).

A.1.2 Peak-to-peak level

The peak-to-peak level is usually calculated using the maximum variation of the pressure from positive to negative within the wave. This represents the maximum change in pressure (differential pressure from positive to negative) as the transient pressure wave propagates. Where the wave is symmetrically distributed in positive and negative pressure, the peak-to-peak level will be twice the peak level, and hence 6 dB higher (i.e. the negative part of the wave has the same amplitude as the positive part).

Peak-to-peak levels of noise are often used to characterise sound transients from impulsive sources such as percussive impact piling and seismic airgun sources.

A.1.3 Sound pressure level

The sound pressure level (SPL) is normally used to characterise noise and vibration of a continuous nature, such as drilling, boring, continuous wave sonar, or background sea and river noise levels. To calculate the SPL, the variation in sound pressure is measured over a specific time period to determine the root mean square (RMS) level of the time-varying acoustic pressure. The SPL_{RMS} can therefore be considered to be a measure of the average unweighted level of the sound over the measurement period.

A.1.4 Sound exposure level

When assessing the noise from transient sources such as blast waves, impact piling, or seismic airgun noise, the issue of the time period of the pressure wave is often addressed by measuring the total energy of the wave. This form of analysis was used by Bebb and Wright (1953, 1954a, 1954b, 1955), and later by Rawlins (1987) to explain the apparent discrepancies in the biological effect of short and long range blast waves on human divers.

The sound exposure level (SEL) sums the acoustic energy over a measurement period, and effectively takes account of both the SPL of the sound source and the duration for which the sound is present in the acoustic environment. Sound exposure (SE) is defined by the equation:

$$SE = \int_0^T p^2(t) dt$$

where p is the acoustic pressure in Pascals (Pa), T is the total duration of the sound in seconds and t is time in seconds. The sound exposure is a measure of the acoustic energy and, therefore, has units of Pascal squared seconds (Pa^2s).

To express the sound exposure on a logarithmic scale, by means of a dB, it is compared with a reference acoustic energy level of $1 \mu Pa$ (P_{ref}^2) and a reference time (T_{ref}). The sound exposure level (SEL) is then defined by

$$SEL = 10 \log_{10} \left(\frac{\int_0^T p^2(t) dt}{P_{ref}^2 T_{ref}} \right)$$

By selecting a common reference pressure (P_{ref}^2) of $1 \mu Pa$ for assessments of underwater noise, the SEL and SPL can be compared using the expression

$$SEL = SPL + 10 \log_{10} T$$

where the SPL is a measure of the average level of the broadband noise and the SEL sums the cumulative broadband noise energy.

Therefore, for continuous sounds of duration less than one second, the SEL will be lower than the SPL. For periods of greater than one second, the SEL will be numerically greater than the SPL (i.e.

for a continuous sound of ten seconds duration, the SEL will be 10 dB higher than the SPL, for a sound of 100 seconds duration, the SEL will be 20 dB higher than the SPL, and so on).

A.2 Source level

The spreading of sound as it travels from the source needs to be included in any assessment of received levels. As the measurement point moves away from the source, a piling operation for instance, the pressure measured will decrease due to spreading. To standardise all source levels, regardless of where they are measured, they are referred back to a conceptual point 1 m away from the point of origin of the noise. Consequently, source levels should be presented with units of 'dB re 1 μ Pa @ 1 m'.

A.3 Sound propagation

Sound propagation is frequently described by the equation

$$L_r = SL - TL$$

where L_r is the sound pressure level at distance r from a source in metres, SL is the (notional) source level at 1 m from the source, and TL is the transmission loss.

The transmission loss is frequently described by the simple equation

$$TL = N \log_{10} r + \alpha r$$

where r is the distance from the source in metres, N is a factor for attenuation due to geometric spreading, and α is a factor for the absorption of sound in water and boundaries (dB.km^{-1}).

Using this form of sound transmission loss, the sound level with range L_r can be described by the expression

$$L_r = SL - N \log_{10} r - \alpha r$$

Appendix B Calibration certificates

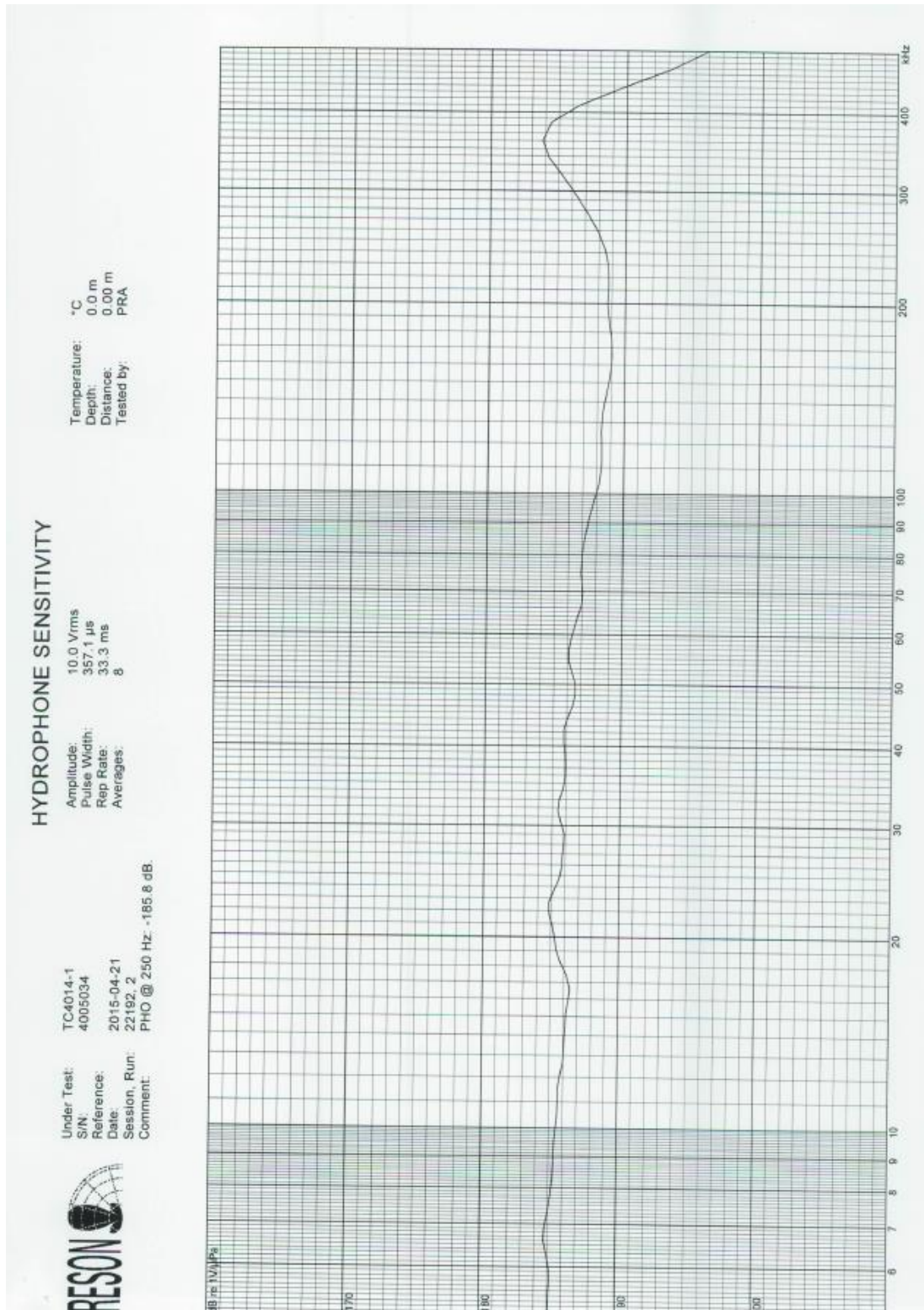


Figure B-1 Calibration certificate for RESON TC4014 hydrophone (S/N 4005034)

HYDROPHONE SENSITIVITY

Temperature: °C
Depth: 0.0 m
Distance: 0.00 m
Tested by: PRA

Amplitude: 10.0 Vrms
Pulse Width: 357.1 µs
Rep Rate: 33.3 ms
Averages: 8

Under Test: TC4014-1
S/N: 4005035
Reference: 2015-04-21
Date: 22/92, 6
Session, Run:
Comment: PHO @ 250 Hz -186.8 dB.

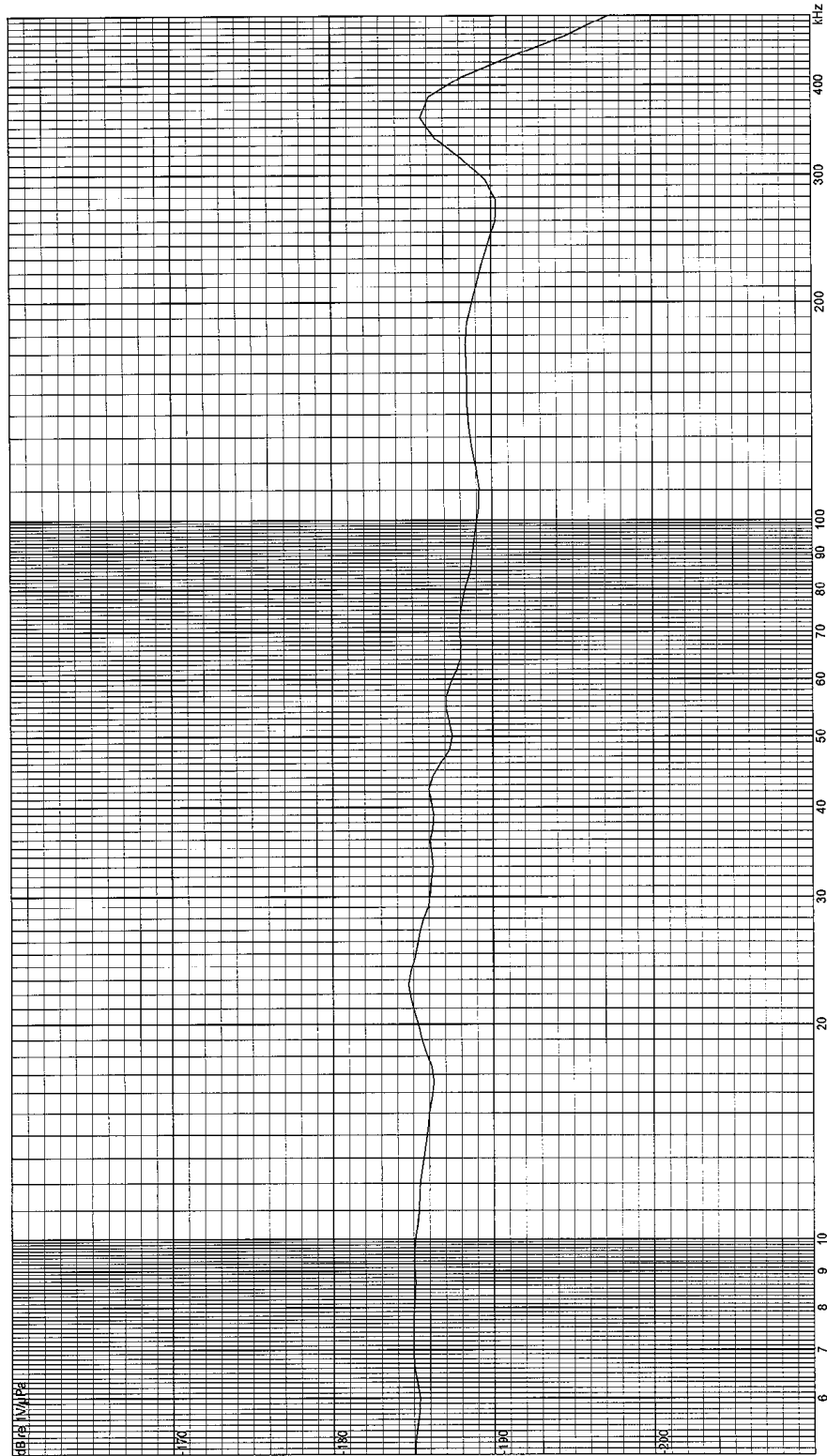


Figure B-2 Calibration certificate for RESON TC4014 hydrophone (S/N 4005035)

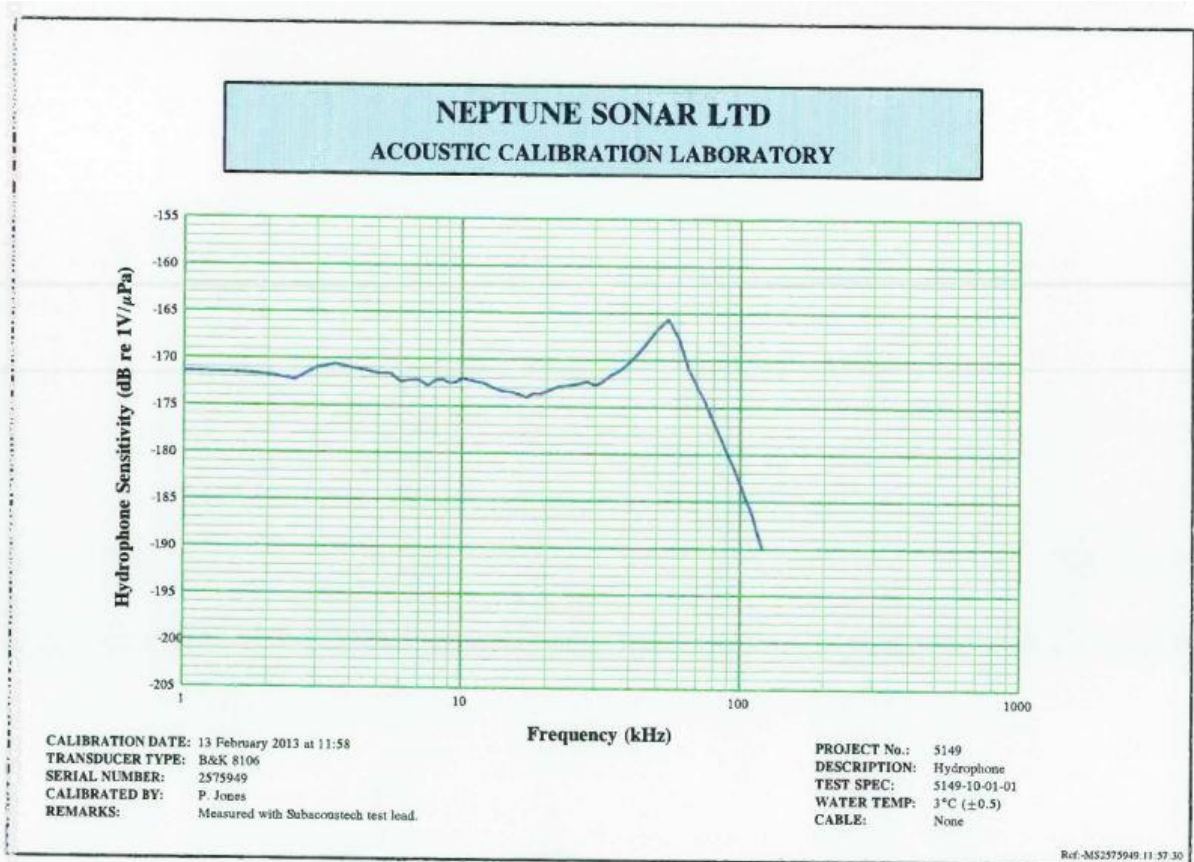


Figure B-3 Calibration certificate for Brüel & Kjær Type 8106 hydrophone (S/N 2575949)

Vibro

CALIBRATION CERTIFICATE

CALIBRATION CERTIFICATE NO.: 0715 Geophone Pack

CLIENT: Subacoustech

INSTRUMENT TYPE: V901 Geophone Pack

SERIAL NUMBER: Red Transducer

CALIBRATION DATE: 13/07/15

CALIBRATED BY: C.H

CALIBRATION ACCURACY:- 610 mv p-p @ 10mm 40Hz

	A channel	B channel	VDV channel
Peak Particle Velocity L	<u>±5</u> %	<u>/</u> %	X <u>/</u> %
Peak Particle Velocity V	<u>±5</u> %	<u>/</u> %	Y <u>/</u> %
Peak Particle Velocity T	<u>±5</u> %	<u>/</u> %	Z <u>/</u> %

AIR OVERPRESSURE CHANNEL - Peak Level Unweighted / dB(Lin)

WE HEREBY CERTIFY THAT THIS SEISMOGRAPH FULLY COMPLIES WITH THE MANUFACTURERS SPECIFICATION

CERTIFIED BY: 

DATE: 13/07/15

THIS CERTIFICATE IS VALID FOR 12 MONTHS

The above calibration was carried out using equipment calibrated as follows:-
Pulsar Acoustic Calibrator 100B, serial number 60796, calibrated April 2015
ISO-TECH IFG 100 Oscillator, serial number 300351, calibrated June 2015
Monitran Vibration Meter, serial number 213608, calibrated June 2015
Precision Gold PG012 Multimeter, serial number 09000182, calibrated June 2015

THIS CALIBRATION IS TRACEABLE TO NATIONAL STANDARDS

VIBROCK LIMITED
Shanakiel
Ilkeston Road
Heanor
Derbyshire DE75 7DR
Tel: 01773 711211
Fax: 01773 711311
Email: vibrock@vibroch.com
Web: www.vibroch.com



INSTCALCERT/2908.05.15

Figure B-4 Calibration certificate for Vibrock V901 geophone

Appendix C Detailed results

Report documentation page

- This is a controlled document.
- Additional copies should be obtained through the Subacoustech Environmental librarian.
- If copied locally, each document must be marked “Uncontrolled copy”.
- Amendment shall be by whole document replacement.
- Proposals for change to this document should be forwarded to Subacoustech Environmental.

Document No.	Draft	Date	Details of change
E494R0100	14	11/25/2015	Initial writing and internal review
E494R0101	-	01/17/2016	First issue to client
E494R0102	-	02/23/2016	Revisions following receipt of piling logs

Originator's current report number	E494R0102
Originator's name and location	T Mason; Subacoustech Environmental Ltd.
Contract number and period covered	E494; July 2015 – February 2016
Sponsor's name and location	Randy Gallien; HDR
Report classification and caveats in use	COMMERCIAL IN CONFIDENCE
Date written	November 2015 – February 2016
Pagination	Cover + iii + 51
References	19
Report title	Measurement and assessment of underwater noise and vibration during construction at the Block Island wind farm, Rhode Island
Translation/Conference details (if translation, give foreign title/if part of a conference, give conference particulars)	
Title classification	Unclassified
Author(s)	A G Collett, T I Mason, R J Barham
Descriptors/keywords	
Abstract	
Abstract classification	Unclassified; Unlimited distribution